Title
The air mycobiome is decoupled from the soil mycobiome in the California San Joaquin Valley

Journal
Molecular Ecology, 31(19)

ISSN
0962-1083

Authors
Wagner, Robert
Montoya, Liliam
Gao, Cheng
et al.

Publication Date
2022-10-01

DOI
10.1111/mec.16640

Running Head: Air mycobiome decoupled from soil

Title: The air mycobiome is decoupled from the soil mycobiome in the California San Joaquin Valley

Authors: Robert Wagner[1], Liliam Montoya[1], Cheng Gao[2], Jennifer R. Head[3], Justin Remais[4], John W. Taylor[1]

[1]Department of Plant & Microbial Biology, University of California Berkeley, Berkeley, CA, USA. [2]Institute of Microbiology, Chinese Academy of Sciences, Beijing, China. [3]Division of Epidemiology, University of California Berkeley, Berkeley, CA, USA. [4]Division of Environmental Health Sciences, University of California Berkeley, Berkeley, CA, USA.

Corresponding author: Robert Wagner (robwagner@berkeley.edu)

Abstract: Dispersal is a key force in the assembly of fungal communities and the air is the dominant route of dispersal for most fungi. Understanding the dynamics of airborne fungi is important for determining their source and for helping to prevent fungal disease. This understanding is important in the San Joaquin Valley of California, which is home to 4.2 million people and where the airborne fungus *Coccidioides* is responsible for the most important fungal disease of otherwise healthy humans, coccidioidomycosis. The San Joaquin Valley is the most productive agricultural region in the United States, with the principal crops grown therein susceptible to fungal pathogens. Here, we characterize the fungal community in soil and air on undeveloped and agricultural land in the San Joaquin Valley using metabarcoding of the internal transcribed spacer 2 variable region of fungal rDNA. Using 1002 individual samples, we report one of the most extensive studies of fungi sampled simultaneously from air and soil using modern sequencing techniques. We find that the air mycobiome in the San Joaquin Valley is distinct from the soil mycobiome, and that the assemblages of airborne fungi from sites as far apart as 160km are far more similar to one another than to the fungal communities in nearby soils. Additionally, we present evidence that airborne fungi in the San Joaquin Valley are subject to dispersal limitation and cyclical intra-annual patterns of community composition. Our findings are broadly applicable to understanding the dispersal of airborne fungi and the taxonomic structure of airborne fungal assemblages.

Keywords: fungi, soil, air, mycobiome, dispersal, *Coccidioides*

Introduction: It has been known that the air harbors microorganisms following Eherenberg's discovery of "infusoria" in dust samples collected off the coast of Africa nearly 200 years ago (Ehrenberg, 1830). Subsequent research has provided the foundation for our understanding of airborne microbial dispersal (Darwin, 1846; Pasteur, 1860), a fundamental process in community assembly (Nemergut et al., 2013; Vellend, 2010). Of particular interest are fungi because they primarily disperse through the air (Magyar et al., 2016; Talbot, 1997), can travel vast distances (Brown & Hovmøller, 2002), and have many dormancy mechanisms at their disposal (Lennon & Jones, 2011; Locey, 2010) which confer protections from damaging environmental conditions during transport (Dijksterhuis, 2019; Wyatt et al., 2013). Fungi provide many important ecosystem services such as establishing mutually beneficial relationships with plant species, breaking down leaf and woody material and cycling carbon and nitrogen in soils (Baldrian, 2017; Becquer et al., 2019; Lustenhouwer et al., 2020; Read & Perez-Moreno, 2003; Stuart & Plett, 2020). Many fungal species, especially airborne fungi, are associated with diseases affecting humans, crops and wild plants and animals (Fisher et al., 2012). Modern studies using high-throughput sequencing to describe the outdoor air microbiome are rare, and those focusing on fungi (the air *myco*biome) rarer still, despite the outdoor air medium harboring diverse, spatially and temporally variable fungal populations (Barberán et al., 2015; Fierer et al., 2008; Frohlich-Nowoisky et al., 2009; Núñez et al., 2019; A. C. Woo et al., 2013).

Fungal disease in the San Joaquin Valley (SJV) in California, which is home to 4.2 million people (US Census Bureau, 2019), is illustrative of the need to better understand airborne fungal dispersal. The fungus *Coccidioides* is a virulent airborne respiratory pathogen that is endemic to the SJV (Dixon, 2001; Egeberg & Ely, 1956; Kollath, Miller, et al., 2019; C. Nguyen et al., 2013; Ophüls, 1905) and is responsible for nearly 200 deaths and $3.9 billion in costs per year in the United States (Centers for Disease Control and Prevention, 2018; Gorris et al., 2021; Huang et al., 2012). Found primarily in California and Arizona, it remains unclear on what environmental medium *Coccidioides* primarily grows, its source of nutrition (Barker et al., 2012; Emmons, 1942; Kollath, Teixeira, et al., 2019; J. W. Taylor & Barker, 2019) or its precise means and range of dispersal (de Perio et al., 2019; Nicas, 2018; Pappagianis & Einstein, 1978; Schneider et al., 1997; Wilken et al., 2015). Agriculturally, the SJV is the most productive region in the United States (Food & Agriculture (CDFA), 2018), and plant pathogenic and parasitic fungi are responsible for significant losses in many of the chief crops grown therein (Baumgartner et al., 2019; Baumgartner & Rizzo, 2002; Camiletti et al., 2022; Holland et al., 2021). Determining the source and dispersal characteristics of airborne fungi can aid in preventing or mitigating fungal disease in humans and crops as well as offering a better understanding of fungal community ecology.

In what is still the most extensive modern outdoor air mycobiome work, significant differences in the distribution of fungi in settled dust have been demonstrated between regions at the continental scale (Barberán et al., 2015) despite a documented capacity amongst airborne fungi for long distance transport (Brown & Hovmøller, 2002; Prospero et al., 2005). The sampling of settled dust by Barberán et al. (2015) was largely focused in population centers and samples were

broadly collected across North America, each at a single timepoint, including one sample from the SJV. A further analyses of the same data that focused on plant pathogens illustrated an association between certain pathogenic fungal taxa and geographic regions of the United States (Dietzel et al., 2019). Few high-throughput sequencing studies, however, have paired aerobiology investigations of outdoor fungal communities with simultaneous sampling of the substrates on which they grow. Abrego et al. (2018) showed that the air mycobiomes of two individual samples taken at a single site were more similar to the air mycobiomes in sites >100km away than to the soil mycobiomes at the same site collected several years prior (Abrego et al., 2018; Mäkipää et al., 2017). Their 2020 follow up publication reported less variation in the air mycobiome than the soil mycobiome, at distances up to 20km, and also across a shift in land use from natural to urban (Abrego et al., 2020). Similarly, Kivlin et. al (2014) showed that the air mycobiomes from five sites, stretching approximately 115km from Irvine, California to the vicinity of Mt San Jacinto, California, did not differ from one another, changed little over a seventeen month sampling period and were distinct from the soil mycobiome (Kivlin et al., 2014). Recently, Schiro et al. (2022) found fungi in dust more closely resembles the soil fungal community nearby than airborne fungi from distant sites, though the dust collected in this study consisted of surface soil that had been suspended using a portable wind tunnel (Schiro et al., 2022).

Here we report the most extensive community-level, high-throughput sequencing study of fungi collected simultaneously from air and soil to date. Many studies have explored the air mycobiome in recent years, though to our knowledge only four other works have investigated both air and soil using high-throughput sequencing, each with an order of magnitude fewer

samples than we present here (Table S1). With just over 1000 samples, we characterized the fungal communities within soils and inferred the assemblage of airborne fungi above these soils via settled dust from both undeveloped land and actively cultivated agricultural land within the SJV in California. Our expectation that fungi in settled dust would most closely resemble the local soil fungal community was surprisingly shown to be false. Instead, assemblages of fungi in settled dust more closely resembled fungi in settled dust from distant sites rather than resembling soil communities collected beneath our dust samplers. Principally, our community level investigation allowed us to discern patterns of fungal dispersal between the soil and airborne mycobiomes in the SJV and generate hypotheses regarding fungal pathogens in the region. By sampling in the SJV, we complement previous work by focusing on a critically important yet overlooked region, and our extensive sampling and temporally explicit approach provides a more comprehensive assessment of regional airborne fungal dispersal than preceding studies. This information will further our understanding of fungal dispersal as well as facilitate connections between epidemiological data on fungal disease of crops and humans with fungal dispersal dynamics, allowing more robust predictions to be generated and prevention strategies employed.

Methods: Fungi in soil and in settled dust were sampled from undeveloped land (defined here as uncultivated and unirrigated land showing few signs of recent disturbance) adjacent to California highway 33 (Hwy33), at five sites spanning 80km, monthly, from November 2017 through October 2018. These sites provide a north-south transect though one of the least developed areas in the SJV (Table S2). Hwy33 sites have aridic soils, receive between 15 and 25cm of annual precipitation, and support a wild vegetation that includes *Nassella spp*., *Sporobolus spp*., *Suaeda*

nigra, *Atriplex polycarpa* and *Adenostoma fasciculatum* (Griffith et al., 2016). Developed land along Hwy33 is primarily cropland, followed by pasture and sites of oil extraction interspersed with small urban areas (Griffith et al., 2016). Fungi in soil and in settled dust were also sampled from experimental sorghum fields at the Kearney Agricultural Research and Extension Center (KARE), 100km northeast of the nearest Hwy33 site, in the summers of 2016, 2017 and 2018 (Gao et al., 2020). There is little undeveloped land near KARE (Griffith et al., 2016). At their furthest, these 6 sites extend across 160km, a substantial portion of the SJV (Figure 1A, Table S2). Soils from agricultural land were collected as shallow soil cores from the upper organic soil layers (Gao et al., 2018, 2020), where both the highest density and a broad diversity of microbial and fungal species are encountered (Fierer et al., 2003; Hao et al., 2021). While soils from agricultural land were collected as shallow soil cores, we chose to collect soils on undeveloped land from within rodent burrows. Fungi generally inhabit places that are protected from stressors such as desiccation, high temperatures and UV irradiation in extreme environments (Makhalanyane et al., 2015; Santiago et al., 2018), and rodent burrows provide such a habitat and are nearly ubiquitous across the landscape in arid and semiarid ecosystems (Davidson & Lightfoot, 2008; Grinnell, 1923; Whitford & Kay, 1999). Our own experience confirmed this ubiquity in the SJV, with hundreds of burrows observed in the immediate vicinity at all Hwy33 sites. Rodent burrows have been shown to be rich in fungal diversity, owing not only to their environmental conditions but also to the nutrients provided by rodents and other macro-organisms that reside within (Hawkins, 1996; Herrera et al., 1999; Miranda et al., 2019; Reichman et al., 1985). Given their unique characteristics when compared to the surrounding landscape, we expect that rodent burrows contribute greatly to soil fungal diversity in arid and semi-arid regions.

Sampling and DNA Extraction: At Hwy33 sites, soil was sampled from within rodent burrows using hemispherical collectors mounted on threaded rods inserted in the burrows as deeply as possible but no deeper than 30cm. Ten burrows were sampled at each site in the first month (November 2017). Thereafter, due to time constraints, sampling was reduced to three burrows for all remaining months. Sampled burrows were not necessarily the same each month though were selected as close as possible to the coordinates sampled the previous month. There were no other selection criteria for burrows. Air was sampled by allowing dust to passively settle into empty, sterile, 10cm Petri dish bottoms placed 50cm off the ground on a polyvinylchloride pipe and protected from precipitation beneath a plastic cone (Figure S1). Three passive dust collectors were placed in a triangular formation at each site with two collectors 5m apart on an east-west axis (the western of which was at the coordinates of soil sampling) that lay 50m north of the third collector. After one month of exposure, Petri dish bottoms were retrieved and covered with sterile lids for transport to the laboratory, and replaced with clean, sterile bottoms, a process that was repeated monthly at each Hwy33 site from November 2017 through October 2018. At KARE, soils were sampled by collecting soil cores 3cm in diameter and 15cm deep, as previously described (Gao et al., 2020), which spans soil depths that incorporate a range of agricultural soil fungal diversity (Schmidt et al., 2019). KARE samples were collected from May through September in 2016, June through October in 2017, and July through October in 2018, with total monthly replicates ranging from 6 to 90 soil samples. Air samples of passively settled dust were taken at KARE in September and October of 2017 (Gao et al., 2020) and from June through October of 2018 as described above with one difference; at KARE, 13 air samplers were arrayed at the corners of nested squares with sides of 10m, 20m, 40m and 80m. Settled dust was

retrieved from all Petri dish bottoms using sterile, DNA-free swabs moistened in sterile, DNA-free, distilled water. Swabs were cut from their wooden sticks, placed into buffer and disrupted by bead beating followed by DNA extraction using the MoBio Powersoil DNA kit (MoBio, Carlsbad, CA, USA). Soil, 0.25g, was added to buffer and DNA extracted using the same kit. DNA was quantified using a Qubit dsDNA HS Assay kit (Life Technologies Inc., Gaithersburg, MD, USA) and then diluted to 5ng μl^{-1}.

PCR Amplification and Sequencing: For Hwy33 samples, the ITS2 region was PCR amplified from extracted DNA with the 5.8SFun (AACTTTYRRCAAYGGATCWCT) and ITS4Fun (AGCCTCCGCTTATTGATATGCTTAART) primers (D. L. Taylor et al., 2016) using the AccuStart II PCR SuperMix kit (Quantabio, Beverly, MA, USA). The reaction mixture contained 2µl of undiluted template DNA, 2.5µl each of 50 µM forward and reverse primer, 12.5µl AccuStart II PCR SuperMix, 2.5µl of nuclease-free water and 3µl BSA. A negative control consisted of 2µl of nuclease-free water in the place of template DNA. Amplification was performed on the Gene Amplification PCR System (Bio-Rad Laboratories, Hercules, CA, USA) under the following conditions: 1 cycle of 96°C for 2 minutes, 35 cycles of 94°C for 30 seconds, 58°C for 40 seconds and 72°C for 2 minutes, and 1 cycle of 72°C for 10 minutes. The PCR product was quantified using the Qubit dsDNA HS Assay kit (Life Technologies Inc., Gaithersburg, MD, USA) and sent to the QB3 Vincent J. Coates Genomics Sequencing Laboratory (University of California, Berkeley, CA, USA), where samples were assigned unique dual indices to avoid barcode bleed / tag-jumping (Carøe & Bohmann, 2020; Zinger et al., 2019), and sequenced on the MiSeq platform using the paired-end PE300 chemistry (Illumina, Inc., CA, USA). For KARE samples, the molecular protocols were identical with the following exceptions:

template DNA was diluted to 5ng μl^{-1}, BSA was not added and 5PRIME HotMaster Mix (Eppendorf-5Prime, Gaithersburg, MD, USA), now discontinued, was used instead of the AccuStart II PCR SuperMix (Gao et al., 2020).

Sequence Processing: All sequence processing was done in Qiime 2 version 2019.10.0 (Bolyen et al., 2019) and sequence runs were visually inspected for quality using the *summarize* command. Sequences were denoised using the *denoise-paired* command in DADA2 (Callahan et al., 2016), and primer sequences were removed, paired-end reads were joined, and bases trimmed at the beginning and end of every read once the median quality score dropped below 25. Unpaired reads (roughly 2% of reads) were discarded. A naïve Bayes classifier was trained with the UNITE database (UNITE Community, 2019) at 97% similarity using the *feature-classifier fit-classifier-naive-bayes* command, and OTUs were assigned with the *feature-classifier classify-sklearn* command (Bokulich et al., 2018; Pedregosa et al., 2011). "Unidentified" taxa could be matched to an unidentified UNITE database sequence entry, indicating that this sequence had been found in the environment, though the taxon associated with it remains unknown. "Unspecified" taxa, on the other hand, were algorithmically categorized by *classify-sklearn*, a machine learning method, at a certain taxonomic level but were not matched to a specific UNITE database entry. All data and metadata supporting the findings of this study have been deposited in the NCBI Sequence Read Archive (www.ncbi.nlm.nih.gov/sra) with the following accession numbers: PRJNA736543 (Wagner, 2021a), PRJNA736167 (Wagner, 2021b) and PRJNA736519 (Wagner, 2021c). All code used to convert raw sequencing data (FASTQ files) into the taxonomic tables used in this study are included as supplementary material.

Statistical Analysis: Statistical analyses used R version 4.0.2 (R Core Team, 2020) and vegan version 2.5.6 (Oksanen et al., 2019). Taxa were analyzed at the species level and those represented by only one DNA sequence amongst all samples were removed. Unidentified and unspecified taxa were also removed for all community-level statistical analyses, though were kept for generation of taxonomic figures. Taxa tables were then transformed (square-rooted to reduce the effect of a few dominant taxa and Wisconsin double standardized) before calculating Bray-Curtis dissimilarity (Bray & Curtis, 1957; Legendre & Gallagher, 2001). Wisconsin double standardization first divides each taxon by the most abundant taxon across all samples, followed by division across all taxa for each sample to calculate proportional relative effect sizes. These transformations make taxa comparable across samples regardless of sample size. Taxa were not rarefied as rarefaction of microbiome data can introduce bias and needlessly throw out data (McMurdie & Holmes, 2014; Willis, 2019). We found no effect on our findings in tests of rarefaction or the inclusion of sequencing depth as a covariate (Weiss et al., 2017).

Differences in the fungal community between factors (land use, site, year, month and sampling medium) were assessed using a nested PERMANOVA (Anderson, 2001) on Bray-Curtis dissimilarities with the adonis2 function. Bray-Curtis dissimilarities were visualized using principal coordinate analysis with ape version 5.6.2 (Paradis & Schliep, 2019) and clustering of principal coordinate scores used ward.D2 distances (Murtagh & Legendre, 2014). Permutations (1000) were left unstratified as stratifying (block permutations) did not change the nested PERMANOVA results. Pairwise differences between land use and sampling medium were assessed using pairwiseadonis (Arbizu, 2019) with 1000 permutations. Significance of the relationship between temporal and geographic distance (distance-decay), and Bray Curtis

dissimilarity, was correlated (Pearson) using the Mantel test (Legendre & Legendre, 2012; Mantel & Valand, 1970) with unstratified permutations (1000). Significant differences between factors in the strength (slope) of the distance-decay relationship were established when a significant interaction was present using linear regression. A linear mixed effects model was used to test for differences in *Onygenales* abundance between land use and sampling medium combinations as fixed effects, and month as a random effect, using lme4 version 1.1.26 (Bates et al., 2015). P-values were calculated by comparing the full model with a null model excluding fixed effects, using a log-likelihood test (Barr et al., 2013), and variance explained was estimated as marginal and conditional r^2 values (Nakagawa & Schielzeth, 2013) using MuMIn version 1.43.17 (Bartoń, 2020). Post-hoc tests comparing factor levels used the Kenward-Rogers method in lsmeans version 2.30.0 and pbkrtest version 0.5.0.1 (Halekoh & Højsgaard, 2014; Lenth, 2016).

Estimating species richness notoriously undercounts the true richness in ecological studies, which is only compounded when rarifying data by the smallest sample size in a given study (Colwell et al., 2012). Methods to alleviate these problems have faced novel challenges with microbial datasets using high-throughput sequencing due to sequencing errors being indistinguishable from novel taxa (Chiu & Chao, 2016). To alleviate these problems, species accumulation curves and estimated species richness were calculated with iNEXT.3D version 1.0.1, which extrapolates species richness based on individual sample sizes using unrarefied data (Chao et al., 2014, 2021; Hsieh et al., 2016). Confidence intervals in iNEXT.3D were calculated from 1000 bootstrap replications. To assess functional potential, OTUs were assigned to functional guilds using FUNGuild version 1.1 (N. H. Nguyen et al., 2016). Guild assignments

were only kept if they reached the “Probable” and “Highly Probable” confidence levels. As each OTU could be assigned to multiple functional guilds, all functional guild assignments were counted to determine the proportional functional potential for each sample (i.e. if an OTU was assigned “Plant Pathogen” and “Saprotroph” it would be counted in both categories). A linear mixed effects model was used to test for temporal shifts in the proportional abundances of taxa in settled dust samples assigned to the “Plant Pathogen” functional guild, with month as a fixed effect and site as a random effect. P-values and r^2 values were calculated as described above. Visualizations were created using ggplot2 version 3.3.2 (Wickham, 2016). No novel code was used to perform the statistical analyses done in this study, though the code used has been included as supplementary material.

Results: A total of 1002 individual soil and air samples were collected and their mycobiota sequenced and characterized using the ITS2 region of fungal ribosomal DNA, with 413 samples from Hwy33 sites and 589 samples from KARE, inclusive of previously published data (Gao et al., 2018, 2020). Hwy33 sites included 175 air and 238 soil samples, while KARE sites included 90 air and 499 soil samples. In total, 1417 known fungal species (non-inclusive of unidentified taxa at higher taxonomic levels) were identified from roughly 44,000,000 reads. The highest number of species was found in Hwy33 (930) and KARE (660) air samples, followed by Hwy33 (563) and KARE (499) soil samples (Figure S2, Table S3). The number of species found along Hwy33 did not significantly differ between individual sites, though there were more species found in air than in soil (Figure S3, Table S4). Of the total number of identified fungal species, a little less than half (626 species) were unique to individual land use and sampling medium

294 combinations. The number of sequence reads assigned to these species was quite small, however,
295 representing only 1.4% of the total number of reads across both land uses and in air and soil. The
296 highest number of uniquely sampled species (270) were found in Hwy33 air and the fewest (95)
297 in KARE air (Figure S4), representing 0.05% and 0.02% of total sequence reads, respectively.
298 172 species were found in common across all sampling mediums and sites, that is, in both soil
299 and air and at both Hwy33 and KARE, representing 87.9% of total sequence reads. Between
300 Hwy33 and KARE, more species were shared in air (503) than in soil (265), though the
301 proportion of sequences in each category was nearly identical at 92.4% and 92.1%, respectively.
302
303 Fungal Community Structure: The most interesting and unexpected result of our analyses is the
304 similarity in fungal assemblages in air over distances as great as 160 km, compared to the
305 distinct nature of soil fungal communities over the same distances. Using principal coordinate
306 analysis (PCoA), all samples separated into three distinct categories representing Hwy33 soil,
307 KARE soil, and a third category containing all air samples from both Hwy33 and KARE (Figure
308 1B). The difference in PCoA-derived mean Bray-Curtis distance between soil and air fungal
309 communities at any individual site was greater than the difference in air between any pair of sites
310 (Figure 1C). In terms of individual predictors of fungal community structure, PERMANOVA
311 analysis showed that land use (Hwy33 vs KARE) and sampling medium (soil vs air) explained
312 18% and 10%, respectively, of the variance in fungal community structure, while month, year,
313 and differences between Hwy33 sites were weak predictors (Table 1). Taken together,
314 interactions between factors represented 18% of explained variance, but only when inclusive of
315 month or sampling medium. All factors showed significant differences ($p \leq 0.001$) between
316 factor levels, likely because of the high number of samples (van der Laan et al., 2010), with

317 variance explained delineating important predictors from inconsequential ones. In general, the
318 fungal assemblage in air more closely resembled the fungal community in soils from Hwy33
319 than from KARE, based on post-hoc PERMANOVA analyses (Table S5). Reducing species to
320 only those shared between soil and settled dust did not substantially change the results of
321 PERMANOVA or PCoA analyses (Figure S5), though subsampling to account for an unbalanced
322 sampling design or heterogeneous dispersion between factor levels greatly reduced the effect of
323 land use from 18% to 10% variance explained (Figure S6). In both cases, land use and sampling
324 medium remained the most important explanatory variables. Likewise, reanalysis in the absence
325 of soils from Hwy33 (Figure S7) or KARE (Figure S8), to test if results were influenced by
326 differences in soil sampling methods, did not change our core findings. Rarifying data did not
327 change our findings and sequencing depth differences between samples could only explain about
328 1% of the total variance observed (Table S6, S7).
329
330 Spatial and Temporal Distance-Decay: Significant patterns of temporal and geographic distance-
331 decay, with Bray-Curtis dissimilarity, were found for fungi in both Hwy33 and KARE samples,
332 and in both the air and the soil (in all cases, Mantel $p = 0.001$) (Figure 2). In air samples, a
333 seasonal pattern of fungal community dissimilarity and temporal distance was evident from the
334 similar parabolic succession relationship seen at both Hwy33 ($r^2 = 0.35$, Mantel $r = 0.38$) and
335 KARE ($r^2 = 0.36$, Mantel $r = 0.17$), with the initial rate of change significantly greater at KARE
336 than at Hwy33 ($p < 0.001$) (Figure 2A). In contrast, the relationship between fungal community
337 dissimilarity and geographic distance in air was very weak across Hwy33 sites ($r^2 = 0.01$, Mantel
338 $r = 0.11$) over a maximum distance of approximately 80km. When airborne fungi from KARE
339 were included in the relationship, which were collected 100-160km from Hwy33 sites, the slope

of the relationship between community dissimilarity and geographic distance in air samples significantly increased ($p < 0.001$) by 36.4% when compared to Hwy33 sites alone ($r^2 = 0.11$, Mantel r = 0.33) (Figure 2B). Within Hwy33 sites, air samples taken no more than 50m apart showed no relationship between dissimilarity and geographic distance ($p > 0.09$, $|\text{Mantel r}| < 0.09$, $r^2 < 0.01$). The relationship between fungal community dissimilarity and temporal distance was weaker in soils than in air at KARE ($r^2 = 0.08$, Mantel r = 0.28), and much weaker at Hwy33 sites ($r^2 = 0.01$, Mantel r = 0.09) (Figure 2C). The difference in temporal decay in soils between KARE and Hwy33 sites is almost certainly due to the former being actively cultivated agricultural land with regular seasonal disturbances due to planting, fertilization, irrigation and harvesting of crops. The temporal distance-decay relationship in soils was also analyzed separately for each year at KARE, which all had significantly different slopes from one another ($p < 0.001$) (Figure S9). Bray-Curtis dissimilarity significantly correlated with temporal distance in KARE soils in 2016 and 2017 (Mantel p = 0.001) but not in 2018 (Mantel p = 0.7). This difference may be due to substantially fewer samples being sequenced and a shorter length of time investigated in 2018 (n = 98, 4 months) than from 2016 (n = 254, 5 months) and 2017 (n = 147, 5 months). With geographic distance, the slope of the relationship with fungal community dissimilarity in soils over approximately 80km along Hwy33 sites ($r^2 = 0.08$, Mantel r = 0.28) was significantly ($p < 0.001$) greater (approximately 2.5 fold) than in air ($r^2 = 0.01$, Mantel r = 0.11) (Figure 2D).

Functional Guilds and Taxonomy: The distribution of functional guild assignments showed distinct sampling medium and land-use specific patterns (Figure 3). Air samples were dominated by the plant pathogen functional guild both along Hwy33 (46.7±0.2%) and at KARE

(71.2±1.2%), while soil samples were dominated by the saprotroph functional guild, also both along Hwy33 (59.2±0.9%) and at KARE (73.9±0.8%) The proportional abundance of taxa assigned to the plant pathogen functional guild in air increased significantly from May through October ($p < 0.001$), though this pattern was less clear during the rest of the year (Figure S10). Plant pathogen functional guild percentages in soils were much lower than in air samples and were similar between soils at Hwy33 (20.1±0.5%) and KARE (22.3±0.8%). The animal pathogen functional guild, alternatively, was most abundant in Hwy33 soils (10.3±0.5%), followed by Hwy33 air (8.6±0.3%) and KARE air (6.6±0.3%), and lowest in KARE soils (2.3±0.3%). Taxonomic proportional abundances were characterized at the phylum, order, and genus levels. Most taxa were Ascomycota in the Pleosporales, Capnodiales and Sordariales (Figure S11, S12). The most common genera in air were *Mycosphaerella* (30.8%) and *Alternaria* (27.9%), which contain numerous plant and crop pathogenic species (Figure 4A-F). *Alternaria* was also the most common genus in soil fungi, though was much more common along Hwy33 (22.2%) than at KARE (9.6%) (Figure 4G-L). Genera of Onygenales, the order that contains *Coccidioides* as well as numerous animal pathogenic fungi (Sigler, 2002), were orders of magnitude more abundant in soils than in the air at both Hwy33 and KARE but did not significantly differ in proportional abundance between soils from Hwy33 and KARE, or between air samples from Hwy33 and KARE (Figure S13). *Coccidioides* was identified in only 4 soil samples from Hwy33 rodent burrows and was not found in any soil cores collected at KARE nor in any air samples. The soil samples that *Coccidioides* was detected in did not have an unusually high or low sequencing depth (Figure S14A), nor were the number of reads assigned to *Coccidioides* exceptional when compared to other taxa (Figure S14B).

Discussion: In the study presented here, we investigated the assemblage of airborne fungi in settled dust and compared it to the soil fungal community in the most productive agricultural region in the United States, the SJV in California. Our study is one of only a handful to simultaneously compare the mycobiome in soil and air using high-throughput sequencing. We showed that the assemblage of airborne fungi collected on both agricultural and undeveloped land, at distances of up to 160km, resemble one another far more than they resemble the fungal communities in nearby soils. We also showed that, regardless of sampling location, the airborne fungal assemblage in the SJV was more similar to the fungal community in rodent burrow soils on undeveloped land than to the fungal community in agricultural soils. The similarity of the airborne fungal community across the SJV, though previously undocumented, is not entirely unexpected. Once airborne, fungal spores can be dispersed across vast distances (Barberán et al., 2015; Cáliz et al., 2018; Griffin, 2007), and the distribution of airborne fungal taxa can change little over tens (Kivlin et al., 2014) to hundreds (Nicolaisen et al., 2017) of kilometers and along altitudinal gradients of up to 1000m (Sánchez-Parra et al., 2021). This degree of mixing is not always the case, however. Airborne fungi in Finnish conifer forests differ from one another at sites approximately 100 to 400km distant from one another (Abrego et al., 2018), and to a lesser degree at distances as short as 1km when sampling across a land-use gradient between forested and urban areas (Abrego et al., 2020). In the coniferous forest study, airborne fungal assemblages from hundreds of kilometers away were more similar to one another than to soil fungi previously characterized at the same sites (Abrego et al., 2018; Mäkipää et al., 2017). These results raise the possibility that the findings we present may not be isolated only to arid environments such as the SJV, but are instead relevant across multiple biomes.

Spatial and Temporal Patterns: Distance-decay relationships are helpful for understanding patterns in community ecology (Anderson et al., 2011; Dray et al., 2012; Nekola & White, 1999; Soininen et al., 2007; Whittaker, 1972). Among studies of fungi, such relationships can illustrate both geographic variation (Bahram et al., 2013; Barberán et al., 2015) and patterns of dispersal limitation (Adams et al., 2013; Peay et al., 2012), both of which are relevant to the current study. The fungi that we sampled in soil and in settled dust showed evidence of dispersal limitation based on significant correlations between Bray-Curtis dissimilarity of the fungal community and geographic distance. Dispersal limitation of airborne fungi has been reported previously in settled dust (Adams et al., 2013; Barberán et al., 2015) and rain spore traps (Peay et al., 2012). Conversely, airborne fungi sampled in southern California showed no evidence of dispersal limitation (Kivlin et al., 2014). The reasons for this difference in findings are likely methodological: Kivlin et al. (2014) sequenced the 18s region of fungal rDNA, which provides a decidedly lower species level resolution than the ITS2 region (Bruns & Taylor, 2016; Schoch et al., 2012) and used an older sequencing technology than the one we used. However, differences may also be related to the frequency and scale of sampling, the geographic region investigated or the sampling methods employed, all of which can influence distance-decay relationships (Clark et al., 2021; Soininen et al., 2007). Our finding that the distance-decay relationship was significantly stronger for soil fungi than airborne fungi reflect our observations of greater community variation in soil fungi than in airborne fungi in the SJV. This result provides support for our main finding that the air mycobiome is more similar than the soil mycobiome, not only with regard to ecological distance, but when incorporating a physical measure of distance as well. While we could assess the distance decay relationship in soils over the 80km separating

undeveloped sites along Hwy33, we felt this relationship could not be extended to soils at KARE due to differences in land management, sampling methods and an absence of rodent burrows on agricultural land. However, the environmental conditions at our undeveloped sites are largely representative of a substantial portion of the undeveloped land in the SJV (Griffith et al., 2016), indicating that our findings regarding the soil fungal community may be generalizable at a larger landscape scale. This point is supported by the fact that rodent burrows, such as the ones we sampled, are exceedingly common across similar arid environments (Davidson & Lightfoot, 2008; Grinnell, 1923; Whitford & Kay, 1999).

As previously noted, the airborne fungi surveyed here and in other studies that use molecular identification techniques are not required to establish and grow (Adams et al., 2013). What is measured is only the DNA that is associated, or was associated, with a living organism. Environmental stressors in the atmosphere, such as ultraviolet irradiation and desiccation, can render airborne fungal spores non-viable (Griffin, 2004; Ulevičius et al., 2004), though dormancy mechanisms can confer a fitness advantage by protecting against such stressors (Nemergut et al., 2013). However, this selective force remains unmeasured, likely inflating the perceived diversity of viable airborne fungi across geographic distances, and possibly underestimating airborne fungal dispersal limitation. The influence of non-viable fungi that plagues studies of airborne fungi is lessened in soils, where unprotected nucleic acids are subject to decomposition (Gordon & Van Norman, 2021). Still, some fungal spores can persist in soils for many years, confusing the detection of growing fungi with dormant fungi (Aime & Miller Jr, 2002; Bruns et al., 2009; N. H. Nguyen, 2018; Sussman et al., 1966). The germination and growth of fungal spores in soils, unlike in air and settled dust, raises the prospect that fitness advantages conferred by

dormancy mechanisms and favorable adaptations to local edaphic conditions contribute to the observed community structure.

The seasonal pattern (temporal-decay) we observed in airborne fungi in the SJV has been reported from other studies based on abundances of individual fungal taxa in air (Almaguer-Chávez et al., 2012; Lacey, 1981; Lagomarsino Oneto et al., 2020; Reyes et al., 2016). Likewise, the distribution of taxa that make up the outdoor airborne fungal assemblage is associated with the frequency and timing of sample collection, whether weekly, seasonally or yearly (Cáliz et al., 2018; Du et al., 2018; Fierer et al., 2008; Nicolaisen et al., 2017). We hypothesize that the seasonal pattern we observed in airborne fungi is due to the annual, agricultural cycle of planting and harvesting, whereupon crops are generally planted in the spring and harvested in the fall (Zhong et al., 2011), as well as the yearly phenology of wild plants in the SJV (Chiariello, 1989). This hypothesis is supported by our observations of monthly shifts in the proportional abundance of taxa assigned to the plant pathogen functional guild as well the dominance of *Alternaria* and *Mycosphaerella* in settled dust samples, genera that contain numerous plant pathogenic and parasitic species (Camiletti et al., 2022; Crous, 2010; Farrar et al., 2004; Fones et al., 2020; Koike et al., 2017). Similar seasonal patterns to the ones we show here have been observed in other agricultural regions, with increased abundances of plant pathogenic fungi in the late summer and fall (Almaguer-Chávez et al., 2012; Nicolaisen et al., 2017). The soil fungal community in the SJV, in contrast to the airborne fungal assemblage, changed little with time, suggesting that shifts in the distribution of fungi present in soils cannot fully explain the corresponding shifts in the distribution of airborne fungi above. While fungi inhabiting soil can survive adverse conditions as vegetative hyphae, through the production of sclerotia (Willetts,

1971) or as spore banks (Baar et al., 1999), fungi inhabiting living tissue on the aerial structures of host plants typically must sporulate for persistence. The high abundance of *Mycosphaerella* in air samples, and its relative near absence in soil samples, indicates that this genus is largely unassociated with soils in the SJV. We presume that airborne *Mycosphaerella*, which constitutes over half of the air mycobiome in some land-use and month combinations, as well as other plant pathogenic and parasitic fungi, are more associated with the crop and wild plant phyllosphere than the soil environment in the SJV.

Land Use and the Influence of Burrowing Rodents: Our results indicate that most airborne fungal taxa in the SJV can be found in both agricultural soils and soils within rodent burrows on undeveloped land. Mean Bray-Curtis dissimilarities, and proportional abundances of taxa indicate that soils from rodent burrows more closely resemble the air mycobiome in the SJV than soils from agricultural fields. Though we believe that the air mycobiome in the SJV is probably more associated with plants than with soils, at some point in their lifecycle most described fungi can be found in soils (Bridge & Spooner, 2001; O'Brien et al., 2005; Tedersoo et al., 2014). Fungi primarily disperse through the air (Magyar et al., 2016; Talbot, 1997), and in arid environments, wind erosion can liberate large volumes of surface soil and dust (Duniway et al., 2019; Field et al., 2010), likely dispersing fungi and fungal spores (Barberán et al., 2015; Dietzel et al., 2019; Schiro et al., 2022). This type of dispersal suggests that, though perhaps not the dominant source of airborne fungi, soil fungi and their spores can contribute significantly to the air mycobiome in arid environments such as those found in the SJV. While the SJV is generally considered an arid environment (Griffith et al., 2016), the physical characteristics of cultivated agricultural land within the SJV are probably less susceptible to wind disturbance than

undeveloped land due to artificial irrigation and crop cover (Duniway et al., 2019). Conversely, on undeveloped lands, burrowing mammals can liberate significant quantities of fine soil material (Black & Montgomery, 1991; Davidson & Lightfoot, 2008; Grinnell, 1923; Whitford & Kay, 1999), and this material is highly susceptible to wind erosion (Wei et al., 2007; Whitford & Kay, 1999). It has been estimated that, in areas where foraging occurs, up to twenty percent of the soil surface is disturbed by burrowing mammals in arid environments each year (Whitford & Kay, 1999). The data we have collected does not allow us to determine the origin of the airborne fungi we found in the SJV, as many variables were left unexplored and the range of locations sampled was limited. However, the susceptibility of soils from rodent burrows to wind erosion could offer a plausible starting point for explaining the higher similarity we found between airborne fungi and fungi from rodent burrow soils, than fungi from agricultural soils.

Methodological Considerations: An important question is to what degree sampling method and study site selection play a role in the observed distribution of fungal species. There are numerous methods for sampling airborne fungi, each with its own unique trade-offs (West & Kimber, 2015). We used passive deposition sampling on petri dishes, which is inexpensive and allows for a high degree of replication. Differences in spore aerodynamic diameter, however, may enrich for specific taxa with larger spores and higher settling velocities when using deposition sampling (C. Woo et al., 2018). Kivlin et al. (2014) sampled airborne fungi on nylon filters that use an active air pump, which can likely capture a wider distribution of particle sizes. However, filters on active samplers such as this slowly become clogged with material (West & Kimber, 2015), which may impact the distribution of fungi sampled over time. Indeed, Kivlin et al. (2014) state that filter replacement was sometimes necessitated due to obstructed airflow. A bigger drawback

523 is the cost of active sampling systems and their need for electricity, which limits replication. For
524 example, our passive sampling method allowed for monthly collection from 13 samplers at
525 KARE for three summers, and 15 samplers among the five Hwy33 sites for one year, whereas
526 Kivlin et. al (2014) collected 1 filter from each of five sites every 2-3 months, over a 17-month
527 period. In both studies by Abrego et al. (2018, 2020), a "cyclone sampler" was used, which
528 likely captures the most representative sample of airborne fungi of the methods mentioned
529 (Abrego et al., 2018), though replication is limited by cost similar to filtration methods. An
530 important consideration regarding the results of ours and the few other metabarcoding studies
531 that have compared airborne fungi and soil fungi is that sampling methods between these two
532 mediums are not equivalent. While the soil fungal community may have taken years to arrive at
533 its current state (Osburn et al., 2021), the airborne fungal assemblage can change with the
534 seasons, as we have shown here. There are likely numerous other differences between these
535 sampling mediums with which to contend, and while we are currently unable to address all of
536 them, it's important to evaluate our results with this caveat in mind.
537
538 The location in the environment where air sampling takes place, particularly sampling height,
539 can influence the distribution of fungal taxa observed (Charalampopoulos et al., 2022; Khattab &
540 Levetin, 2008; Mahaffee, 2014). Sampling closer to the ground (0.5 – 1.5m) better represents
541 local taxonomic distributions of airborne fungi while sampling higher up (10-30m) is more likely
542 to represent regional distributions (Lacey & Venette, 1995; West & Kimber, 2015). Sampling
543 very high up (>100m) appears to homogenize fungal aerobiota (Núñez & Moreno, 2020;
544 Sánchez-Parra et al., 2021; Tipton et al., 2019). Both our study and those of Abrego et al. (2018,
545 2020) sampled close to the soil surface and found small but significant differences in the

546 distribution of airborne taxa between sites. It is possible that our study and Abrego et al. (2018,
547 2020) preferentially sampled more localized fungal taxa. Sampling at low heights near the
548 saltation layer (the height range where wind causes particles to skip across the soil surface)
549 enriches for particles from the surrounding area (Ho et al., 2014; Martin & Kok, 2017). In
550 contrast, Kivlin et al. (2014) sampled at 7m and found no significant differences among sites or
551 between seasons, while we showed clear difference with both. Though Kivlin et al. (2014) used
552 different sequencing methods than ours, it is possible that sampling at a greater height also
553 homogenized the distribution of fungi sampled with respect to time as well as location. This
554 possibility is supported by fungal sampling at elevations above 3000m in which the distribution
555 of airborne fungal taxa can become completely decoupled with time from the seasonal to decadal
556 scale (Tipton et al., 2019).
557
558 Difficulty in Detecting *Coccidioides*: Our inability to detect *Coccidioides* in all but four samples
559 prevent us from saying much that is ecologically relevant regarding *Coccidioides* in either soil or
560 air. It is notable however that the sequencing depth and the total number of reads assigned to
561 *Coccidioides* in samples where *Coccidioides* was detected were neither remarkably high nor low.
562 This finding suggests that the likelihood of finding *Coccidioides* in soils may be more associated
563 with an uneven distribution across the landscape (Greene et al., 2000; Maddy, 1958; Stewart &
564 Meyer, 1932) rather than its presence at some minimum abundance. Detecting *Coccidioides* in
565 air samples has only been accomplished three times from ambient air (Ajello et al., 1965;
566 Daniels et al., 2002; Gade et al., 2020), and once from dust generated through disturbance of the
567 soil surface with a leaf blower (Chow et al., 2016). In all three cases, a high-throughput pump
568 was used to sample thousands of liters of air, which contrasts greatly with our passive deposition

sampling method. It is possible that our sampling method did not allow for the reliable detection of *Coccidioides*, which may only be present in the air in extremely small abundances. Our finding that fungi in the order Onygenales are far more common in soils than in settled dust, on both agricultural and undeveloped land, allows for speculation that soil disturbance may be important for dispersal and infection of animal pathogenic fungi (including *Coccidioides*). The higher proportional abundance of taxa assigned to the animal pathogenic fungal guild in the air and soil of undisturbed land than those of agricultural land hints at possible source dynamics, though more work is needed here. Regardless, high-throughput air sampling techniques should be used in any future attempts to capture airborne *Coccidioides* fungi and a more sensitive *Coccidioides* detection strategy, such as using the CocciENV qPCR assay (Bowers et al., 2019) should be applied in future work investigating *Coccidioides* in either soil or air.

Conclusion: The study presented here provides an analysis of the most extensive sampling effort of fungi in both soil and air to date using high-throughput sequencing methods. By comparing the settled dust mycobiome with the spatially associated soil mycobiome from two distinct sources (rodent burrows on undeveloped land and soil cores from agricultural land), we show that the airborne fungal assemblage in the San Joaquin Valley in California is far more similar between sites over one hundred kilometers away than to nearby soil fungal communities. Our results indicate that the air mycobiome in the San Joaquin Valley experiences seasonal cycles which we hypothesize are the result of the cultivation of crop plants on agricultural land and the phenology of wild plants. We show that, despite the relative similarity of the air mycobiome among sites when compared to the soil mycobiome, significant geographic patterns are apparent.

This pattern is elucidated most clearly through the evidence we provide for airborne fungal dispersal limitation in the San Joaquin Valley. Finally, we hypothesize that the broad array of methodological differences used to explore airborne fungi in the past are likely responsible for differences in results, and that future work should seek to either standardize methods or present results in the context of the methods used. Taken together, our study provides an important exploration of airborne fungal dispersal in the San Joaquin Valley in California, which will be important for gaining a better understand of how fungal pathogens spread in the outdoor environment. This information will be useful for helping to prevent airborne fungal disease as well as for providing a broader understanding of fungal community ecology.

Acknowledgements: This work was supported by National Institutes of Health, National Institute of Allergy and Infectious Disease grant R01AI148336, University of California Office of the President grant VFR-19-633952, and Department of Energy grant DE-SC0014081. We would like to thank Bridget Barker for help with DNA extractions. The authors have no conflict of interest.

References

Abrego, N., Crosier, B., Somervuo, P., Ivanova, N., Abrahamyan, A., Abdi, A., Hämäläinen, K., Junninen, K., Maunula, M., & Purhonen, J. (2020). Fungal communities decline with urbanization—More in air than in soil. *The ISME Journal*, *14*(11), 2806–2815.

Abrego, N., Norros, V., Halme, P., Somervuo, P., Ali-Kovero, H., & Ovaskainen, O. (2018). Give me a sample of air and I will tell which species are found from your region: Molecular identification of fungi from airborne spore samples. *Molecular Ecology Resources*, *18*(3), 511–524.

Adams, R. I., Miletto, M., Taylor, J. W., & Bruns, T. D. (2013). Dispersal in microbes: Fungi in indoor air are dominated by outdoor air and show dispersal limitation at short distances. *The ISME Journal*, *7*(7), 1262–1273.

Aime, M. C., & Miller Jr, O. K. (2002). Delayed germination of basidiospores in temperate species of Crepidotus (Fr.) Staude. *Canadian Journal of Botany*, *80*(3), 280–287.

Ajello, L., Maddy, K., Crecelius, G., Hugenholtz, P., & Hall, L. (1965). Recovery of Coccidioides immitis from the air. *Sabouraudia*, *4*(2), 92–95.

Almaguer-Chávez, M., Rojas-Flores, T., Dobal-Amador, V., Batista-Mainegra, A., Rives-Rodríguez, N., Jesús-Aira, M., Hernández-Lauzardo, A. N., & Hernández-Rodríguez, A. (2012). Aerobiological dynamics of potentially pathogenic fungi in a rice agroecosystem in La Habana, Cuba. *Aerobiologia*, *28*(2), 177–183.

Anderson, M. J. (2001). A new method for non-parametric multivariate analysis of variance. *Austral Ecology*, *26*(1), 32–46.

Anderson, M. J., Crist, T. O., Chase, J. M., Vellend, M., Inouye, B. D., Freestone, A. L., Sanders, N. J., Cornell, H. V., Comita, L. S., Davies, K. F., Harrison, S. P., Kraft, N. J. B., Stegen, J. C., & Swenson, N. G. (2011). Navigating the multiple meanings of β diversity: A roadmap for the practicing ecologist: Roadmap for beta diversity. *Ecology Letters*, *14*(1), 19–28. https://doi.org/10.1111/j.1461-0248.2010.01552.x

Arbizu, P. (2019). *PairwiseAdonis: Pairwise Multilevel Comparison using Adonis. 2017*.

Baar, J., Horton, T. R., Kretzer, A., & Bruns, T. D. (1999). Mycorrhizal colonization of Pinus muricata from resistant propagules after a stand-replacing wildfire. *New Phytologist*, *143*(2), 409–418.

Bahram, M., Koljalg, U., Courty, P.-E., Diedhiou, A. G., Kjøller, R., Polme, S., Ryberg, M., Veldre, V., & Tedersoo, L. (2013). The distance decay of

similarity in communities of ectomycorrhizal fungi in different ecosystems and scales. *Journal of Ecology*, *101*(5), 1335–1344.

Baldrian, P. (2017). Forest microbiome: Diversity, complexity and dynamics. *FEMS Microbiology Reviews*, *41*(2), 109–130.

Barberán, A., Ladau, J., Leff, J. W., Pollard, K. S., Menninger, H. L., Dunn, R. R., & Fierer, N. (2015). Continental-scale distributions of dust-associated bacteria and fungi. *Proceedings of the National Academy of Sciences*, *112*(18), 5756–5761.

Barker, B. M., Tabor, J. A., Shubitz, L. F., Perrill, R., & Orbach, M. J. (2012). Detection and phylogenetic analysis of Coccidioides posadasii in Arizona soil samples. *Fungal Ecology*, *5*(2), 163–176. https://doi.org/10.1016/j.funeco.2011.07.010

Barr, D. J., Levy, R., Scheepers, C., & Tily, H. J. (2013). Random effects structure for confirmatory hypothesis testing: Keep it maximal. *Journal of Memory and Language*, *68*(3), 255–278. https://doi.org/10.1016/j.jml.2012.11.001

Bartoń, K. (2020). *MuMIn: Multi-Model Inference*. https://CRAN.R-project.org/package=MuMIn

Bates, D., Mächler, M., Bolker, B., & Walker, S. (2015). Fitting Linear Mixed-Effects Models Using lme4. *Journal of Statistical Software*, *67*(1), 1–48. https://doi.org/10.18637/jss.v067.i01

Baumgartner, K., Hillis, V., Lubell, M., Norton, M., & Kaplan, J. (2019). Managing grapevine trunk diseases in California's southern San Joaquin Valley. *American Journal of Enology and Viticulture*, *70*(3), 267–276.

Baumgartner, K., & Rizzo, D. M. (2002). Spread of Armillaria root disease in a California vineyard. *American Journal of Enology and Viticulture*, *53*(3), 197–203.

Becquer, A., Guerrero-Galán, C., Eibensteiner, J. L., Houdinet, G., Bücking, H., Zimmermann, S. D., & Garcia, K. (2019). The ectomycorrhizal contribution to tree nutrition. In *Advances in Botanical Research* (Vol. 89, pp. 77–126). Elsevier.

Black, T. A., & Montgomery, D. R. (1991). Sediment transport by burrowing mammals, Marin County, California. *Earth Surface Processes and Landforms*, *16*(2), 163–172.

Bokulich, N. A., Kaehler, B. D., Rideout, J. R., Dillon, M., Bolyen, E., Knight, R., Huttley, G. A., & Gregory Caporaso, J. (2018). Optimizing taxonomic classification of marker-gene amplicon sequences with QIIME 2's q2-feature-classifier plugin. *Microbiome*, *6*(1), 90. https://doi.org/10.1186/s40168-018-0470-z

Bolyen, E., Rideout, J. R., Dillon, M. R., Bokulich, N. A., Abnet, C. C., Al-Ghalith, G. A., Alexander, H., Alm, E. J., Arumugam, M., Asnicar, F., Bai, Y., Bisanz, J. E., Bittinger, K., Brejnrod, A., Brislawn, C. J., Brown, C. T., Callahan, B. J., Caraballo-Rodríguez, A. M., Chase, J., … Caporaso, J. G. (2019). Reproducible, interactive, scalable and extensible microbiome

data science using QIIME 2. *Nature Biotechnology*, *37*(8), 852–857. https://doi.org/10.1038/s41587-019-0209-9

Bowers, J., Parise, K., Kelley, E., Lemmer, D., Schupp, J., Driebe, E., Engelthaler, D., Keim, P., & Barker, B. (2019). Direct detection of Coccidioides from Arizona soils using CocciENV, a highly sensitive and specific real-time PCR assay. *Medical Mycology*, *57*(2), 246–255.

Bray, J. R., & Curtis, J. T. (1957). An Ordination of the Upland Forest Communities of Southern Wisconsin. *Ecological Monographs*, *27*(4), 325–349. https://doi.org/10.2307/1942268

Bridge, P., & Spooner, B. (2001). Soil fungi: Diversity and detection. *Plant and Soil*, *232*(1), 147–154.

Brown, J. K., & Hovmøller, M. S. (2002). Aerial dispersal of pathogens on the global and continental scales and its impact on plant disease. *Science*, *297*(5581), 537–541.

Bruns, T. D., Peay, K. G., Boynton, P. J., Grubisha, L. C., Hynson, N. A., Nguyen, N. H., & Rosenstock, N. P. (2009). Inoculum potential of Rhizopogon spores increases with time over the first 4 yr of a 99-yr spore burial experiment. *New Phytologist*, *181*(2), 463–470.

Bruns, T. D., & Taylor, J. W. (2016). Comment on “Global assessment of arbuscular mycorrhizal fungus diversity reveals very low endemism.” *Science*, *351*(6275), 826–826. https://doi.org/10.1126/science.aad4228

Cáliz, J., Triadó-Margarit, X., Camarero, L., & Casamayor, E. O. (2018). A long-term survey unveils strong seasonal patterns in the airborne

microbiome coupled to general and regional atmospheric circulations. *Proceedings of the National Academy of Sciences*, *115*(48), 12229–12234.

Callahan, B. J., McMurdie, P. J., Rosen, M. J., Han, A. W., Johnson, A. J. A., & Holmes, S. P. (2016). DADA2: High-resolution sample inference from Illumina amplicon data. *Nature Methods*, *13*(7), 581–583. https://doi.org/10.1038/nmeth.3869

Camiletti, B. X., Lichtemberg, P. S., Paredes, J. A., Carraro, T. A., Velascos, J., & Michailides, T. J. (2022). Characterization, pathogenicity, and fungicide sensitivity of Alternaria isolates associated with preharvest fruit drop in California citrus. *Fungal Biology*.

Carøe, C., & Bohmann, K. (2020). Tagsteady: A metabarcoding library preparation protocol to avoid false assignment of sequences to samples. *Molecular Ecology Resources*, *20*(6), 1620–1631.

Centers for Disease Control and Prevention. (2018). *Valley fever (Coccidioidomycosis) Statistics*. https://www.cdc.gov/fungal/diseases/coccidioidomycosis/statistics.html

Chao, A., Gotelli, N. J., Hsieh, T. C., Sander, E. L., Ma, K. H., Colwell, R. K., & Ellison, A. M. (2014). Rarefaction and extrapolation with Hill numbers: A framework for sampling and estimation in species diversity studies. *Ecological Monographs*, *84*(1), 45–67. https://doi.org/10.1890/13-0133.1

Chao, A., Henderson, P. A., Chiu, C.-H., Moyes, F., Hu, K.-H., Dornelas, M., & Magurran, A. E. (2021). Measuring temporal change in alpha diversity: A framework integrating taxonomic, phylogenetic and functional diversity and the iNEXT. 3D standardization. *Methods in Ecology and Evolution*, *12*(10), 1926–1940.

Charalampopoulos, A., Damialis, A., & Vokou, D. (2022). Spatiotemporal assessment of aeromycoflora under differing urban green space, sampling height, and meteorological regimes: The atmospheric fungiscape of Thessaloniki, Greece. *International Journal of Biometeorology*, 1–15.

Chiariello, N. (1989). Phenology of California grasslands. In *Grassland structure and function* (pp. 47–58). Springer.

Chiu, C.-H., & Chao, A. (2016). Estimating and comparing microbial diversity in the presence of sequencing errors. *PeerJ*, *4*, e1634.

Chow, N. A., Griffin, D. W., Barker, B. M., Loparev, V. N., & Litvintseva, A. P. (2016). Molecular detection of airborne Coccidioides in Tucson, Arizona. *Medical Mycology*, *54*(6), 584–592.

Clark, D. R., Underwood, G. J., McGenity, T. J., & Dumbrell, A. J. (2021). What drives study-dependent differences in distance–decay relationships of microbial communities? *Global Ecology and Biogeography*, *30*(4), 811–825.

Colwell, R. K., Chao, A., Gotelli, N. J., Lin, S.-Y., Mao, C. X., Chazdon, R. L., & Longino, J. T. (2012). Models and estimators linking individual-based

and sample-based rarefaction, extrapolation and comparison of assemblages. *Journal of Plant Ecology*, *5*(1), 3–21.

Crous, P. W. (2010). *Taxonomy and phylogeny of the genus Mycosphaerella and its anamorphs* [PhD Thesis]. University of Pretoria.

Daniels, J., Wilson, W., DeSantis, T., Gouveia, F., Anderson, G., Shinn, J., Pletcher, R., Johnson, S., & Pappagianis, D. (2002). *Development of a Quantitative TaqManTM-PCR Assay and Feasibility of Atmosphoric Collection for Coccidioides Immits for Ecological Studies*. Lawrence Livermore National Lab., CA (US).

Darwin, C. (1846). An account of the Fine Dust which often falls on Vessels in the Atlantic Ocean. *Quarterly Journal of the Geological Society*, *2*(1–2), 26–30.

Davidson, A., & Lightfoot, D. (2008). Burrowing rodents increase landscape heterogeneity in a desert grassland. *Journal of Arid Environments*, *72*(7), 1133–1145.

de Perio, M. A., Materna, B. L., Sondermeyer Cooksey, G. L., Vugia, D. J., Su, C., Luckhaupt, S. E., McNary, J., & Wilken, J. A. (2019). Occupational coccidioidomycosis surveillance and recent outbreaks in California. *Medical Mycology*, *57*(Supplement_1), S41–S45.

Dietzel, K., Valle, D., Fierer, N., U'Ren, J. M., & Barberán, A. (2019). Geographical distribution of fungal plant pathogens in dust across the United States. *Frontiers in Ecology and Evolution*, *7*, 304.

Dijksterhuis, J. (2019). Fungal spores: Highly variable and stress-resistant vehicles for distribution and spoilage. *Food Microbiology*, *81*, 2–11.

Dixon, D. (2001). Coccidioides immitis as a select agent of bioterrorism. *Journal of Applied Microbiology*, *91*(4), 602–605.

Dray, S., Pélissier, R., Couteron, P., Fortin, M.-J., Legendre, P., Peres-Neto, P. R., Bellier, E., Bivand, R., Blanchet, F. G., De Cáceres, M., & others. (2012). Community ecology in the age of multivariate multiscale spatial analysis. *Ecological Monographs*, *82*(3), 257–275.

Du, P., Du, R., Ren, W., Lu, Z., Zhang, Y., & Fu, P. (2018). Variations of bacteria and fungi in PM2.5 in Beijing, China. *Atmospheric Environment*, *172*, 55–64. https://doi.org/10.1016/j.atmosenv.2017.10.048

Duniway, M. C., Pfennigwerth, A. A., Fick, S. E., Nauman, T. W., Belnap, J., & Barger, N. N. (2019). Wind erosion and dust from US drylands: A review of causes, consequences, and solutions in a changing world. *Ecosphere*, *10*(3), e02650.

Egeberg, R., & Ely, A. F. (1956). Coccidioides immitis in the soil of the southern San Joaquin Valley. *American Journal of Medical Sciences*, *231*(2), 151–154.

Ehrenberg, C. (1830). Neue Beobachlungen über blutartige Erscheinungen in Aegypten, Arabien und Sibirien, nebst einer Uebersicht und Kritik der früher bekannnten. *Annalen Der Physik*, *94*(4), 477–514.

Emmons, C. W. (1942). Isolation of Coccidioides from soil and rodents. *Public Health Reports (1896-1970)*, 109–111.

Farrar, J. J., Pryor, B. M., & Davis, R. M. (2004). Alternaria diseases of carrot. *Plant Disease*, *88*(8), 776–784.

Field, J. P., Belnap, J., Breshears, D. D., Neff, J. C., Okin, G. S., Whicker, J. J., Painter, T. H., Ravi, S., Reheis, M. C., & Reynolds, R. L. (2010). The ecology of dust. *Frontiers in Ecology and the Environment*, *8*(8), 423–430.

Fierer, N., Liu, Z., Rodríguez-Hernández, M., Knight, R., Henn, M., & Hernandez, M. T. (2008). Short-term temporal variability in airborne bacterial and fungal populations. *Applied and Environmental Microbiology*, *74*(1), 200–207.

Fierer, N., Schimel, J. P., & Holden, P. A. (2003). Variations in microbial community composition through two soil depth profiles. *Soil Biology and Biochemistry*, *35*(1), 167–176.

Fisher, M. C., Henk, D. A., Briggs, C. J., Brownstein, J. S., Madoff, L. C., McCraw, S. L., & Gurr, S. J. (2012). Emerging fungal threats to animal, plant and ecosystem health. *Nature*, *484*(7393), 186–194.

Fones, H. N., Bebber, D. P., Chaloner, T. M., Kay, W. T., Steinberg, G., & Gurr, S. J. (2020). Threats to global food security from emerging fungal and oomycete crop pathogens. *Nature Food*, *1*(6), 332–342.

Food, C. D. of, & Agriculture (CDFA). (2018). California Agricultural Statistics Review, 2017–2018. *State of California*.

Frohlich-Nowoisky, J., Pickersgill, D. A., Despres, V. R., & Poschl, U. (2009). High diversity of fungi in air particulate matter. *Proceedings of the National Academy of Sciences*, *106*(31), 12814–12819. https://doi.org/10.1073/pnas.0811003106

Gade, L., McCotter, O. Z., Bowers, J. R., Waddell, V., Brady, S., Carvajal, J. A., Sunenshine, R., Komatsu, K. K., Engelthaler, D. M., Chiller, T., & Litvintseva, A. P. (2020). The detection of Coccidioides from ambient air in Phoenix, Arizona: Evidence of uneven distribution and seasonality. *Medical Mycology*, *58*(4), 552–559. https://doi.org/10.1093/mmy/myz093

Gao, C., Montoya, L., Xu, L., Madera, M., Hollingsworth, J., Purdom, E., Hutmacher, R. B., Dahlberg, J. A., Coleman-Derr, D., Lemaux, P. G., & others. (2018). Strong succession in arbuscular mycorrhizal fungal communities. *The ISME Journal*, *13*(1), 214–226.

Gao, C., Montoya, L., Xu, L., Madera, M., Hollingsworth, J., Purdom, E., Singan, V., Vogel, J., Hutmacher, R. B., Dahlberg, J. A., Coleman-Derr, D., Lemaux, P. G., & Taylor, J. W. (2020). Fungal community assembly in drought-stressed sorghum shows stochasticity, selection, and universal ecological dynamics. *Nature Communications*, *11*(1), 34. https://doi.org/10.1038/s41467-019-13913-9

Gordon, M., & Van Norman, K. (2021). Mycelial DNA persistence in a forest soil. *Environmental DNA*, *3*(6), 1208–1213.

Gorris, M. E., Neumann, J. E., Kinney, P. L., Sheahan, M., & Sarofim, M. C. (2021). Economic valuation of coccidioidomycosis (Valley fever) projections in the United States in response to climate change. *Weather, Climate, and Society*, *13*(1), 107–123.

Greene, D. R., Koenig, G., Fisher, M. C., & Taylor, J. W. (2000). Soil isolation and molecular identification of Coccidioides immitis. *Mycologia*, *92*(3), 406–410.

Griffin, D. W. (2004). Terrestrial microorganisms at an altitude of 20,000 m in Earth's atmosphere. *Aerobiologia*, *20*(2), 135–140.

Griffin, D. W. (2007). Atmospheric movement of microorganisms in clouds of desert dust and implications for human health. *Clinical Microbiology Reviews*, *20*(3), 459–477.

Griffith, G. E., Omernik, J. M., Smith, D. W., Cook, T. D., Tallyn, E., Moseley, K., & Johnson, C. B. (2016). Ecoregions of California. *US Geological Survey Open-File Report*, *1021*.

Grinnell, J. (1923). The burrowing rodents of California as agents in soil formation. *Journal of Mammalogy*, *4*(3), 137–149.

Halekoh, U., & Højsgaard, S. (2014). A Kenward-Roger Approximation and Parametric Bootstrap Methods for Tests in Linear Mixed Models – The R Package pbkrtest. *Journal of Statistical Software*, *59*(9), 1–30.

Hao, J., Chai, Y. N., Lopes, L. D., Ordóñez, R. A., Wright, E. E., Archontoulis, S., & Schachtman, D. P. (2021). The effects of soil depth on the structure

of microbial communities in agricultural soils in Iowa (United States). *Applied and Environmental Microbiology*, *87*(4), e02673-20.

Hawkins, L. K. (1996). Burrows of kangaroo rats are hotspots for desert soil fungi. *Journal of Arid Environments*, *32*(3), 239–249.

Herrera, J., Kramer, C., & Reichman, O. (1999). Microfungal community changes in rodent food stores over space and time. *Microbial Ecology*, *38*(1), 79–91.

Ho, T. D., Valance, A., Dupont, P., & El Moctar, A. O. (2014). Aeolian sand transport: Length and height distributions of saltation trajectories. *Aeolian Research*, *12*, 65–74.

Holland, L. A., Trouillas, F. P., Nouri, M. T., Lawrence, D. P., Crespo, M., Doll, D. A., Duncan, R. A., Holtz, B. A., Culumber, C. M., Yaghmour, M. A., & others. (2021). Fungal pathogens associated with canker diseases of almond in california. *Plant Disease*, *105*(2), 346–360.

Hsieh, T. C., Ma, K. H., & Chao, A. (2016). iNEXT: An R package for rarefaction and extrapolation of species diversity (H ill numbers). *Methods in Ecology and Evolution*, *7*(12), 1451–1456. https://doi.org/10.1111/2041-210X.12613

Huang, J. Y., Bristow, B., Shafir, S., & Sorvillo, F. (2012). Coccidioidomycosis-associated Deaths, United States, 1990–2008. *Emerging Infectious Diseases*, *18*(11), 1723–1728. https://doi.org/10.3201/eid1811.120752

Khattab, A., & Levetin, E. (2008). Effect of sampling height on the concentration of airborne fungal spores. *Annals of Allergy, Asthma & Immunology*, *101*(5), 529–534.

Kivlin, S. N., Winston, G. C., Goulden, M. L., & Treseder, K. K. (2014). Environmental filtering affects soil fungal community composition more than dispersal limitation at regional scales. *Fungal Ecology*, *12*, 14–25.

Koike, S. T., Smith, R. F., Cahn, M. D., & Pryor, B. M. (2017). Association of the carrot pathogen Alternaria dauci with new diseases, alternaria leaf speck, of lettuce and celery in California. *Plant Health Progress*, *18*(2), 136–143.

Kollath, D. R., Miller, K. J., & Barker, B. M. (2019). The mysterious desert dwellers: *Coccidioides immitis and Coccidioides posadasii* , causative fungal agents of coccidioidomycosis. *Virulence*, *10*(1), 222–233. https://doi.org/10.1080/21505594.2019.1589363

Kollath, D. R., Teixeira, M. M., Funke, A., Miller, K. J., & Barker, B. M. (2019). Investigating the Role of Animal Burrows on the Ecology and Distribution of Coccidioides spp. In Arizona Soils. *Mycopathologia*. https://doi.org/10.1007/s11046-019-00391-2

Lacey, J. (1981). The aerobiology of conidial fungi. *Biology of Conidial Fungi*, *1*, 373–416.

Lacey, J., & Venette, J. (1995). Outdoor air sampling techniques. *Bioaerosols Handbook*, 407–471.

Lagomarsino Oneto, D., Golan, J., Mazzino, A., Pringle, A., & Seminara, A. (2020). Timing of fungal spore release dictates survival during atmospheric transport. *Proceedings of the National Academy of Sciences*, *117*(10), 5134–5143.

Legendre, P., & Gallagher, E. D. (2001). Ecologically meaningful transformations for ordination of species data. *Oecologia*, *129*(2), 271–280. https://doi.org/10.1007/s004420100716

Legendre, P., & Legendre, L. (2012). *Numerical ecology*. Elsevier.

Lennon, J. T., & Jones, S. E. (2011). Microbial seed banks: The ecological and evolutionary implications of dormancy. *Nature Reviews Microbiology*, *9*(2), 119–130.

Lenth, R. V. (2016). Least-Squares Means: The R Package lsmeans. *Journal of Statistical Software*, *69*(1), 1–33. https://doi.org/10.18637/jss.v069.i01

Locey, K. J. (2010). Synthesizing traditional biogeography with microbial ecology: The importance of dormancy. *Journal of Biogeography*, *37*(10), 1835–1841.

Lustenhouwer, N., Maynard, D. S., Bradford, M. A., Lindner, D. L., Oberle, B., Zanne, A. E., & Crowther, T. W. (2020). A trait-based understanding of wood decomposition by fungi. *Proceedings of the National Academy of Sciences*, *117*(21), 11551–11558.

Maddy, K. T. (1958). The geographic distribution of coccidioides immitis and possible ecologic implications. *Arizona Med.*, *15*(3).

946 Magyar, D., Vass, M., & Li, D.-W. (2016). Dispersal strategies of microfungi. In
947 *Biology of microfungi* (pp. 315–371). Springer.
948 Mahaffee, W. F. (2014). Use of airborne inoculum detection for disease
949 management decisions. In *Detection and diagnostics of plant*
950 *pathogens* (pp. 39–54). Springer.
951 Makhalanyane, T. P., Valverde, A., Gunnigle, E., Frossard, A., Ramond, J.-B., &
952 Cowan, D. A. (2015). Microbial ecology of hot desert edaphic systems.
953 *FEMS Microbiology Reviews*, *39*(2), 203–221.
954 Mäkipää, R., Rajala, T., Schigel, D., Rinne, K. T., Pennanen, T., Abrego, N., &
955 Ovaskainen, O. (2017). Interactions between soil-and dead wood-
956 inhabiting fungal communities during the decay of Norway spruce logs.
957 *The ISME Journal*, *11*(9), 1964–1974.
958 Mantel, N., & Valand, R. S. (1970). A technique of nonparametric multivariate
959 analysis. *Biometrics*, 547–558.
960 Martin, R. L., & Kok, J. F. (2017). Wind-invariant saltation heights imply linear
961 scaling of aeolian saltation flux with shear stress. *Science Advances*,
962 *3*(6), e1602569.
963 McMurdie, P. J., & Holmes, S. (2014). Waste not, want not: Why rarefying
964 microbiome data is inadmissible. *PLoS Computational Biology*, *10*(4),
965 e1003531.
966 Miranda, V., Rothen, C., Yela, N., Aranda-Rickert, A., Barros, J., Calcagno, J., &
967 Fracchia, S. (2019). Subterranean desert rodents (genus Ctenomys)

create soil patches enriched in root endophytic fungal propagules. *Microbial Ecology*, *77*(2), 451–459.

Murtagh, F., & Legendre, P. (2014). Ward's Hierarchical Agglomerative Clustering Method: Which Algorithms Implement Ward's Criterion? *Journal of Classification*, *31*(3), 274–295. https://doi.org/10.1007/s00357-014-9161-z

Nakagawa, S., & Schielzeth, H. (2013). A general and simple method for obtaining R2 from generalized linear mixed-effects models. *Methods in Ecology and Evolution*, *4*(2), 133–142.

Nekola, J. C., & White, P. S. (1999). The distance decay of similarity in biogeography and ecology. *Journal of Biogeography*, *26*(4), 867–878.

Nemergut, D. R., Schmidt, S. K., Fukami, T., O'Neill, S. P., Bilinski, T. M., Stanish, L. F., Knelman, J. E., Darcy, J. L., Lynch, R. C., Wickey, P., & Ferrenberg, S. (2013). Patterns and Processes of Microbial Community Assembly. *Microbiology and Molecular Biology Reviews*, *77*(3), 342–356. https://doi.org/10.1128/MMBR.00051-12

Nguyen, C., Barker, B. M., Hoover, S., Nix, D. E., Ampel, N. M., Frelinger, J. A., Orbach, M. J., & Galgiani, J. N. (2013). Recent advances in our understanding of the environmental, epidemiological, immunological, and clinical dimensions of coccidioidomycosis. *Clinical Microbiology Reviews*, *26*(3), 505–525.

Nguyen, N. H. (2018). Longevity of light-and dark-colored basidiospores from saprotrophic mushroom-forming fungi. *Mycologia*, *110*(1), 131–135.

Nguyen, N. H., Song, Z., Bates, S. T., Branco, S., Tedersoo, L., Menke, J., Schilling, J. S., & Kennedy, P. G. (2016). FUNGuild: An open annotation tool for parsing fungal community datasets by ecological guild. *Fungal Ecology*, *20*, 241–248. https://doi.org/10.1016/j.funeco.2015.06.006

Nicas, M. (2018). A point-source outbreak of Coccidioidomycosis among a highway construction crew. *Journal of Occupational and Environmental Hygiene*, *15*(1), 57–62.

Nicolaisen, M., West, J. S., Sapkota, R., Canning, G. G., Schoen, C., & Justesen, A. F. (2017). Fungal communities including plant pathogens in near surface air are similar across northwestern Europe. *Frontiers in Microbiology*, *8*, 1729.

Núñez, A., de Paz, G. A., Rastrojo, A., Ferencova, Z., Gutiérrez-Bustillo, A. M., Alcamí, A., Moreno, D. A., & Guantes, R. (2019). Temporal patterns of variability for prokaryotic and eukaryotic diversity in the urban air of Madrid (Spain). *Atmospheric Environment*, *217*, 116972.

Núñez, A., & Moreno, D. A. (2020). The differential vertical distribution of the airborne biological particles reveals an atmospheric reservoir of microbial pathogens and aeroallergens. *Microbial Ecology*, *80*(2), 322–333.

O'Brien, H. E., Parrent, J. L., Jackson, J. A., Moncalvo, J.-M., & Vilgalys, R. (2005). Fungal community analysis by large-scale sequencing of environmental samples. *Applied and Environmental Microbiology*, *71*(9), 5544–5550.

Oksanen, J., Blanchet, F. G., Friendly, M., Kindt, R., Legendre, P., McGlinn, D., Minchin, P. R., O'Hara, R. B., Simpson, G. L., Solymos, P., Stevens, M. H. H., Szoecs, E., & Wagner, H. (2019). *vegan: Community Ecology Package*. https://CRAN.R-project.org/package=vegan

Ophüls, W. (1905). Further observations on a pathogenic mould formerly described as a protozoon (Coccidioides immitis, Coccidioides pyogenes). *The Journal of Experimental Medicine*, *6*(4–6), 443.

Osburn, E. D., Aylward, F. O., & Barrett, J. (2021). Historical land use has long-term effects on microbial community assembly processes in forest soils. *ISME Communications*, *1*(1), 1–4.

Pappagianis, D., & Einstein, H. (1978). Tempest from Tehachapi takes toll or Coccidioides conveyed aloft and afar. *Western Journal of Medicine*, *129*(6), 527.

Paradis, E., & Schliep, K. (2019). ape 5.0: An environment for modern phylogenetics and evolutionary analyses in R. *Bioinformatics*, *35*, 526–528.

Pasteur, L. (1860). *De l'origine des ferments: Nouvelles expériences relatives aux générations dites spontanées*.

Peay, K. G., Schubert, M. G., Nguyen, N. H., & Bruns, T. D. (2012). Measuring ectomycorrhizal fungal dispersal: Macroecological patterns driven by microscopic propagules. *Molecular Ecology*, *21*(16), 4122–4136.

Pedregosa, F., Varoquaux, G., Gramfort, A., Michel, V., Thirion, B., Grisel, O., Blondel, M., Prettenhofer, P., Weiss, R., Dubourg, V., Vanderplas, J.,

Passos, A., & Cournapeau, D. (2011). Scikit-learn: Machine Learning in Python. *Journal of Machine Learning Research*, *12*, 2825–2830.

Prospero, J. M., Blades, E., Mathison, G., & Naidu, R. (2005). Interhemispheric transport of viable fungi and bacteria from Africa to the Caribbean with soil dust. *Aerobiologia*, *21*(1), 1–19.

R Core Team. (2020). *R: A Language and Environment for Statistical Computing*. R Foundation for Statistical Computing. https://www.R-project.org/

Read, D., & Perez-Moreno, J. (2003). Mycorrhizas and nutrient cycling in ecosystems–a journey towards relevance? *New Phytologist*, *157*(3), 475–492.

Reichman, O., Wicklow, D. T., & Rebar, C. (1985). Ecological and mycological characteristics of caches in the mounds of Dipodomys spectabilis. *Journal of Mammalogy*, *66*(4), 643–651.

Reyes, E. S., de la Cruz, D. R., & Sánchez, J. S. (2016). First fungal spore calendar of the middle-west of the Iberian Peninsula. *Aerobiologia*, *32*(3), 529–539.

Sánchez-Parra, B., Núñez, A., García, A. M., Campoy, P., & Moreno, D. A. (2021). Distribution of airborne pollen, fungi and bacteria at four altitudes using high-throughput DNA sequencing. *Atmospheric Research*, *249*, 105306.

Santiago, I. F., Gonçalves, V. N., Gómez-Silva, B., Galetovic, A., & Rosa, L. H. (2018). Fungal diversity in the Atacama Desert. *Antonie Van Leeuwenhoek*, *111*(8), 1345–1360.

Schiro, G., Chen, Y., Blankinship, J. C., & Barberán, A. (2022). Ride the dust: Linking dust dispersal and spatial distribution of microorganisms across an arid landscape (Accepted). *Environmental Microbiology*. https://doi.org/10.1111/1462-2920.15998

Schmidt, R., Mitchell, J., & Scow, K. (2019). Cover cropping and no-till increase diversity and symbiotroph: Saprotroph ratios of soil fungal communities. *Soil Biology and Biochemistry*, *129*, 99–109.

Schneider, E., Hajjeh, R. A., Spiegel, R. A., Jibson, R. W., Harp, E. L., Marshall, G. A., Gunn, R. A., McNeil, M. M., Pinner, R. W., Baron, R. C., & others. (1997). A coccidioidomycosis outbreak following the Northridge, Calif, earthquake. *Jama*, *277*(11), 904–908.

Schoch, C. L., Seifert, K. A., Huhndorf, S., Robert, V., Spouge, J. L., Levesque, C. A., Chen, W., Consortium, F. B., List, F. B. C. A., Bolchacova, E., & others. (2012). Nuclear ribosomal internal transcribed spacer (ITS) region as a universal DNA barcode marker for Fungi. *Proceedings of the National Academy of Sciences*, *109*(16), 6241–6246.

Sigler, L. (2002). The onygenaceae and other fungi from the order onygenales. *Pathogenic Fungi in Humans and Animals. New York: Marcel Dekker Inc. p*, 195–314.

Soininen, J., McDonald, R., & Hillebrand, H. (2007). The distance decay of similarity in ecological communities. *Ecography*, *30*(1), 3–12.

Stewart, R., & Meyer, K. (1932). Isolation of Coccidioides immitis (Stiles) from the soil. *Proceedings of the Society for Experimental Biology and Medicine*, *29*(8), 937–938.

Stuart, E. K., & Plett, K. L. (2020). Digging deeper: In search of the mechanisms of carbon and nitrogen exchange in ectomycorrhizal symbioses. *Frontiers in Plant Science*, 1658.

Sussman, A. S., Halvorson, H. O., & others. (1966). Spores: Their dormancy and germination. *Spores: Their Dormancy and Germination.*

Talbot, N. J. (1997). Fungal biology: Growing into the air. *Current Biology*, *7*(2), R78–R81.

Taylor, D. L., Walters, W. A., Lennon, N. J., Bochicchio, J., Krohn, A., Caporaso, J. G., & Pennanen, T. (2016). Accurate Estimation of Fungal Diversity and Abundance through Improved Lineage-Specific Primers Optimized for Illumina Amplicon Sequencing. *Applied and Environmental Microbiology*, *82*(24), 7217–7226. https://doi.org/10.1128/AEM.02576-16

Taylor, J. W., & Barker, B. M. (2019). The endozoan, small-mammal reservoir hypothesis and the life cycle of Coccidioides species. *Medical Mycology*, *57*(Supplement_1), S16–S20. https://doi.org/10.1093/mmy/myy039

Tedersoo, L., Bahram, M., Põlme, S., Kõljalg, U., Yorou, N. S., Wijesundera, R., Ruiz, L. V., Vasco-Palacios, A. M., Thu, P. Q., Suija, A., & others. (2014). Global diversity and geography of soil fungi. *Science*, *346*(6213), 1256688.

Tipton, L., Zahn, G., Datlof, E., Kivlin, S. N., Sheridan, P., Amend, A. S., & Hynson, N. A. (2019). Fungal aerobiota are not affected by time nor environment over a 13-y time series at the Mauna Loa Observatory. *Proceedings of the National Academy of Sciences*, *116*(51), 25728–25733.

Ulevičius, V., Pečiulytė, D., Lugauskas, A., & Andriejauskienė, J. (2004). Field study on changes in viability of airborne fungal propagules exposed to UV radiation. *Environmental Toxicology: An International Journal*, *19*(4), 437–441.

UNITE Community. (2019). *UNITE QIIME release for Fungi 2 Version 18.11.2018.* UNITE Community. https://doi.org/10.15156/BIO/786349

US Census Bureau. (2019). *American Community Survey 2015—2019 ACS 5-Year Data Profile*. https://www.census.gov/acs/www/data/data-tables-and-tools/data-profiles/2019/

van der Laan, M., Hsu, J.-P., Peace, K. E., & Rose, S. (2010). Statistics ready for a revolution: Next generation of statisticians must build tools for massive data sets. *AMSTAT News: The Membership Magazine of the American Statistical Association*, *399*, 38–39.

Vellend, M. (2010). Conceptual Synthesis in Community Ecology. *The Quarterly Review of Biology*, *85*(2), 183–206. https://doi.org/10.1086/652373

Wagner, R. (2021a). California Highway 33 Rodent Burrow and Surface Soil Mycobiome. *Sequence Read Archive. BioProject: PRJNA736543*.

Wagner, R. (2021b). California San Joaquin Valley Air Mycobiome. *Sequence Read Archive. BioProject: PRJNA736167*.

Wagner, R. (2021c). California San Joaquin Valley Soil Mycobiome. *Sequence Read Archive. BioProject: PRJNA736519*.

Wei, X., Li, S., Yang, P., & Cheng, H. (2007). Soil erosion and vegetation succession in alpine Kobresia steppe meadow caused by plateau pika—A case study of Nagqu County, Tibet. *Chinese Geographical Science*, *17*(1), 75–81.

Weiss, S., Xu, Z. Z., Peddada, S., Amir, A., Bittinger, K., Gonzalez, A., Lozupone, C., Zaneveld, J. R., Vázquez-Baeza, Y., Birmingham, A., & others. (2017). Normalization and microbial differential abundance strategies depend upon data characteristics. *Microbiome*, *5*(1), 1–18.

West, J. S., & Kimber, R. (2015). Innovations in air sampling to detect plant pathogens. *Annals of Applied Biology*, *166*(1), 4–17.

Whitford, W. G., & Kay, F. R. (1999). Biopedturbation by mammals in deserts: A review. *Journal of Arid Environments*, *41*(2), 203–230.

Whittaker, R. H. (1972). EVOLUTION AND MEASUREMENT OF SPECIES DIVERSITY. *TAXON*, *21*(2–3), 213–251. https://doi.org/10.2307/1218190

Wickham, H. (2016). *ggplot2: Elegant Graphics for Data Analysis*. Springer-Verlag New York. https://ggplot2.tidyverse.org

Wilken, J. A., Sondermeyer, G., Shusterman, D., McNary, J., Vugia, D. J., McDowell, A., Borenstein, P., Gilliss, D., Ancock, B., Prudhomme, J., & others. (2015). Coccidioidomycosis among workers constructing solar power farms, California, USA, 2011–2014. *Emerging Infectious Diseases*, *21*(11), 1997.

Willetts, H. (1971). The survival of fungal sclerotia under adverse environmental conditions. *Biological Reviews*, *46*(3), 387–407.

Willis, A. D. (2019). Rarefaction, Alpha Diversity, and Statistics. *Frontiers in Microbiology*, *10*, 2407. https://doi.org/10.3389/fmicb.2019.02407

Woo, A. C., Brar, M. S., Chan, Y., Lau, M. C., Leung, F. C., Scott, J. A., Vrijmoed, L. L., Zawar-Reza, P., & Pointing, S. B. (2013). Temporal variation in airborne microbial populations and microbially-derived allergens in a tropical urban landscape. *Atmospheric Environment*, *74*, 291–300.

Woo, C., An, C., Xu, S., Yi, S.-M., & Yamamoto, N. (2018). Taxonomic diversity of fungi deposited from the atmosphere. *The ISME Journal*, *12*(8), 2051–2060. https://doi.org/10.1038/s41396-018-0160-7

Wyatt, T. T., Wösten, H. A., & Dijksterhuis, J. (2013). Fungal spores for dispersion in space and time. *Advances in Applied Microbiology*, *85*, 43–91.

Zhong, L., Hawkins, T., Biging, G., & Gong, P. (2011). A phenology-based approach to map crop types in the San Joaquin Valley, California. *International Journal of Remote Sensing*, *32*(22), 7777–7804.

Zinger, L., Bonin, A., Alsos, I. G., Bálint, M., Bik, H., Boyer, F., Chariton, A. A., Creer, S., Coissac, E., Deagle, B. E., & others. (2019). DNA metabarcoding—Need for robust experimental designs to draw sound ecological conclusions. In *Molecular ecology* (Vol. 28, Issue 8, pp. 1857–1862). Wiley Online Library.

Data Accessibility and Benefit-Sharing Statement

Data Accessibility: All data supporting the findings of this study have been deposited in the NCBI Sequence Read Archive (www.ncbi.nlm.nih.gov/sra) with the following accession

numbers: PRJNA736519, PRJNA736167 and PRJNA736543. All metadata, bioinformatics code and statistical code needed to replicate this study is included as supplementary material.

Benefit-Sharing: The people living in the region from which samples were collected will benefit through a better understanding of the ecological dynamics of local airborne fungal pathogens. This understanding can inform prevention and mitigation strategies regarding fungal pathogens of humans, such as *Coccidioides*, as well as fungal pathogens of crops, wild plants, and domesticated and wild animals in the region studied.

Figure Captions

Figure 1. (A) Location of sampling sites on undeveloped land (Hwy33) and agricultural land (KARE) in the San Joaquin Valley with counties labeled. Inset shows the location of labeled counties within California. (B) Principal coordinate analysis of the Bray-Curtis dissimilarity

between ITS2-identified fungal species, demarcated by land use (Hwy33 vs KARE) and sampling medium (soil vs air), which separates into three distinct groups: agricultural (KARE) soil, wild (Hwy33) soil, and air from both agricultural and wild land (KARE *and* Hwy33). (C) Hierarchically clustered mean Bray-Curtis distances derived from principal coordinates between each pair of individual sites and sampling mediums. Distances were greatest between KARE and Hwy33 soils, and between soil and air samples, and least when comparing between only air samples. Air samples from both land uses were more similar to soils from Hwy33 than soils from KARE. Black boxes indicate comparisons between soil and air at the same site, and between air at KARE and air at each Hwy33 site.

Figure 2. Effect of geographic distance and temporal distance on the composition of fungal communities. Relationships are between Bray-Curtis dissimilarity in air (A, B) and soil (C, D) samples. Temporal distance showed a stronger annual pattern in air (A) than in soils (C), while geographic distance (and land-use change) showed little difference across air samples (B). Likewise, geographic distance among Hwy33 air samples was small compared to moderate differences between soil samples (D). r = Mantel statistic. r^2 = linear model coefficient of determination. The linear model for Hwy33 air and KARE air (A) both use a 2nd order polynomial, and the reported slope is the initial rate of change. Geographic distance decay between soils (D) excludes KARE because of differences in sampling methods between land use types. Mantel $p < 0.001$ in all cases. Points jittered up to ±3 units on the x-axis for visibility. Note: x-axis range differs between panels.

Figure 3. Mean proportional abundance of fungal guilds as a function of month, site and sampling medium. All guilds assigned to multi-guild taxa were counted. Only guilds representing at least 1% of the community across all samples were included. Only Funguild version 1.1 “Probable” and “Highly Probable” guild assignments were used. Note that November and December (2017) precede January – October (2018) for Hwy33.

Figure 4. Mean proportional abundance of the top 30 most abundant genera, among all genera, as a function of month, site and sampling medium. Values are means between replicates, and across years (for KARE samples). unidentified = all pooled genera matching an unidentified reference sequence. unspecified = sequences binned into a taxonomic level without a reference sequence. Note that November and December (2017) precede January – October (2018) for Hwy33.

Table 1. PERMANOVA coefficient table for the Bray-Curtis dissimilarity among samples as a function of land use, site, year, month and sampling medium and the interactions between them in a fully nested model (adonis2 function). Permutations = 1000 (unstratified). n = 1002. df = degrees of freedom. F = pseudo F-ratio (Anderson, 2001). Note: very low p-values are likely a result of greatly increased sensitivity due to high replication (van der Laan et al., 2010), whereas r^2 and F values can better differentiate between important and trivial independent variables.

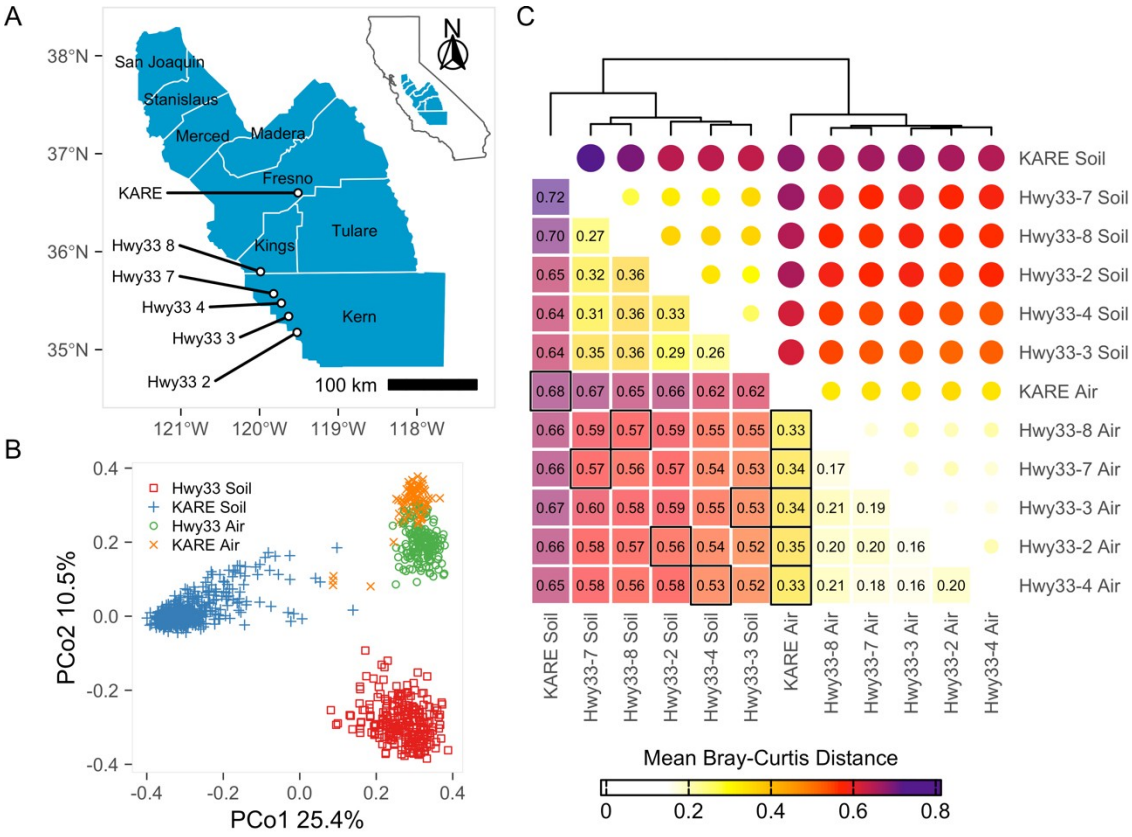

Figure 1. (A) Location of sampling sites on undeveloped land (Hwy33) and agricultural land (KARE) in the San Joaquin Valley with counties labeled. Inset shows the location of labeled counties within California. (B) Principal coordinate analysis of the Bray-Curtis dissimilarity between ITS2-identified fungal species, demarcated by land use (Hwy33 vs KARE) and sampling medium (soil vs air), which separates into three distinct groups: agricultural (KARE) soil, wild (Hwy33) soil, and air from both agricultural and wild land (KARE *and* Hwy33). (C) Hierarchically clustered mean Bray-Curtis distances derived from principal coordinates between each pair of individual sites and sampling mediums. Distances were greatest between KARE and Hwy33 soils, and between soil and air samples, and least when comparing between only air samples. Air samples from both land uses were more similar to soils from Hwy33 than soils from KARE. Black boxes indicate comparisons between soil and air at the same site, and between air at KARE and air at each Hwy33 site.

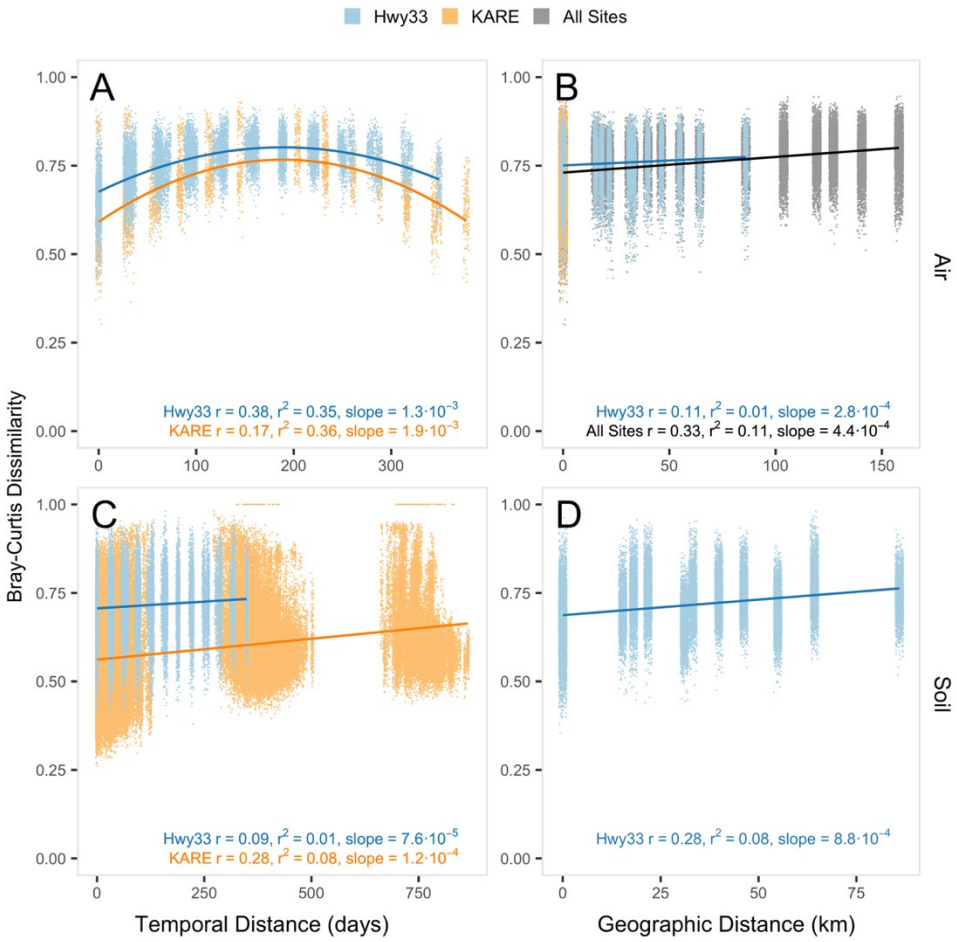

Figure 2. Effect of geographic distance and temporal distance on the composition of fungal communities. Relationships are between Bray-Curtis dissimilarity in air (A, B) and soil (C, D) samples. Temporal distance showed a stronger annual pattern in air (A) than in soils (C), while geographic distance (and land-use change) showed little difference across air samples (B). Likewise, geographic distance among Hwy33 air samples was small compared to moderate differences between soil samples (D). r = Mantel statistic. r^2 = linear model coefficient of determination. The linear model for Hwy33 air and KARE air (A) both use a 2nd order polynomial, and the reported slope is the initial rate of change. Geographic distance decay between soils (D) excludes KARE because of differences in sampling methods between land use types. Mantel $p < 0.001$ in all cases. Points jittered up to ±3 units on the x-axis for visibility. Note: x-axis range differs between panels.

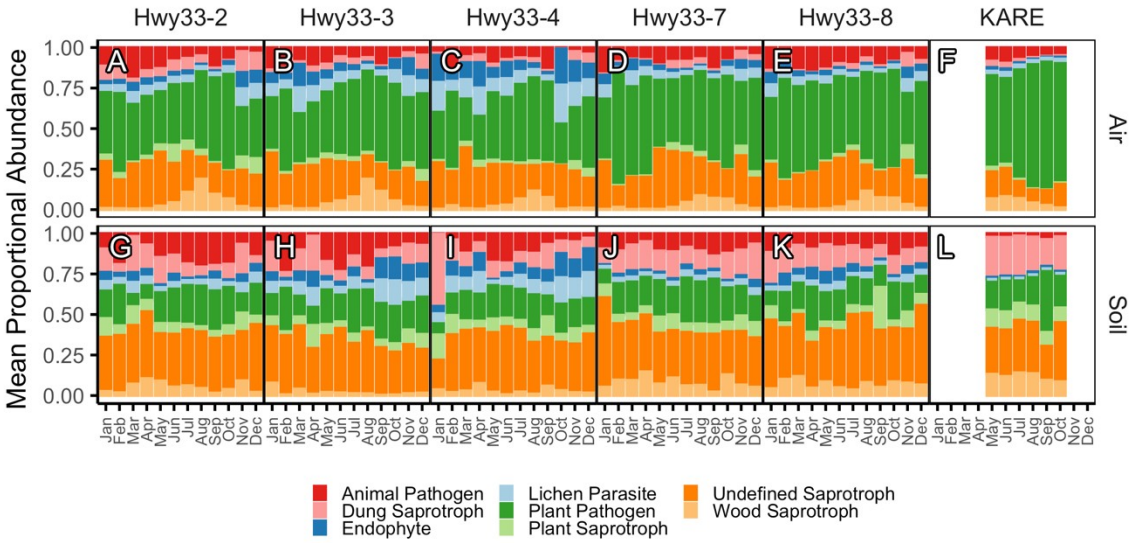

Figure 3. Mean proportional abundance of fungal guilds as a function of month, site and sampling medium. All guilds assigned to multi-guild taxa were counted. Only guilds representing at least 1% of the community across all samples were included. Only Funguild version 1.1 "Probable" and "Highly Probable" guild assignments were used. Note that November and December (2017) precede January – October (2018) for Hwy33.

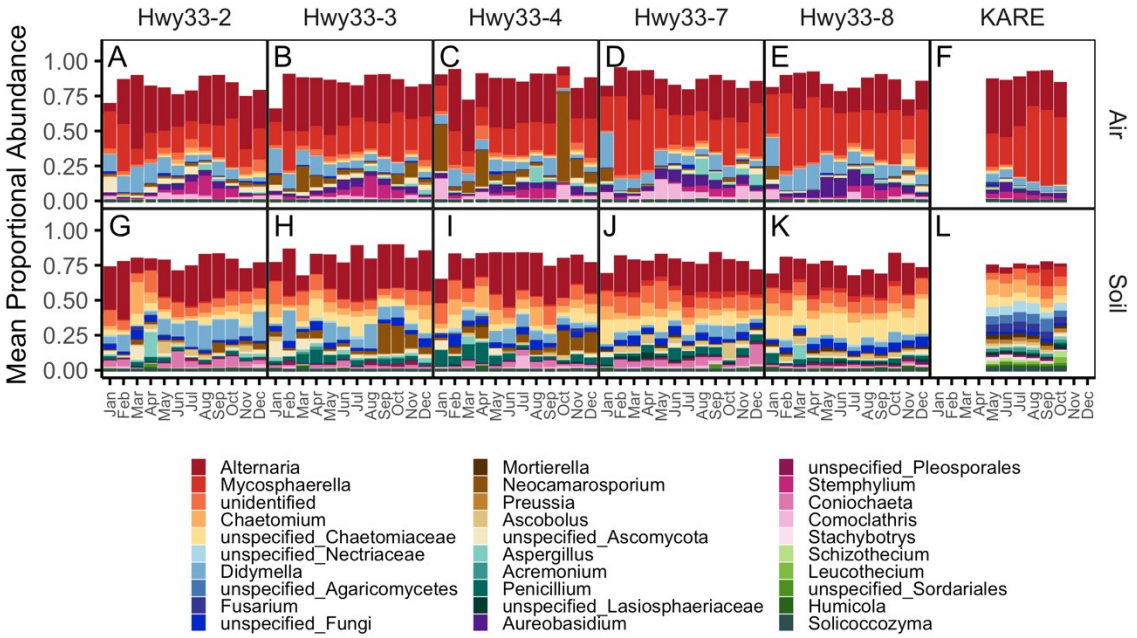

Figure 4. Mean proportional abundance of the top 30 most abundant genera, among all genera, as a function of month, site and sampling medium. Values are means between replicates, and across years (for KARE samples). unidentified = all pooled genera matching an unidentified reference sequence. unspecified = sequences binned into a taxonomic level without a reference sequence. Note that November and December (2017) precede January – October (2018) for Hwy33.

Table 1. PERMANOVA coefficient table for the Bray-Curtis dissimilarity among samples as a function of land use, site, year, month and sampling medium and the interactions between them in a fully nested model (adonis2 function). Permutations = 1000 (unstratified). n = 1002. df = degrees of freedom. F = pseudo F-ratio (Anderson, 2001). Note: very low p-values are likely a result of greatly increased sensitivity due to high replication (van der Laan et al., 2010), whereas r^2 and F values can differentiate between important and trivial independent variables.

Model (adonis2 function):
~ Land Use + Site + Year + Month + Medium + Medium*Land Use/Site/Year/Month

	df	Sum of Squares	r^2	F	p value
Land Use	1	64.74	0.18	381.06	0.001
Site	4	7.73	0.02	11.38	0.001
Year	1	12.08	0.03	71.11	0.001
Month	11	17.6	0.05	9.42	0.001
Medium	1	35.95	0.10	211.58	0.001
Land Use : Medium	1	15.56	0.04	91.58	0.001
Land Use : Site : Medium	4	4.62	0.01	6.79	0.001
Land Use : Site : Year : Medium	10	5.15	0.01	3.03	0.001
Land Use : Site : Year : Month : Medium	104	41.56	0.12	2.35	0.001
Residual	864	146.79	0.42		
Total	1001	351.78	1.00		

Supplemental Information for:

The air mycobiome is decoupled from the soil mycobiome in the California San Joaquin Valley

Robert Wagner, Liliam Montoya, Cheng Gao, Jennifer R. Head, Justin Remais, John W. Taylor

Figure S1. Photograph of settled dust sampler used to sample the air mycobiome in the San Joaquin Valley. The sampler rests atop a polyvinylchloride pipe that is slipped over and secured to a reinforcing rod driven into the ground so that the sampler is 50cm above the soil surface. A plastic cone was affixed to the top of the sampler to prevent precipitation from impacting the open petri dish within. The sides of the sampler were open to ambient air to allow dust carried on air currents to passively settle on the petri dish. Vertical deposition during periods of still air may have been inhibited.

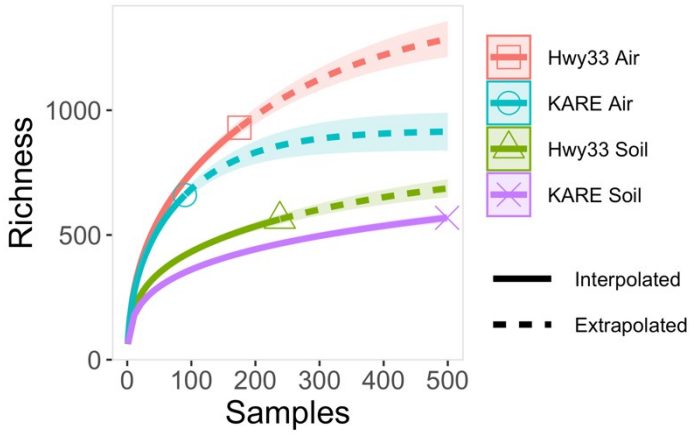

Figure S2. Species richness as a function of sampling effort across all sites. Points and interpolated lines represent actual sampling effort. Extrapolated lines estimate species richness at higher potential sampling efforts. Shaded regions = 95% confidence interval derived from a bootstrap estimate of variance with 1000 replications.

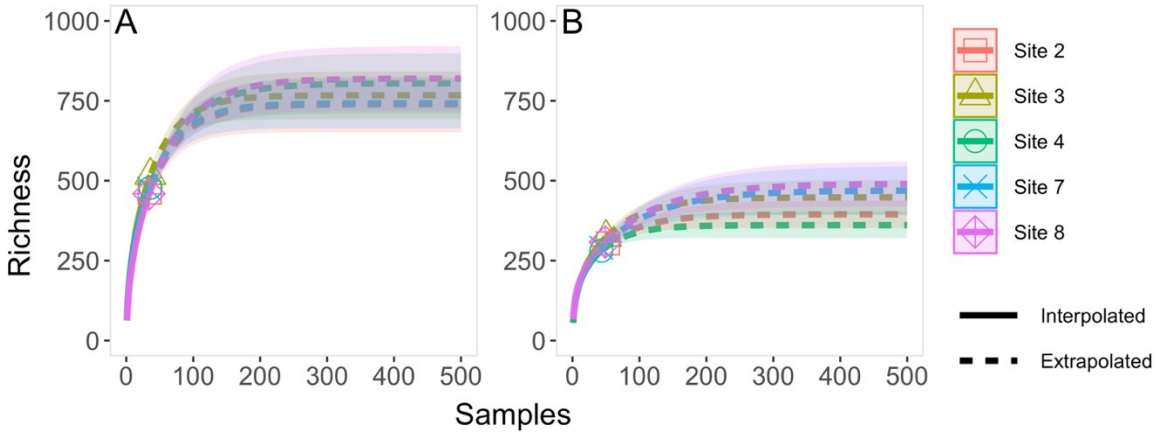

Figure S3. Species richness as a function of sampling effort at Hwy33 sites for air and settled dust samplers (A) and rodent burrow soils (B). Points and interpolated lines represent actual sampling effort. Extrapolated lines estimate species richness at higher potential sampling efforts. Shaded regions = 95% confidence interval derived from a bootstrap estimate of variance with 1000 replications.

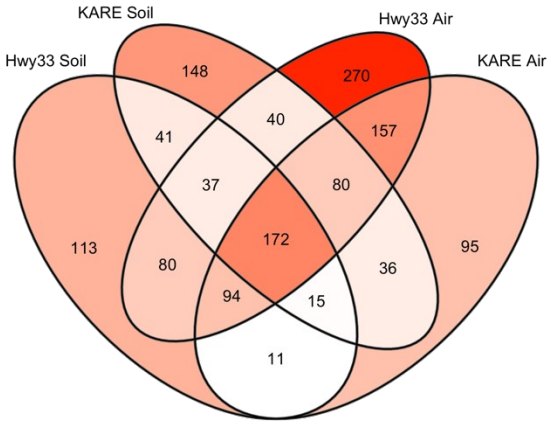

Figure S4. Venn diagram showing the number of species unique to, and shared between, each land use type (Hwy33 vs KARE) and sampling medium (soil vs air) combination.

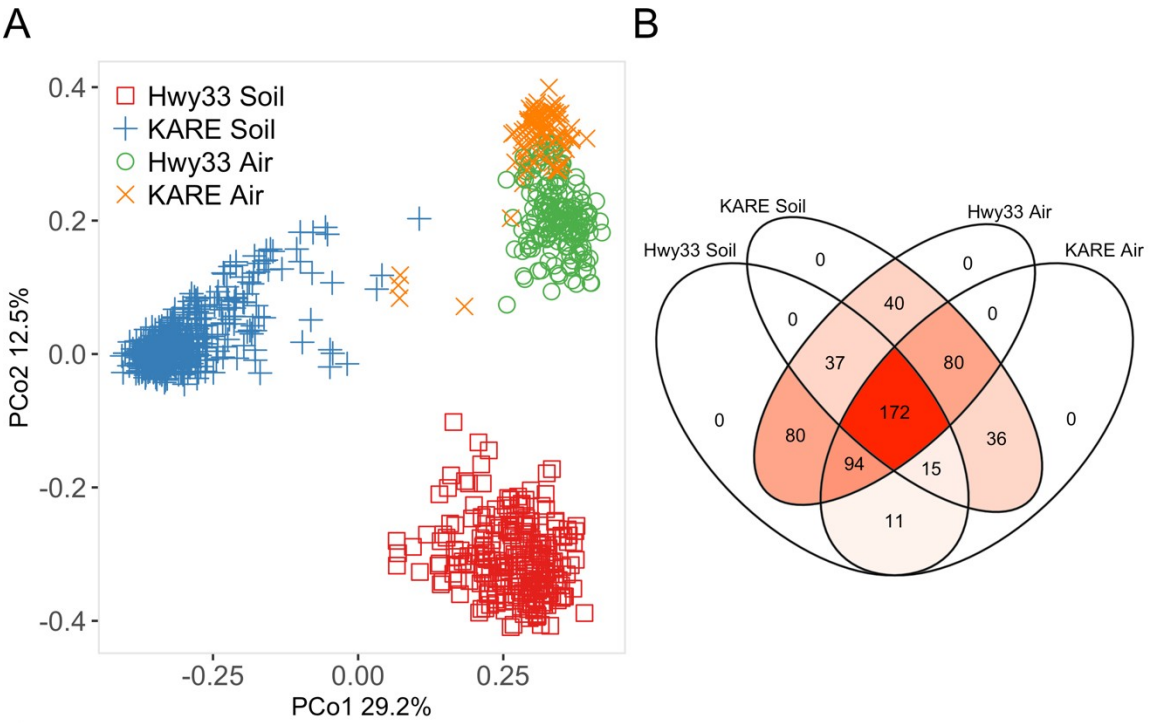

C

	Df	SumOfSqs	r^2	F	p
Land Use	1	69.9	0.21	497.54	0.001
Site	4	7.56	0.02	13.46	0.001
Year	1	11.43	0.03	81.37	0.001
Month	11	17.69	0.05	11.44	0.001
Medium	1	40.67	0.12	289.45	0.001
Land Use : Medium	1	15.8	0.05	112.46	0.001
Land Use : Site : Medium	4	4.16	0.01	7.4	0.001
Land Use : Site : Year : Medium	10	4.69	0.01	3.34	0.001
Land Use : Site : Year : Month : Medium	104	36.78	0.11	2.52	0.001
Residual	863	121.25	0.37		
Total	1000	329.93	1		

Figure S5. Principal coordinate analysis limited to species found in both air and soil samples, which separates into the same three groups as the full dataset: agricultural (KARE) soil, undeveloped (Hwy33) soil, and air from both agricultural and undeveloped land (KARE and Hwy33) (A). Venn diagram showing the number of species unique to, and shared between, each land-use and sampling medium combination (B). Nested PERMANOVA coefficient table (C).

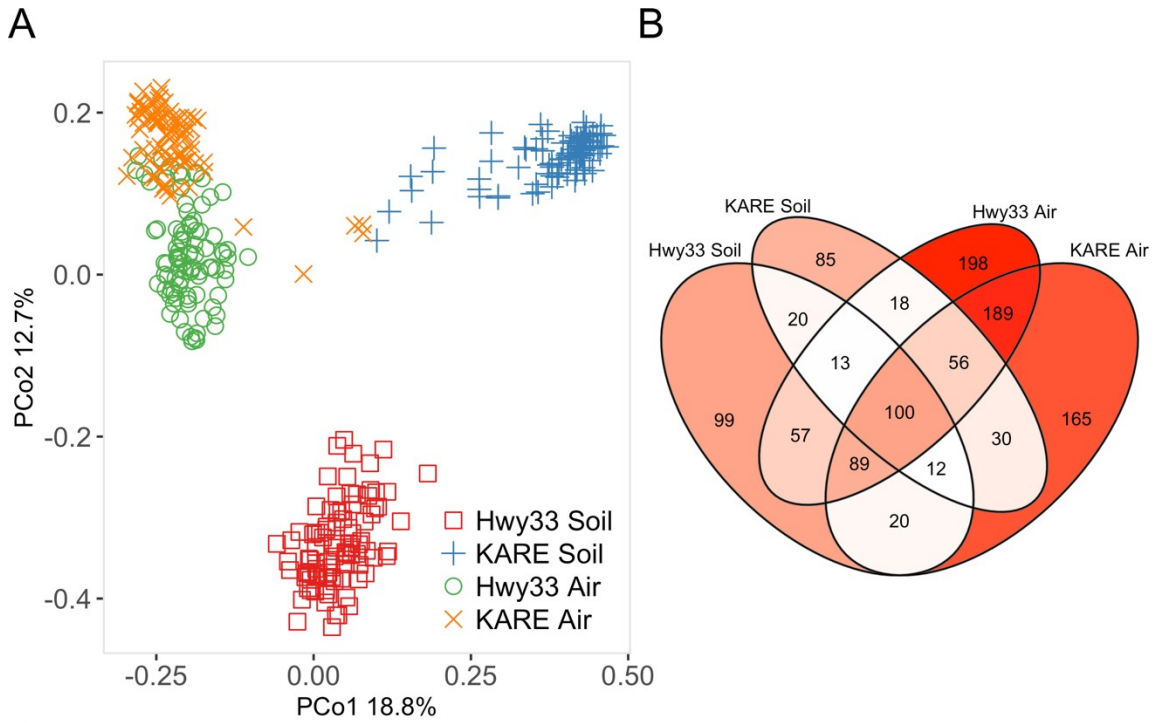

C

	Df	SumOfSqs	r^2	F	p
Land Use	1	11.82	0.1	73.25	0.001
Site	4	3.23	0.03	5	0.001
Year	1	6.57	0.06	40.72	0.001
Month	11	10.3	0.09	5.8	0.001
Medium	1	13.3	0.11	82.38	0.001
Land Use : Medium	1	6.03	0.05	37.36	0.001
Land Use : Site : Medium	4	2.22	0.02	3.44	0.001
Land Use : Site : Year : Medium	10	3.61	0.03	2.24	0.001
Land Use : Site : Year : Month : Medium	82	22.37	0.19	1.69	0.001
Residual	244	39.39	0.33		
Total	359	118.85	1		

Figure S6. Principal coordinate analysis after balancing the number of samples from the four combinations of land-use and sampling medium (Hwy33 Soil, Hwy33 Air, KARE Soil, KARE Air) by randomly selecting 90 samples from the abundantly sampled groups to match the lower number from KARE Air. (A). Venn diagram showing the number of species unique to, and shared between, each land-use and sampling medium combination (B). Nested PERMANOVA coefficient table (C).

A

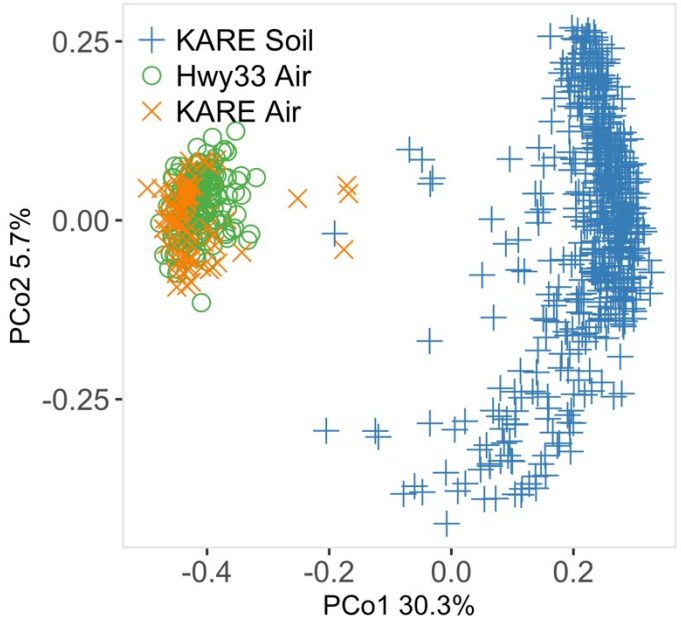

B

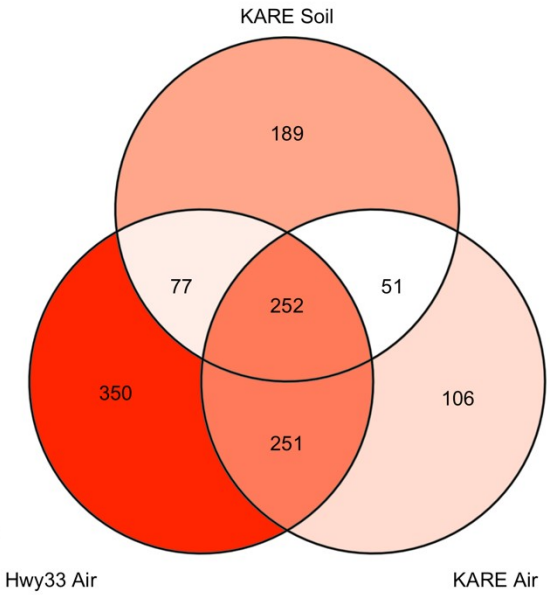

C

	Df	SumOfSqs	r^2	F	p
Land Use	1	41.7	0.17	253.85	0.001
Site	4	2.51	0.01	3.81	0.001
Year	1	12.78	0.05	77.8	0.001
Month	11	19.82	0.08	10.97	0.001
Medium	1	25.81	0.11	157.11	0.001
Land Use : Site : Year : Medium	5	2.81	0.01	3.43	0.001
Land Use : Site : Year : Month : Medium	54	23.96	0.1	2.7	0.001
Residual	686	112.69	0.47		
Total	763	242.08	1		

Figure S7. Principal coordinate analysis after removing all Hwy33 soil samples from the analysis, leaving only three combinations of land-use and sampling medium (KARE Soil, Hwy33 Air and KARE Air) (A). Venn diagram showing the number of species unique to, and shared between, each land-use and sampling medium combination (B). Nested PERMANOVA coefficient table (C).

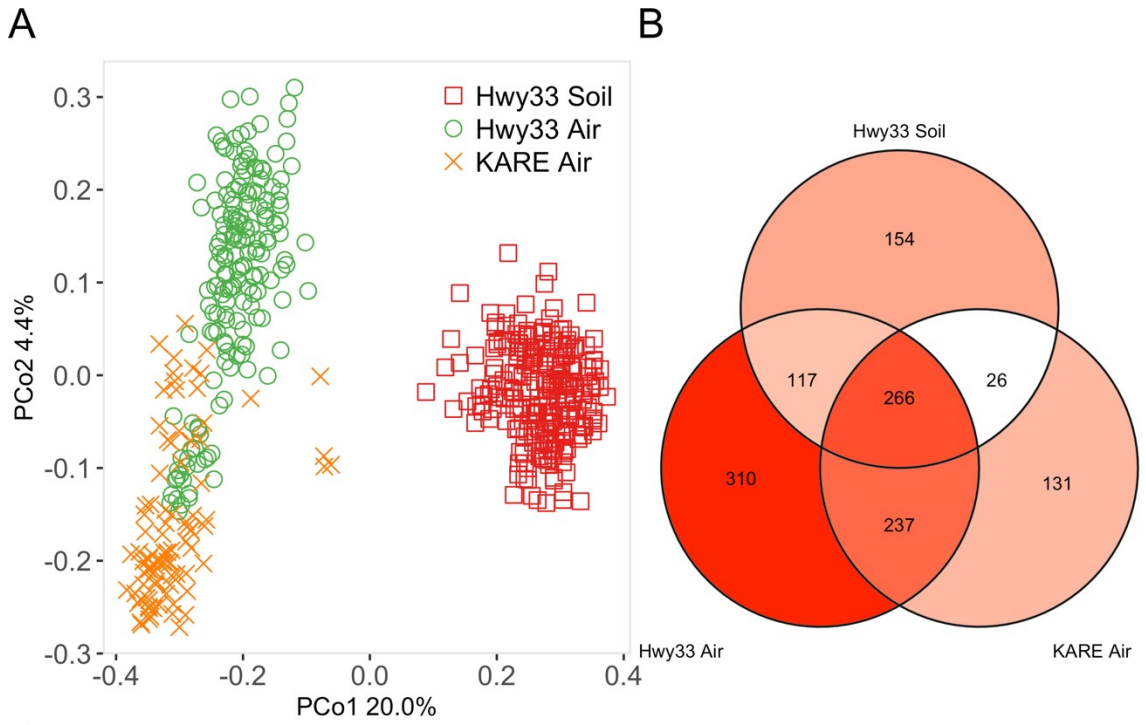

C

	Df	SumOfSqs	r^2	F	p
Land Use	1	13.9	0.08	70.19	0.001
Site	4	7.79	0.04	9.84	0.001
Year	1	2.27	0.01	11.48	0.001
Month	11	10.63	0.06	4.88	0.001
Medium	1	24.12	0.14	121.81	0.001
Land Use : Site : Medium	4	4.71	0.03	5.94	0.001
Land Use : Site : Year : Medium	9	3.53	0.02	1.98	0.001
Land Use : Site : Year : Month : Medium	95	33.98	0.19	1.81	0.001
Residual	376	74.47	0.42		
Total	502	175.39	1		

Figure S8. Principal coordinate analysis after removing all KARE soil samples from the analysis, leaving only three combinations of land-use and sampling medium (Hwy33 Soil, Hwy33 Air and KARE Air) (A). Venn diagram showing the number of species unique to, and shared between, each land-use and sampling medium combination (B). Nested PERMANOVA coefficient table (C).

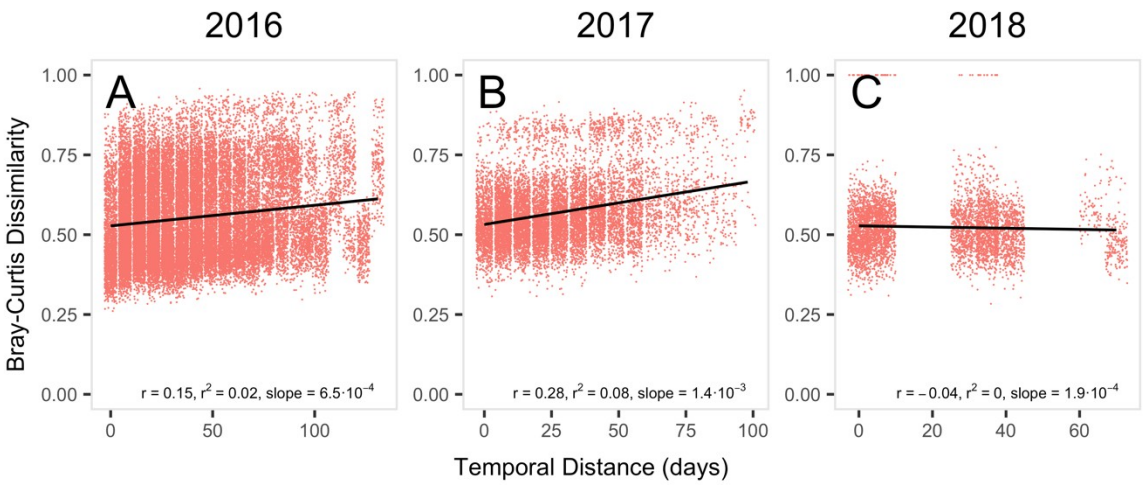

Figure S9. Bray-Curtis dissimilarity as a function of temporal distance (days) at KARE in 2016 (A), 2017 (B) and 2018 (C). Significant relationships were present in 2016 and 2017 but not in 2018. Mantel p = 0.001 in 2016 and 2017. Mantel p = 0.7 in 2018. n = 254 in 2016, 147 in 2017 and 98 in 2018. r = Mantel statistic. r^2 = linear model coefficient of determination. Slopes differed significantly between all pairs of years ($p < 0.001$). Points jittered up to ±3 units on the x-axis for visibility. Note: x-axis range differs between panels.

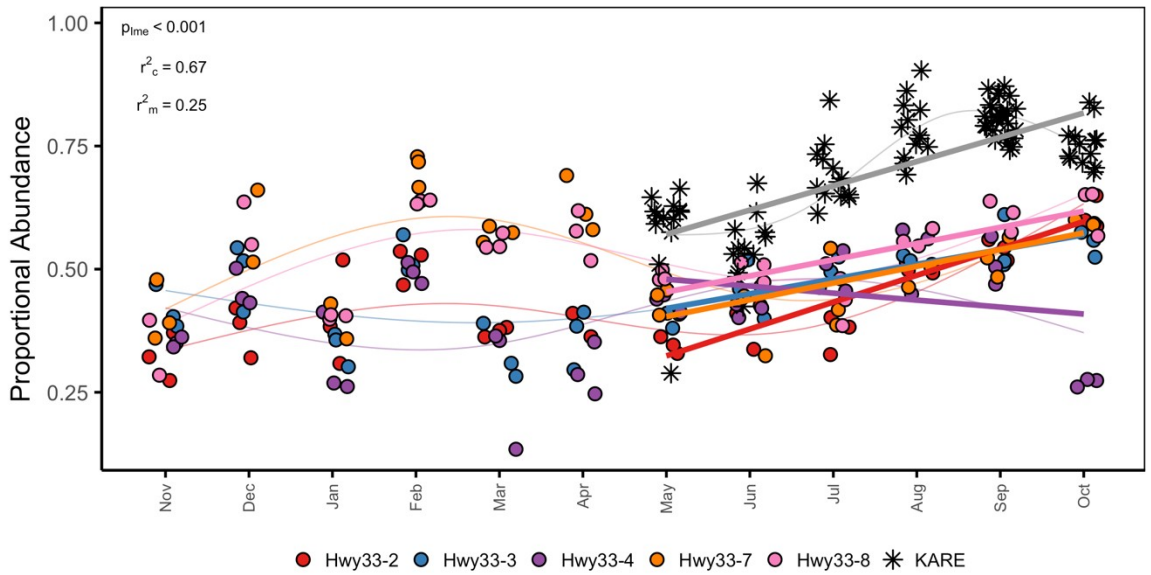

Figure S10. Proportional abundance of airborne taxa assigned to the Plant Pathogen functional guild as a function of month and site. For settled dust samples collected from May through October (n = 180), a linear mixed effects model was calculated with month as a fixed effect and site as a random effect. P_{lme} = p-value obtained from log-likelihood test between full model (site and month) and null model (excluding month). r^2_c = conditional r^2 (fixed effect [month] + random effect [site]). r^2_m = marginal r^2 (only random effect [site]). Thick lines = linear regression lines for each site from May through October. Thin lines = natural cubic spline regressions (3 degrees of freedom) for each site. Note: x-axis is from November 2017 through October 2018. Points represent individual settled dust samples and are jittered on the x-axis for clarity.

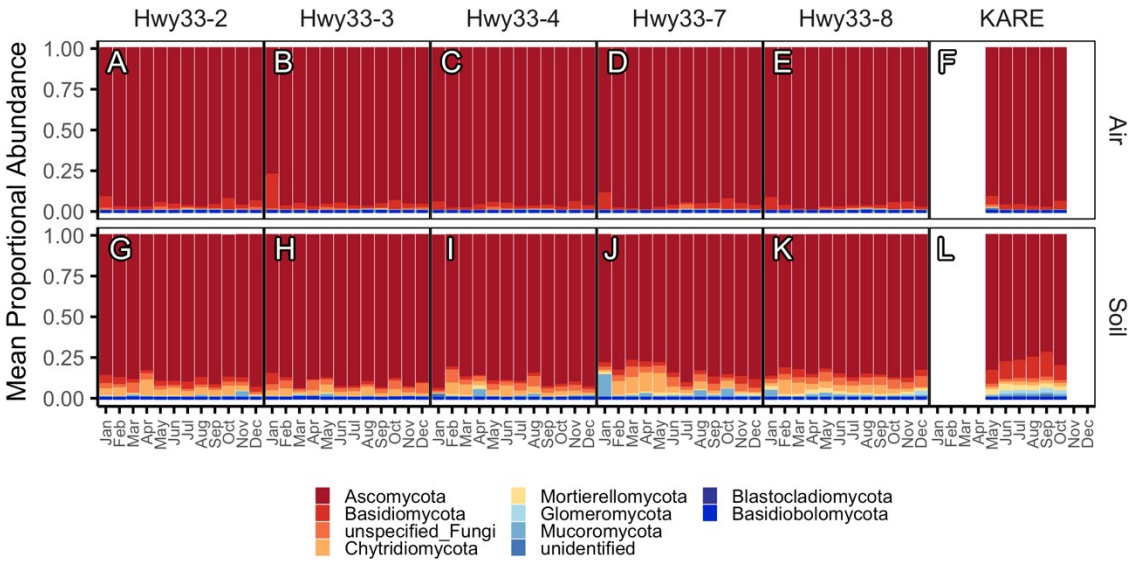

Figure S11. Mean proportional abundance of the top 10 most abundant phyla, among all phyla, as a function of month, site and sampling medium. Values are means between replicates, and across years (for KARE samples). unidentified = all pooled phyla matching unidentified reference sequences. unspecified = sequences binned into a taxonomic level without a reference sequence. Note that November and December (2017) precede January – October (2018) for Hwy33.

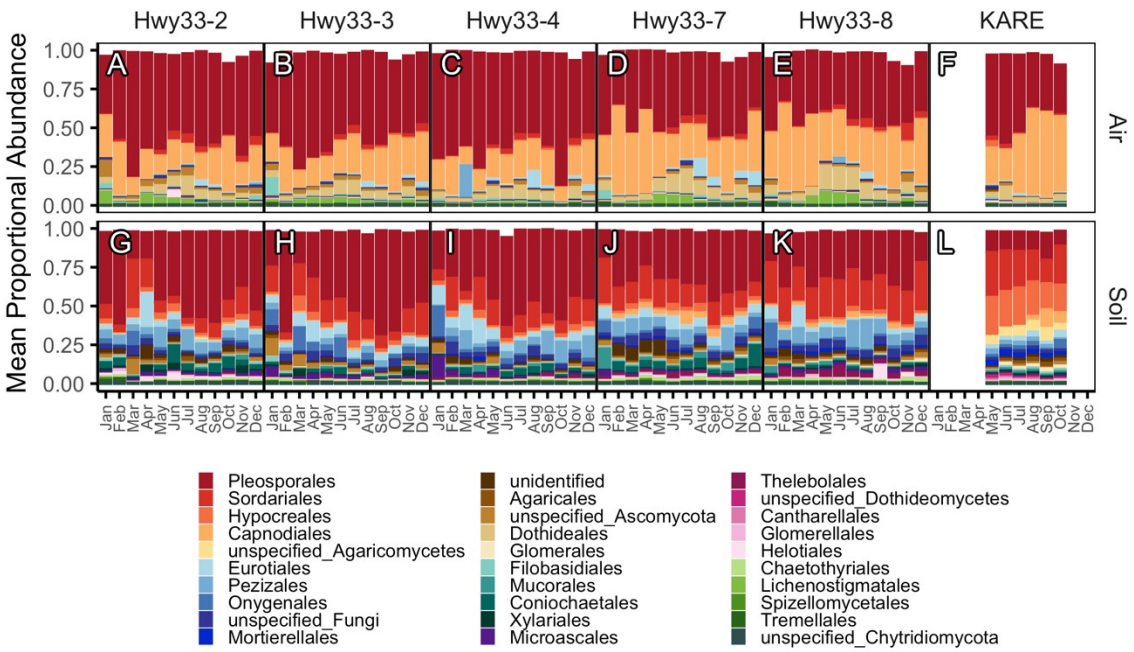

Figure S12. Mean proportional abundance of the top 30 most abundant orders, among all orders, as a function of month, site and sampling medium from ITS2 sequences. Values are means between replicates, and across years (for KARE samples). unidentified = all pooled orders matching unidentified reference sequences. unspecified = sequences binned into a taxonomic level without a reference sequence. Note that November and December (2017) precede January – October (2018) for Hwy33.

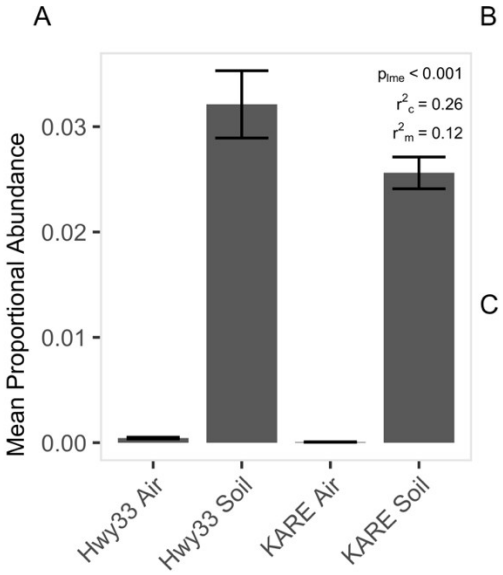

	mean	sd	sem	n
Hwy33 Air	0.00044	0.00116	0.00009	175
Hwy33 Soil	0.03211	0.04924	0.00319	238
KARE Air	0.00006	0.00016	0.00002	90
KARE Soil	0.02561	0.03373	0.00151	500

	Estimate	df	t	p
Hwy33 Air - Hwy33 Soil	−0.033	993.577	−10.064	<0.001
Hwy33 Air - KARE Air	−0.007	996.572	−1.589	0.385
Hwy33 Air - KARE Soil	−0.032	959.467	−9.387	<0.001
Hwy33 Soil - KARE Air	0.026	993.843	5.957	<0.001
Hwy33 Soil - KARE Soil	0.001	935.139	0.449	0.97
KARE Air - KARE Soil	−0.025	992.468	−6.407	<0.001

Figure S13. Mean proportional abundance of Onygenales genera as a function of land use (Hwy33 vs KARE) and sampling medium (soil vs air) (A, B). A linear mixed effects model was calculated with a factor combining land use and sampling medium “site-medium” (Hwy33 Air, KARE Soil, etc.) as a fixed effect and sampling month as a random effect. P_{lme} = p-value obtained from log-likelihood test between full model (site-medium and month) and null model (excluding site-medium). r^2_c = conditional r^2 (fixed effect[site-medium] + random effect [month]). r^2_m = marginal r^2 (only random effect [month]). Error bars = SEM. Pairwise comparison of individual factor levels obtained from the mixed effects model (C).

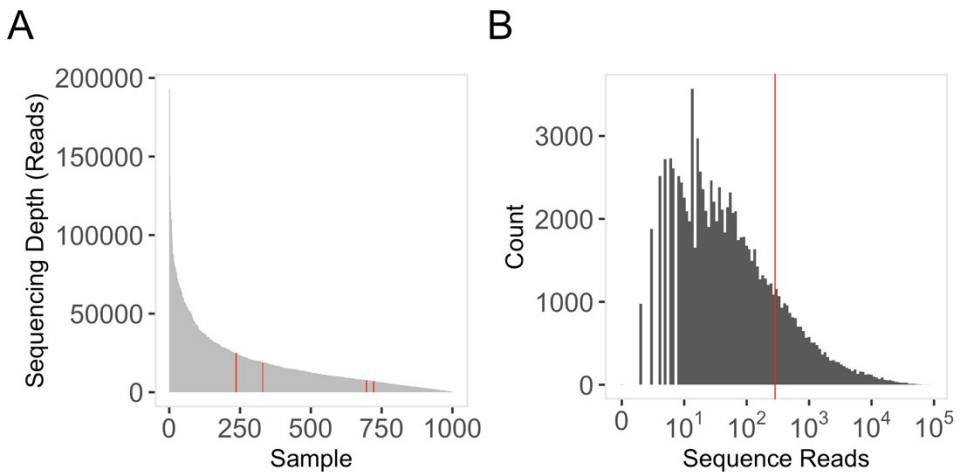

Figure S14. Sequencing depth as a function of sample, ordered from highest to lowest, with samples where *Coccidioides* was detected in red (A). Distribution of total sequence reads assigned to each species across all samples on a logarithmic scale. Vertical red bar indicates the position of *Coccidioides* reads in the distribution (B).

Table S1. The current study (yellow, bold text) and publications investigating the outdoor air mycobiome *with* the soil mycobiome (tan) and the outdoor air mycobiome *without* the soil mycobiome (blue) using high-throughput sequencing methods. In some cases, elevation and sampler height values were estimated based on methods and site descriptions. This list is extensive, though not necessarily exhaustive.

Study	Air Samples	Soil Samples	Location	Sampling Method	Elevation	Sampler Height	DNA Region	Sequencer
Current Study	**265**	**737**	**California**	**Deposition**	**103m - 361m**	**0.5m**	**ITS2**	**Illumina Miseq**
(Schiro et al., 2022)*	12	87	Arizona	Impaction	600m - 1400m	0m - 0.05m	ITS1	Illumina Miseq
(Abrego et al., 2020)	90	90	Finland	Impaction	7m - 100m	0m	ITS2	Illumina Miseq
(Abrego et al., 2018)	134	35	Finland	Impaction	0m - 126m	0m - 10m	ITS1, ITS2	Roche 454
(Kivlin et al., 2014)	25 - 40	63	California	Filtration	520m - 1680m	7m	18s	Roche 454
(Redondo et al., 2022)	322	-	Sweden	Deposition	15m - 50m	1.5m	ITS2	PacBio SMRT
(Niu et al., 2021)	11	-	Tianjin	Impaction	6m	21m	ITS1	Illumina HiSeq
(Sánchez-Parra et al., 2021)	15	-	Spain	Impaction	1000m	1.5m - 1000m	ITS1, ITS2	Illumina Miseq
(Redondo et al., 2020)	1157	-	Sweden	Deposition, Impaction	50m - 110m	1m - 8m	ITS2	PacBio SMRT
(Núñez & Moreno, 2020)	8	-	Spain	Impaction	640m	80m - 250m	ITS1, ITS2	Illumina Miseq
(Tipton et al., 2019)	383	-	Hawaii	Filtration	3397m	Unknown	ITS1	Illumina Miseq
(Tignat-Perrier et al., 2019)	75	-	Global	Filtration	Variable	Unknown	ITS2	Illumina Miseq
(Du et al., 2018)	104	-	Beijing	Filtration	88m	30m	ITS1	Illumina Miseq
(Chen et al., 2018)	98	-	Canada	Deposition, Impaction	20 - 60m	0m - 1.2m	ITS1, ITS2	Roche 454
(Cáliz et al., 2018)	150	-	Spain	Deposition, Filtration	1800m	Unknown	18s	Illumina Miseq
(Woo et al., 2018)	58	-	South Korea	Deposition, Filtration	109m	20m	ITS1	Illumina Miseq
(Castaño et al., 2017)	64	-	Spain	Deposition	670m	30cm	ITS2	Illumina Miseq
(Nicolaisen et al., 2017)	193	-	Europe	Impaction	9m - 130m	10m - 15m	ITS1	Roche 454
(Yan et al., 2016)	81	-	Beijing	Impaction	51m	8m	ITS1	Illumina Miseq
(Barberán et al., 2015)	1289	-	United States	Deposition	Variable	2m - Unknown	ITS1	Illumina Miseq, HiSeq
(Womack et al., 2015)	4	-	Amazonia	Impaction	67m	48m	D1/D2 LSU	Illumina Miseq, HiSeq
(Peay & Bruns, 2014)	178	-	California	Deposition	64m	Unknown	ITS1, ITS2	Roche 454
(Adams et al., 2013)	84	-	United States	Deposition	Unknown	Unknown	ITS1	Roche 454
(Yamamoto et al., 2012)	20	-	Connecticut	Filtration	12m	22m	ITS1, ITS2	Roche 454
(Fröhlich-Nowoisky et al., 2012)	136	-	Global	Variable	Variable	Variable	ITS1, ITS2	ABI Prism 3xxx
(Frohlich-Nowoisky et al.,	42	-	Germany	Filtration, Impaction	127m	16m	ITS1, 18s	ABI Prism 3xxx

2009)								
(Bowers et al., 2009)	11	-	Colorado	Filtration	3200m	4m	18s	ABI Prism 3xxx
(Fierer et al., 2008)	5	-	Colorado	Impaction	1660m	1.5m	18s	ABI Prism 3730

*Sampling was from dust generated by artificially disturbing the soil surface.

Table S2. Site latitude and longitude in decimal degrees and distance from California Highway 33 (Hwy33 sites).

Site	Latitude	Longitude	Distance from highway (Hwy33)
Hwy33 2	35.176195	-119.52282	56m
Hwy33 3	35.339717	-119.63083	90m
Hwy33 4	35.474297	-119.72277	147m
Hwy33 7	35.570672	-119.82144	515m
Hwy33 8	35.795795	-119.98771	80m
KARE	36.600289	-119.51099	NA

Table S3. Species richness as a function of sampling effort. Richness estimates were calculated in iNEXT at 500 samples. 95% confidence interval derived from a bootstrap estimate of variance with 1000 replications.

Site	Observed	Estimated	Std. Error	Lower 95% CI	Upper 95% CI
Hwy33 Air	930	1409.53	56.65	1298.5	1520.56
KARE Air	660	918.97	35.97	848.47	989.48
Hwy33 Soil	563	779.97	36.41	708.6	851.34
KARE Soil	569	759.3	34.37	691.93	826.66

Table S4. Species richness as a function of sampling effort for Hwy33 samples. Richness estimates were calculated in iNEXT at 500 samples. 95% confidence interval derived from a bootstrap estimate of variance with 1000 replications.

Medium	Site	Observed	Estimated	Std. Error	Lower 95% CI	Upper 95% CI
Air	Site 2	463	738.84	41.69	657.13	820.55
Air	Site 3	517	767.13	38.00	692.66	841.61
Air	Site 4	478	804.67	50.11	706.46	902.89
Air	Site 7	475	742.44	42.95	658.26	826.62
Air	Site 8	459	819.94	50.26	721.43	918.45
Soil	Site 2	304	394.88	22.47	350.85	438.91
Soil	Site 3	323	448.13	27.31	394.60	501.66
Soil	Site 4	281	361.11	21.44	319.09	403.12
Soil	Site 7	290	469.80	37.60	396.11	543.49
Soil	Site 8	308	490.68	36.97	418.21	563.14

Table S5. Pairwise PERMANOVA coefficient table for the Bray-Curtis dissimilarity among samples as a function of a factor combining land use and sampling medium (pairwiseadonis function). Permutations = 1000 (unstratified). n = 1002. F = pseudo F-ratio (Anderson, 2001). Note: very low p-values are likely a result of greatly increased sensitivity due to high replication (van der Laan et al., 2010), whereas r^2 and F values can differentiate between important and trivial independent variables.

	Sum of Squares	F	r^2	p value	Adjusted p value
KARE Soil vs Hwy33 Soil	65.28	310.8	0.30	0.001	0.006
KARE Soil vs Hwy33 Air	54.89	257.5	0.28	0.001	0.006
KARE Soil vs KARE Air	35.01	180.7	0.23	0.001	0.006
Hwy33 Soil vs Hwy33 Air	26.04	95.3	0.19	0.001	0.006
Hwy33 Soil vs KARE Air	24.38	96.1	0.23	0.001	0.006
Hwy33 Air vs KARE Air	5.89	21.6	0.08	0.001	0.006

Table S6. PERMANOVA coefficient table (*using community data rarefied to the mean sequencing depth*) for the Bray-Curtis dissimilarity among samples as a function of land use, site, year, month and sampling medium and the interactions between them in a fully nested model (adonis2 function). Permutations = 1000 (unstratified). n = 1002. df = degrees of freedom. F = pseudo F-ratio (Anderson, 2001). Note: very low p-values are likely a result of greatly increased sensitivity due to high replication (van der Laan et al., 2010), whereas r^2 and F values can better differentiate between important and trivial independent variables.

Model ~ Land Use + Site + Year + Month + Medium + Medium*Land Use/Site/Year/Month

	df	Sum of Squares	r^2	F	p value
Land Use	1	65.93	0.19	404.59	0.001
Site	4	7.57	0.02	11.61	0.001
Year	1	11.81	0.03	72.45	0.001
Month	11	17.91	0.05	9.99	0.001
Medium	1	37.06	0.11	227.41	0.001
Land Use : Medium	1	15.61	0.05	95.8	0.001
Land Use : Site : Medium	4	4.45	0.01	6.82	0.001

			0.01		
Land Use : Site : Year : Medium	10	4.98		3.05	0.001
Land Use : Site : Year : Month : Medium	104	40.37	0.12	2.38	0.001
Residual	864	140.8	0.41		
Total	1001	346.47	1		

Table S7. PERMANOVA coefficient table (*including sample sequencing depth as a predictor variable*) for the Bray-Curtis dissimilarity among samples as a function of land use, site, year, month and sampling medium and the interactions between them in a fully nested model (adonis2 function). Permutations = 1000 (unstratified). n = 1002. df = degrees of freedom. F = pseudo F-ratio (Anderson, 2001). Note: very low p-values are likely a result of greatly increased sensitivity due to high replication (van der Laan et al., 2010), whereas r^2 and F values can better differentiate between important and trivial independent variables.

Model
~ Land Use + Site + Year + Month + Medium + Sequencing Depth + Medium*Land Use/Site/Year/Month

	df	Sum of Squares	r^2	F	p value
Land Use	1	64.74	0.18	384.67	0.001
Site	4	7.73	0.02	11.48	0.001

Year	1	12.08	0.03	71.79	0.001
Month	11	17.6	0.05	9.51	0.001
Medium	1	35.95	0.1	213.59	0.001
Sequencing Depth	1	2.92	0.01	17.38	0.001
Land Use : Medium	1	14.88	0.04	88.43	0.001
Land Use : Site : Medium	4	4.62	0.01	6.87	0.001
Land Use : Site : Year : Medium	10	5.31	0.02	3.16	0.001
Land Use : Site : Year : Month : Medium	104	40.69	0.12	2.32	0.001
Residual	863	145.25	0.41		
Total	1001	351.78	1		

References

Abrego, N., Crosier, B., Somervuo, P., Ivanova, N., Abrahamyan, A., Abdi, A., Hämäläinen, K., Junninen, K., Maunula, M., & Purhonen, J. (2020).

Fungal communities decline with urbanization—More in air than in soil. *The ISME Journal*, *14*(11), 2806–2815.

Abrego, N., Norros, V., Halme, P., Somervuo, P., Ali-Kovero, H., & Ovaskainen, O. (2018). Give me a sample of air and I will tell which species are found from your region: Molecular identification of fungi from airborne spore samples. *Molecular Ecology Resources*, *18*(3), 511–524.

Adams, R. I., Miletto, M., Taylor, J. W., & Bruns, T. D. (2013). Dispersal in microbes: Fungi in indoor air are dominated by outdoor air and show dispersal limitation at short distances. *The ISME Journal*, *7*(7), 1262–1273.

Anderson, M. J. (2001). A new method for non-parametric multivariate analysis of variance. *Austral Ecology*, *26*(1), 32–46.

Barberán, A., Ladau, J., Leff, J. W., Pollard, K. S., Menninger, H. L., Dunn, R. R., & Fierer, N. (2015). Continental-scale distributions of dust-associated bacteria and fungi. *Proceedings of the National Academy of Sciences*, *112*(18), 5756–5761.

Bowers, R. M., Lauber, C. L., Wiedinmyer, C., Hamady, M., Hallar, A. G., Fall, R., Knight, R., & Fierer, N. (2009). Characterization of airborne microbial communities at a high-elevation site and their potential to act as atmospheric ice nuclei. *Applied and Environmental Microbiology*, *75*(15), 5121–5130.

Cáliz, J., Triadó-Margarit, X., Camarero, L., & Casamayor, E. O. (2018). A long-term survey unveils strong seasonal patterns in the airborne

microbiome coupled to general and regional atmospheric circulations. *Proceedings of the National Academy of Sciences*, *115*(48), 12229–12234.

Castaño, C., Oliva, J., Martinez de Aragon, J., Alday, J. G., Parladé, J., Pera, J., & Bonet, J. A. (2017). Mushroom emergence detected by combining spore trapping with molecular techniques. *Applied and Environmental Microbiology*, *83*(13), e00600-17.

Chen, W., Hambleton, S., Seifert, K. A., Carisse, O., Diarra, M. S., Peters, R. D., Lowe, C., Chapados, J. T., & Lévesque, C. A. (2018). Assessing performance of spore samplers in monitoring aeromycobiota and fungal plant pathogen diversity in Canada. *Applied and Environmental Microbiology*, *84*(9), e02601-17.

Du, P., Du, R., Ren, W., Lu, Z., Zhang, Y., & Fu, P. (2018). Variations of bacteria and fungi in PM2.5 in Beijing, China. *Atmospheric Environment*, *172*, 55–64. https://doi.org/10.1016/j.atmosenv.2017.10.048

Fierer, N., Liu, Z., Rodríguez-Hernández, M., Knight, R., Henn, M., & Hernandez, M. T. (2008). Short-term temporal variability in airborne bacterial and fungal populations. *Applied and Environmental Microbiology*, *74*(1), 200–207.

Fröhlich-Nowoisky, J., Burrows, S., Xie, Z., Engling, G., Solomon, P., Fraser, M., Mayol-Bracero, O., Artaxo, P., Begerow, D., Conrad, R., & others.

(2012). Biogeography in the air: Fungal diversity over land and oceans. *Biogeosciences*, *9*(3), 1125–1136.

Frohlich-Nowoisky, J., Pickersgill, D. A., Despres, V. R., & Poschl, U. (2009). High diversity of fungi in air particulate matter. *Proceedings of the National Academy of Sciences*, *106*(31), 12814–12819. https://doi.org/10.1073/pnas.0811003106

Kivlin, S. N., Winston, G. C., Goulden, M. L., & Treseder, K. K. (2014). Environmental filtering affects soil fungal community composition more than dispersal limitation at regional scales. *Fungal Ecology*, *12*, 14–25.

Nicolaisen, M., West, J. S., Sapkota, R., Canning, G. G., Schoen, C., & Justesen, A. F. (2017). Fungal communities including plant pathogens in near surface air are similar across northwestern Europe. *Frontiers in Microbiology*, *8*, 1729.

Niu, M., Hu, W., Cheng, B., Wu, L., Ren, L., Deng, J., Shen, F., & Fu, P. (2021). Influence of rainfall on fungal aerobiota in the urban atmosphere over Tianjin, China: A case study. *Atmospheric Environment: X*, *12*, 100137.

Núñez, A., & Moreno, D. A. (2020). The differential vertical distribution of the airborne biological particles reveals an atmospheric reservoir of microbial pathogens and aeroallergens. *Microbial Ecology*, *80*(2), 322–333.

Peay, K. G., & Bruns, T. D. (2014). Spore dispersal of basidiomycete fungi at the landscape scale is driven by stochastic and deterministic processes

and generates variability in plant–fungal interactions. *New Phytologist*, *204*(1), 180–191.

Redondo, M. A., Berlin, A., Boberg, J., & Oliva, J. (2020). Vegetation type determines spore deposition within a forest–agricultural mosaic landscape. *FEMS Microbiology Ecology*, *96*(6), fiaa082.

Redondo, M. A., Oliva, J., Elfstrand, M., Boberg, J., Capador-Barreto, H. D., Karlsson, B., & Berlin, A. (2022). Host genotype interacts with aerial spore communities and influences the needle mycobiome of Norway spruce. *Environmental Microbiology*.

Sánchez-Parra, B., Núñez, A., García, A. M., Campoy, P., & Moreno, D. A. (2021). Distribution of airborne pollen, fungi and bacteria at four altitudes using high-throughput DNA sequencing. *Atmospheric Research*, *249*, 105306.

Schiro, G., Chen, Y., Blankinship, J. C., & Barberán, A. (2022). Ride the dust: Linking dust dispersal and spatial distribution of microorganisms across an arid landscape (Accepted). *Environmental Microbiology*. https://doi.org/10.1111/1462-2920.15998

Tignat-Perrier, R., Dommergue, A., Thollot, A., Keuschnig, C., Magand, O., Vogel, T. M., & Larose, C. (2019). Global airborne microbial communities controlled by surrounding landscapes and wind conditions. *Scientific Reports*, *9*(1), 1–11.

Tipton, L., Zahn, G., Datlof, E., Kivlin, S. N., Sheridan, P., Amend, A. S., & Hynson, N. A. (2019). Fungal aerobiota are not affected by time nor

environment over a 13-y time series at the Mauna Loa Observatory. *Proceedings of the National Academy of Sciences*, *116*(51), 25728–25733.

van der Laan, M., Hsu, J.-P., Peace, K. E., & Rose, S. (2010). Statistics ready for a revolution: Next generation of statisticians must build tools for massive data sets. *AMSTAT News: The Membership Magazine of the American Statistical Association*, *399*, 38–39.

Womack, A. M., Artaxo, P., Ishida, F. Y., Mueller, R. C., Saleska, S. R., Wiedemann, K. T., Bohannan, B. J., & Green, J. L. (2015). Characterization of active and total fungal communities in the atmosphere over the Amazon rainforest. *Biogeosciences*, *12*(21), 6337–6349.

Woo, C., An, C., Xu, S., Yi, S.-M., & Yamamoto, N. (2018). Taxonomic diversity of fungi deposited from the atmosphere. *The ISME Journal*, *12*(8), 2051–2060. https://doi.org/10.1038/s41396-018-0160-7

Yamamoto, N., Bibby, K., Qian, J., Hospodsky, D., Rismani-Yazdi, H., Nazaroff, W. W., & Peccia, J. (2012). Particle-size distributions and seasonal diversity of allergenic and pathogenic fungi in outdoor air. *The ISME Journal*, *6*(10), 1801–1811.

Yan, D., Zhang, T., Su, J., Zhao, L.-L., Wang, H., Fang, X.-M., Zhang, Y.-Q., Liu, H.-Y., & Yu, L.-Y. (2016). Diversity and composition of airborne fungal community associated with particulate matters in Beijing during haze and non-haze days. *Frontiers in Microbiology*, *7*, 487.

Bioinformatics Code for:

The air mycobiome is decoupled from the soil mycobiome in the California San Joaquin Valley

Robert Wagner, Liliam Montoya, Cheng Gao, Jennifer R. Head, Justin Remais, John W. Taylor

```
# import FASTAs into artifact object (make sure to set the correct path!)
qiime tools import --type 'SampleData[PairedEndSequencesWithQuality]' --
input-path /fastq --input-format CasavaOneEightSingleLanePerSampleDirFmt
--output-path demux.qza

# generate summary
qiime demux summarize --i-data demux.qza --o-visualization demux.qzv
qiime tools view demux.qzv

# denoise with dada2 (truncate read ends)
# Forward primer = 5.8s-Fun (AACTTT...CAA.GGATC.CT)
# Reverse primer = ITS4-Fun (AGCCTCCGCTTATTGATATGCTTAA.T)
# Quality cutoff at >= 25
# (trim parameters below differ between runs but adhere to the quality
# cutoff)
qiime dada2 denoise-paired --i-demultiplexed-seqs demux.qza --p-trim-left-
f 22 --p-trunc-len-f 300 --p-trim-left-r 28 --p-trunc-len-r 258 --p-n-
threads 7 --o-representative-sequences rep-seqs-dada2.qza --o-table table-
dada2.qza --o-denoising-stats stats-dada2.qza

# generate visualization for denoise
qiime metadata tabulate --m-input-file stats-dada2.qza --o-visualization
stats-dada2.qzv
qiime tools view stats-dada2.qzv
```

```
# rename files
mv rep-seqs-dada2.qza rep-seqs.qza
mv table-dada2.qza table.qza

# import UNITE database
qiime tools import --type 'FeatureData[Sequence]' --input-path
sh_refs_qiime_ver8_97_s_02.02.2019.fasta --output-path reference.qza
qiime tools import --type 'FeatureData[Taxonomy]' --input-format
HeaderlessTSVTaxonomyFormat --input-path
sh_taxonomy_qiime_ver8_97_s_02.02.2019.txt --output-path taxonomy.qza

# train naive bayes classifier
qiime feature-classifier fit-classifier-naive-bayes --i-reference-reads
reference.qza --i-reference-taxonomy taxonomy.qza --o-classifier
classifier.qza

# run sklearn naive bayes classifier
qiime feature-classifier classify-sklearn --verbose --p-n-jobs 7 --i-
classifier classifier.qza --i-reads rep-seqs.qza --o-classification taxonomy-
output.qza

qiime metadata tabulate \
  --m-input-file taxonomy-output.qza \
  --o-visualization taxonomy-output.qzv

qiime tools view taxonomy-output.qzv

# collapse taxa table
qiime taxa collapse --i-table table.qza --i-taxonomy taxonomy-output.qza
--p-level 7 --o-collapsed-table table-collapsed.qza

# export fearture table to biom file and convert biom file to tsv
qiime tools export \
  --input-path table-collapsed.qza \
  --output-path exported-feature-table
cd exported-feature-table
biom convert -i feature-table.biom -o feature-table.tsv --to-tsv




### R code ###

# next, open the tsv file in R and make taxa tables at each taxonomic
level.

# load libraries
library(reshape2)

# load otu data
```

```
d.otus = read.table("feature-table.tsv", sep = "\t", skip = 1,
comment.char = "")

d.otus = t(d.otus)
colnames(d.otus) = d.otus[1,]
colnames(d.otus)[1] = "sample"
d.otus = d.otus[-1,]
d.otus = as.data.frame(d.otus)
d.otus = sapply(d.otus, as.numeric)
d.otus = as.data.frame(d.otus)

# melt otu data into long format
d.melt = melt(d.otus, id=c("sample"))

# remove taxa level prefix from otu names
d.melt$variable = gsub("[a-z]__", "", d.melt$variable)

# make kingdom column
function.kingdom = function(x) substr(x, 1, unlist(gregexpr(";", x))[1] -
1)
d.melt$kingdom = lapply(d.melt$variable, function.kingdom)

# make phylum column
function.phylum = function(x) substr(x, unlist(gregexpr(";", x))[1] + 1,
unlist(gregexpr(";", x))[2] - 1)
d.melt$phylum = unlist(lapply(d.melt$variable, function.phylum))

# make class column
function.class = function(x) substr(x, unlist(gregexpr(";", x))[2] + 1,
unlist(gregexpr(";", x))[3] - 1)
d.melt$class = unlist(lapply(d.melt$variable, function.class))

# make order column
function.order = function(x) substr(x, unlist(gregexpr(";", x))[3] + 1,
unlist(gregexpr(";", x))[4] - 1)
d.melt$order = unlist(lapply(d.melt$variable, function.order))

# make family column
function.family = function(x) substr(x, unlist(gregexpr(";", x))[4] + 1,
unlist(gregexpr(";", x))[5] - 1)
d.melt$family = unlist(lapply(d.melt$variable, function.family))

# make genus column
function.genus = function(x) substr(x, unlist(gregexpr(";", x))[5] + 1,
unlist(gregexpr(";", x))[6] - 1)
d.melt$genus = unlist(lapply(d.melt$variable, function.genus))

# make species column
function.species= function(x) substr(x, unlist(gregexpr(";", x))[6] + 1,
nchar(x))
d.melt$species = unlist(lapply(d.melt$variable, function.species))
```

```
# replace __ wih Unknown
d.melt[d.melt == "__"] = "unspecified"

# append "unspecified" with next highest identified taxa level
unspecified.phylum = function (x) paste("unspecified_", substr(x, 1,
unlist(gregexpr(";", x))[1]-1), sep = "")
d.melt[d.melt$phylum=="unspecified",][,5:10] =
unlist(lapply(d.melt[d.melt$phylum=="unspecified",]$variable,
unspecified.phylum))

unspecified.class = function (x) paste("unspecified_", substr(x,
unlist(gregexpr(";", x))[1]+1, unlist(gregexpr(";", x))[2]-1), sep = "")
d.melt[d.melt$class=="unspecified",][,6:10] =
unlist(lapply(d.melt[d.melt$class=="unspecified",]$variable,
unspecified.class))

unspecified.order = function (x) paste("unspecified_", substr(x,
unlist(gregexpr(";", x))[2]+1, unlist(gregexpr(";", x))[3]-1), sep = "")
d.melt[d.melt$order=="unspecified",][,7:10] =
unlist(lapply(d.melt[d.melt$order=="unspecified",]$variable,
unspecified.order))

unspecified.family = function (x) paste("unspecified_", substr(x,
unlist(gregexpr(";", x))[3]+1, unlist(gregexpr(";", x))[4]-1), sep = "")
d.melt[d.melt$family=="unspecified",][,8:10] =
unlist(lapply(d.melt[d.melt$family=="unspecified",]$variable,
unspecified.family))

unspecified.genus = function (x) paste("unspecified_", substr(x,
unlist(gregexpr(";", x))[4]+1, unlist(gregexpr(";", x))[5]-1), sep = "")
d.melt[d.melt$genus=="unspecified",][,9:10] =
unlist(lapply(d.melt[d.melt$genus=="unspecified",]$variable,
unspecified.genus))

unspecified.species = function (x) paste("unspecified_", substr(x,
unlist(gregexpr(";", x))[5]+1, unlist(gregexpr(";", x))[6]-1), sep = "")
d.melt[d.melt$species=="unspecified",][,10] =
unlist(lapply(d.melt[d.melt$species=="unspecified",]$variable,
unspecified.species))

# cast molten data at each taxonomic level
d.cast.phylum = dcast(d.melt, sample ~ phylum, sum)
d.cast.class = dcast(d.melt, sample ~ class, sum)
d.cast.order = dcast(d.melt, sample ~ order, sum)
d.cast.family = dcast(d.melt, sample ~ family, sum)
d.cast.genus = dcast(d.melt, sample ~ genus, sum)
d.cast.species = dcast(d.melt, sample ~ species, sum)
```

Statistics Code for:

The air mycobiome is decoupled from the soil mycobiome in the California San Joaquin Valley

Robert Wagner, Liliam Montoya, Cheng Gao, Jennifer R. Head, Justin Remais, John W. Taylor

```
### PCoA and PERMANOVA

# load libraries
library(vegan)
library(ape)
library(lsmeans)
library(psych)
library(data.table)

# load data
d = read.csv("d.combined.species.csv")

# remove unidentified and unspecified taxa
d = d[,-grep("unspecified", colnames(d))]
d = d[,-grep("unidentified", colnames(d))]

# remove rows containing no taxa
```

```
d = d[which(rowSums(d[,10:dim(d)[2]]) != 0),]

# load meta data
d.meta = d[,1:9]

# make data matrix
d.matrix = as.matrix(d[,10:dim(d)[2]])
# remove rare species (optional)
d.matrix.removed.rare = d.matrix[,colSums(d.matrix) > 1]
# first squareroot and wisconsin 2x transform data
d.matrix.transformed = sqrt(d.matrix.removed.rare)
d.matrix.transformed = wisconsin(d.matrix.transformed)
# next, create dissimilarity matrix with transformed data (bray-curtis)
d.dist = vegdist(d.matrix.transformed, method="bray")

# ordination (PCoA)
myPCoA = pcoa(d.dist)

# Permutational multivariate analysis of variance (PerMANOVA)
# note: Site = "Land Use", site = "Site", year = "Year", month = "Month",
type = "Medium"
adonis2(d.dist ~ Site + site + year + month + type + Site/site/year/month/
type, d.meta, parallel = 8, method = "bray", permutations = 1000)

# Permutational multivariate analysis of variance (PerMANOVA) (with
strata[or "blocks"])
# https://github.com/vegandevs/vegan/issues/427
# https://stats.stackexchange.com/questions/350462/can-you-perform-a-
permanova-analysis-on-nested-data
# https://stats.stackexchange.com/questions/188519/adonis-in-vegan-order-
of-variables-or-use-of-strata/238962#238962

perm = how(nperm = 1000)
setBlocks(perm) = with(d.meta, type)
adonis2(d.dist ~ Site + site + year + month + type + Site/site/year/month/
type, d.meta, parallel = 8, method = "bray", permutations = perm)



### Distance Decay

# load libraries
library(vegan)
library(ape)

# load data
d = read.csv("d.combined.species.csv")

# remove unidentified and unspecified taxa
d = d[,-grep("unspecified", colnames(d))]
d = d[,-grep("unidentified", colnames(d))]
```

```
# remove rows containing no taxa
d = d[which(rowSums(d[,10:dim(d)[2]]) != 0),]

# load meta data
d.meta = d[,1:9]

# make data matrix
d.matrix = as.matrix(d[,10:dim(d)[2]])
# remove rare species (optional)
d.matrix.removed.rare = d.matrix[,colSums(d.matrix) > 1]
# first squareroot and wisconsin 2x transform data
d.matrix.transformed = sqrt(d.matrix.removed.rare)
d.matrix.transformed = wisconsin(d.matrix.transformed)
# next, create dissimilarity matrix with transformed data (bray-curtis)
d.dist = vegdist(d.matrix.transformed, method="bray")

# create a dissimilarity matrix with transformed data
d.dist = vegdist(d.matrix.transformed, method="bray")
d.dist.air = vegdist(d.matrix.transformed[d.meta$type=="Air",],
method="bray")
d.dist.soil = vegdist(d.matrix.transformed[d.meta$type=="Soil",],
method="bray")
d.dist.hwy33.air = vegdist(d.matrix.transformed[d.meta$site!="KARE" &
d.meta$type=="Air",], method="bray")
d.dist.hwy33.soil = vegdist(d.matrix.transformed[d.meta$site!="KARE" &
d.meta$type=="Soil",], method="bray")
d.dist.kare.air = vegdist(d.matrix.transformed[d.meta$site=="KARE" &
d.meta$type=="Air",], method="bray")
d.dist.kare.soil = vegdist(d.matrix.transformed[d.meta$site=="KARE" &
d.meta$type=="Soil",], method="bray")

# make another site and type factor for all sites
d.meta$sitetype2 = as.factor(paste(d.meta$site, d.meta$type, sep = "-"))

# create latitude and longitude table by site
d.lat.long =
read.csv("/Users/user/Desktop/Cocci2020/data.meta/sites.lat.long.csv")
d.lat.long[d.lat.long$site!="KARE",]$site = paste("Hwy33-",
d.lat.long[d.lat.long$site!="KARE",]$site, sep = "")

d.geo = d.lat.long[match(d.meta$site, d.lat.long$site),]

# create euclidean distance matrix
d.dist.geo = vegdist(d.geo[,2:3], method="euclidean")*111
d.dist.geo.air = vegdist(d.geo[d.meta$type=="Air",2:3],
method="euclidean")*111
d.dist.geo.soil = vegdist(d.geo[d.meta$type=="Soil",2:3],
method="euclidean")*111
d.dist.geo.hwy33.air = vegdist(d.geo[d.meta$site!="KARE" &
d.meta$type=="Air",2:3], method="euclidean")*111
```

```
d.dist.geo.hwy33.soil = vegdist(d.geo[d.meta$site!="KARE" &
d.meta$type=="Soil",2:3], method="euclidean")*111
d.dist.geo.kare.air = vegdist(d.geo[d.meta$site=="KARE" &
d.meta$type=="Air",2:3], method="euclidean")*111
d.dist.geo.kare.soil = vegdist(d.geo[d.meta$site=="KARE" &
d.meta$type=="Soil",2:3], method="euclidean")*111

# create a vector of julian dates
d.meta$date = paste(d.meta$year, d.meta$month, d.meta$day, sep = "-")
date.samples = strptime(d.meta$date, "%Y-%B-%e")
d.time = as.integer(round(julian(date.samples), 0))

# create a temporal (euclidean) distance matrix from julian dates
d.dist.time = vegdist(d.time, method="euclidean")
d.dist.time.air = vegdist(d.time[d.meta$type=="Air"], method="euclidean")
d.dist.time.soil = vegdist(d.time[d.meta$type=="Soil"],
method="euclidean")
d.dist.time.hwy33.air = vegdist(d.time[d.meta$site!="KARE" &
d.meta$type=="Air"], method="euclidean")
d.dist.time.hwy33.soil = vegdist(d.time[d.meta$site!="KARE" &
d.meta$type=="Soil"], method="euclidean")
d.dist.time.kare.air = vegdist(d.time[d.meta$site=="KARE" &
d.meta$type=="Air"], method="euclidean")
d.dist.time.kare.soil = vegdist(d.time[d.meta$site=="KARE" &
d.meta$type=="Soil"], method="euclidean")



# air

# fit linear models for dist ~ time for air hwy33, air KARE and both
combined
fit.time.air.hwy33 = lm(d.dist.hwy33.air ~ d.dist.time.hwy33.air +
I(d.dist.time.hwy33.air^2))
fit.time.air.hwy33.linear = lm(d.dist.hwy33.air ~ d.dist.time.hwy33.air)
prd.time.air.hwy33 = data.frame(d.dist.time.hwy33.air = seq(from =
range(d.dist.time.hwy33.air)[1], to = range(d.dist.time.hwy33.air)[2],
length.out = 100))
err.time.air.hwy33 = predict(fit.time.air.hwy33, newdata =
prd.time.air.hwy33, se.fit = TRUE)

prd.time.air.hwy33$lci = err.time.air.hwy33$fit - 1.96 *
err.time.air.hwy33$se.fit
prd.time.air.hwy33$fit = err.time.air.hwy33$fit
prd.time.air.hwy33$uci = err.time.air.hwy33$fit + 1.96 *
err.time.air.hwy33$se.fit

fit.time.air.kare = lm(d.dist.kare.air ~ d.dist.time.kare.air +
I(d.dist.time.kare.air^2))
fit.time.air.kare.linear = lm(d.dist.kare.air ~ d.dist.time.kare.air)
```

```
prd.time.air.kare = data.frame(d.dist.time.kare.air = seq(from =
range(d.dist.time.kare.air)[1], to = range(d.dist.time.kare.air)[2],
length.out = 100))
err.time.air.kare = predict(fit.time.air.kare, newdata = prd.time.air.kare,
se.fit = TRUE)

prd.time.air.kare$lci = err.time.air.kare$fit - 1.96 *
err.time.air.kare$se.fit
prd.time.air.kare$fit = err.time.air.kare$fit
prd.time.air.kare$uci = err.time.air.kare$fit + 1.96 *
err.time.air.kare$se.fit

fit.time.air = lm(d.dist.air ~ d.dist.time.air + I(d.dist.time.air^2))
prd.time.air = data.frame(d.dist.time.air = seq(from =
range(d.dist.time.air)[1], to = range(d.dist.time.air)[2], length.out =
100))
err.time.air = predict(fit.time.air, newdata = prd.time.air, se.fit = TRUE)

prd.time.air$lci = err.time.air$fit - 1.96 * err.time.air$se.fit
prd.time.air$fit = err.time.air$fit
prd.time.air$uci = err.time.air$fit + 1.96 * err.time.air$se.fit

# fit mantel tests for dist ~ time for air hwy33, air KARE and both
combined
mantel.time.hwy33.air = mantel(d.dist.time.hwy33.air, d.dist.hwy33.air,
method="pearson", permutations=999, parallel = 8)
mantel.time.kare.air = mantel(d.dist.time.kare.air, d.dist.kare.air,
method="pearson", permutations=999, parallel = 8)
mantel.time.air = mantel(d.dist.time.air, d.dist.air, method="pearson",
permutations=999, parallel = 8)

# define points for plotting dist ~ time
df.time.air = data.frame(x = as.numeric(d.dist.time.air), y =
as.numeric(d.dist.air))
df.time.hwy33.air = data.frame(x = as.numeric(d.dist.time.hwy33.air), y =
as.numeric(d.dist.hwy33.air))
df.time.kare.air = data.frame(x = as.numeric(d.dist.time.kare.air), y =
as.numeric(d.dist.kare.air))


# fit linear models for dist ~ geo for air hwy33, air KARE and both
combined
fit.geo.air.hwy33 = lm(d.dist.hwy33.air ~ d.dist.geo.hwy33.air)
prd.geo.air.hwy33 = data.frame(d.dist.geo.hwy33.air = seq(from =
range(d.dist.geo.hwy33.air)[1], to = range(d.dist.geo.hwy33.air)[2],
length.out = 100))
err.geo.air.hwy33 = predict(fit.geo.air.hwy33, newdata = prd.geo.air.hwy33,
se.fit = TRUE)

prd.geo.air.hwy33$lci = err.geo.air.hwy33$fit - 1.96 *
err.geo.air.hwy33$se.fit
```

```
prd.geo.air.hwy33$fit = err.geo.air.hwy33$fit
prd.geo.air.hwy33$uci = err.geo.air.hwy33$fit + 1.96 *
err.geo.air.hwy33$se.fit

fit.geo.air.kare = lm(d.dist.kare.air ~ d.dist.geo.kare.air)
prd.geo.air.kare = data.frame(d.dist.geo.kare.air = seq(from =
range(d.dist.geo.kare.air)[1], to = range(d.dist.geo.kare.air)[2],
length.out = 100))
err.geo.air.kare = predict(fit.geo.air.kare, newdata = prd.geo.air.kare,
se.fit = TRUE)

prd.geo.air.kare$lci = err.geo.air.kare$fit - 1.96 * err.geo.air.kare$se.fit
prd.geo.air.kare$fit = err.geo.air.kare$fit
prd.geo.air.kare$uci = err.geo.air.kare$fit + 1.96 * err.geo.air.kare$se.fit

fit.geo.air = lm(d.dist.air ~ d.dist.geo.air)
prd.geo.air = data.frame(d.dist.geo.air = seq(from = range(d.dist.geo.air)
[1], to = range(d.dist.geo.air)[2], length.out = 100))
err.geo.air = predict(fit.geo.air, newdata = prd.geo.air, se.fit = TRUE)

prd.geo.air$lci = err.geo.air$fit - 1.96 * err.geo.air$se.fit
prd.geo.air$fit = err.geo.air$fit
prd.geo.air$uci = err.geo.air$fit + 1.96 * err.geo.air$se.fit

# fit mantel tests for dist ~ geo for air hwy33, air KARE and both combined
mantel.geo.hwy33.air = mantel(d.dist.geo.hwy33.air, d.dist.hwy33.air,
method="pearson", permutations=999, parallel = 8)
mantel.geo.kare.air = mantel(d.dist.geo.kare.air, d.dist.kare.air,
method="pearson", permutations=999, parallel = 8)
mantel.geo.air = mantel(d.dist.geo.air, d.dist.air, method="pearson",
permutations=999, parallel = 8)

# define points for plotting dist ~ geo
df.geo.air = data.frame(x = as.numeric(d.dist.geo.air), y =
as.numeric(d.dist.air))
df.geo.hwy33.air = data.frame(x = as.numeric(d.dist.geo.hwy33.air), y =
as.numeric(d.dist.hwy33.air))
df.geo.kare.air = data.frame(x = as.numeric(d.dist.geo.kare.air), y =
as.numeric(d.dist.kare.air))

## test for significant difference between intercepts/slopes between hwy33
and KARE

# time
d.dist.time.hwy33.air.df = data.frame(
        dist = as.matrix(d.dist.hwy33.air)
[lower.tri(as.matrix(d.dist.hwy33.air))],
        time = as.matrix(d.dist.time.hwy33.air)
[lower.tri(as.matrix(d.dist.time.hwy33.air))],
        site = "hwy33"
)
```

```
d.dist.time.kare.air.df = data.frame(
        dist = as.matrix(d.dist.kare.air)
[lower.tri(as.matrix(d.dist.kare.air))],
        time = as.matrix(d.dist.time.kare.air)
[lower.tri(as.matrix(d.dist.time.kare.air))],
        site = "kare"
)

d.dist.time.air.df = rbind(
        d.dist.time.hwy33.air.df,
        d.dist.time.kare.air.df
)

y = d.dist.time.air.df$dist
x = d.dist.time.air.df$time
site = d.dist.time.air.df$site

fit.time.air.mtest = lm(y ~ site*(x + I(x^2)))
summary(fit.time.air.mtest)

# geo
d.dist.geo.hwy33.air.df = data.frame(
        dist = as.matrix(d.dist.hwy33.air)
[lower.tri(as.matrix(d.dist.hwy33.air))],
        geo = as.matrix(d.dist.geo.hwy33.air)
[lower.tri(as.matrix(d.dist.geo.hwy33.air))],
        site = "hwy33"
)

d.dist.geo.air.df = data.frame(
        dist = as.matrix(d.dist.air)[lower.tri(as.matrix(d.dist.air))],
        geo = as.matrix(d.dist.geo.air)
[lower.tri(as.matrix(d.dist.geo.air))],
        site = "all"
)

d.dist.geo.air.df = rbind(
        d.dist.geo.hwy33.air.df,
        d.dist.geo.air.df
)

y = d.dist.geo.air.df$dist
x = d.dist.geo.air.df$geo
site = d.dist.geo.air.df$site

fit.geo.air.mtest = lm(y ~ site*x)
summary(fit.geo.air.mtest)
```

```
# soil

# fit linear models for dist ~ time for soil hwy33, soil KARE and both
combined
fit.time.soil.hwy33 = lm(d.dist.hwy33.soil ~ d.dist.time.hwy33.soil)
prd.time.soil.hwy33 = data.frame(d.dist.time.hwy33.soil = seq(from =
range(d.dist.time.hwy33.soil)[1], to = range(d.dist.time.hwy33.soil)[2],
length.out = 100))
err.time.soil.hwy33 = predict(fit.time.soil.hwy33, newdata =
prd.time.soil.hwy33, se.fit = TRUE)

prd.time.soil.hwy33$lci = err.time.soil.hwy33$fit - 1.96 *
err.time.soil.hwy33$se.fit
prd.time.soil.hwy33$fit = err.time.soil.hwy33$fit
prd.time.soil.hwy33$uci = err.time.soil.hwy33$fit + 1.96 *
err.time.soil.hwy33$se.fit

fit.time.soil.kare = lm(d.dist.kare.soil ~ d.dist.time.kare.soil)
#fit.time.soil.kare = lm(d.dist.kare.soil ~ d.dist.time.kare.soil +
I(d.dist.time.kare.soil^2))
prd.time.soil.kare = data.frame(d.dist.time.kare.soil = seq(from =
range(d.dist.time.kare.soil)[1], to = range(d.dist.time.kare.soil)[2],
length.out = 100))
err.time.soil.kare = predict(fit.time.soil.kare, newdata =
prd.time.soil.kare, se.fit = TRUE)

prd.time.soil.kare$lci = err.time.soil.kare$fit - 1.96 *
err.time.soil.kare$se.fit
prd.time.soil.kare$fit = err.time.soil.kare$fit
prd.time.soil.kare$uci = err.time.soil.kare$fit + 1.96 *
err.time.soil.kare$se.fit

fit.time.soil = lm(d.dist.soil ~ d.dist.time.soil)
prd.time.soil = data.frame(d.dist.time.soil = seq(from =
range(d.dist.time.soil)[1], to = range(d.dist.time.soil)[2], length.out =
100))
err.time.soil = predict(fit.time.soil, newdata = prd.time.soil, se.fit =
TRUE)

prd.time.soil$lci = err.time.soil$fit - 1.96 * err.time.soil$se.fit
prd.time.soil$fit = err.time.soil$fit
prd.time.soil$uci = err.time.soil$fit + 1.96 * err.time.soil$se.fit

# fit mantel tests for dist ~ time for soil hwy33, soil KARE and both
combined
mantel.time.hwy33.soil = mantel(d.dist.time.hwy33.soil, d.dist.hwy33.soil,
method="pearson", permutations=999, parallel = 8)
mantel.time.kare.soil = mantel(d.dist.time.kare.soil, d.dist.kare.soil,
method="pearson", permutations=999, parallel = 8)
```

```
mantel.time.soil = mantel(d.dist.time.soil, d.dist.soil, method="pearson",
permutations=999, parallel = 8)

# define points for plotting dist ~ time
df.time.soil = data.frame(x = as.numeric(d.dist.time.soil), y =
as.numeric(d.dist.soil))
df.time.hwy33.soil = data.frame(x = as.numeric(d.dist.time.hwy33.soil), y
= as.numeric(d.dist.hwy33.soil))
df.time.kare.soil = data.frame(x = as.numeric(d.dist.time.kare.soil), y =
as.numeric(d.dist.kare.soil))




# fit linear models for dist ~ geo for soil hwy33, soil KARE and both
combined
fit.geo.soil.hwy33 = lm(d.dist.hwy33.soil ~ d.dist.geo.hwy33.soil)
prd.geo.soil.hwy33 = data.frame(d.dist.geo.hwy33.soil = seq(from =
range(d.dist.geo.hwy33.soil)[1], to = range(d.dist.geo.hwy33.soil)[2],
length.out = 100))
err.geo.soil.hwy33 = predict(fit.geo.soil.hwy33, newdata =
prd.geo.soil.hwy33, se.fit = TRUE)

prd.geo.soil.hwy33$lci = err.geo.soil.hwy33$fit - 1.96 *
err.geo.soil.hwy33$se.fit
prd.geo.soil.hwy33$fit = err.geo.soil.hwy33$fit
prd.geo.soil.hwy33$uci = err.geo.soil.hwy33$fit + 1.96 *
err.geo.soil.hwy33$se.fit

fit.geo.soil.kare = lm(d.dist.kare.soil ~ d.dist.geo.kare.soil)
prd.geo.soil.kare = data.frame(d.dist.geo.kare.soil = seq(from =
range(d.dist.geo.kare.soil)[1], to = range(d.dist.geo.kare.soil)[2],
length.out = 100))
err.geo.soil.kare = predict(fit.geo.soil.kare, newdata = prd.geo.soil.kare,
se.fit = TRUE)

prd.geo.soil.kare$lci = err.geo.soil.kare$fit - 1.96 *
err.geo.soil.kare$se.fit
prd.geo.soil.kare$fit = err.geo.soil.kare$fit
prd.geo.soil.kare$uci = err.geo.soil.kare$fit + 1.96 *
err.geo.soil.kare$se.fit

fit.geo.soil = lm(d.dist.soil ~ d.dist.geo.soil)
prd.geo.soil = data.frame(d.dist.geo.soil = seq(from =
range(d.dist.geo.soil)[1], to = range(d.dist.geo.soil)[2], length.out =
100))
err.geo.soil = predict(fit.geo.soil, newdata = prd.geo.soil, se.fit = TRUE)

prd.geo.soil$lci = err.geo.soil$fit - 1.96 * err.geo.soil$se.fit
prd.geo.soil$fit = err.geo.soil$fit
```

```
prd.geo.soil$uci = err.geo.soil$fit + 1.96 * err.geo.soil$se.fit

# fit mantel tests for dist ~ geo for soil hwy33, soil KARE and both
combined
mantel.geo.hwy33.soil = mantel(d.dist.geo.hwy33.soil, d.dist.hwy33.soil,
method="pearson", permutations=999, parallel = 8)
mantel.geo.kare.soil = mantel(d.dist.geo.kare.soil, d.dist.kare.soil,
method="pearson", permutations=999, parallel = 8)
mantel.geo.soil = mantel(d.dist.geo.soil, d.dist.soil, method="pearson",
permutations=999, parallel = 8)

# define points for plotting dist ~ geo
df.geo.soil = data.frame(x = as.numeric(d.dist.geo.soil), y =
as.numeric(d.dist.soil))
df.geo.hwy33.soil = data.frame(x = as.numeric(d.dist.geo.hwy33.soil), y =
as.numeric(d.dist.hwy33.soil))
df.geo.kare.soil = data.frame(x = as.numeric(d.dist.geo.kare.soil), y =
as.numeric(d.dist.kare.soil))

# test for significant difference between intercepts/slopes between hwy33
and KARE

# time
d.dist.time.hwy33.soil.df = data.frame(
        dist = as.matrix(d.dist.hwy33.soil)
[lower.tri(as.matrix(d.dist.hwy33.soil))],
        time = as.matrix(d.dist.time.hwy33.soil)
[lower.tri(as.matrix(d.dist.time.hwy33.soil))],
        site = "hwy33"
)

d.dist.time.kare.soil.df = data.frame(
        dist = as.matrix(d.dist.kare.soil)
[lower.tri(as.matrix(d.dist.kare.soil))],
        time = as.matrix(d.dist.time.kare.soil)
[lower.tri(as.matrix(d.dist.time.kare.soil))],
        site = "kare"
)

d.dist.time.soil.df = rbind(
        d.dist.time.hwy33.soil.df,
        d.dist.time.kare.soil.df
)

y = d.dist.time.soil.df$dist
x = d.dist.time.soil.df$time
site = d.dist.time.soil.df$site

fit.time.soil.mtest = lm(y ~ site*(x))
summary(fit.time.soil.mtest)
```

```
# geo
d.dist.geo.hwy33.soil.df = data.frame(
        dist = as.matrix(d.dist.hwy33.soil)
[lower.tri(as.matrix(d.dist.hwy33.soil))],
        geo = as.matrix(d.dist.geo.hwy33.soil)
[lower.tri(as.matrix(d.dist.geo.hwy33.soil))],
        site = "hwy33"
)

d.dist.geo.soil.df = data.frame(
        dist = as.matrix(d.dist.soil)[lower.tri(as.matrix(d.dist.soil))],
        geo = as.matrix(d.dist.geo.soil)
[lower.tri(as.matrix(d.dist.geo.soil))],
        site = "all"
)

d.dist.geo.soil.df = rbind(
        d.dist.geo.hwy33.soil.df,
        d.dist.geo.soil.df
)

y = d.dist.geo.soil.df$dist
x = d.dist.geo.soil.df$geo
site = d.dist.geo.soil.df$site

fit.geo.soil.mtest = lm(y ~ site*x)
summary(fit.geo.soil.mtest)

# combine and export mtest results
fit.mtest.combined = rbind(
        summary(fit.time.air.mtest)$coefficients,
        summary(fit.geo.air.mtest)$coefficients,
        summary(fit.time.soil.mtest)$coefficients,
        summary(fit.geo.soil.mtest)$coefficients
)
fit.mtest.combined = round(fit.mtest.combined, 4)

# compare slopes for geographic distance decay between hwy33 air and all
air
# (see if land use is a significant interaction term)

# Make lm and anova table with "site" as interaction term
m.interaction = lm(dist ~ geo*site, data = d.dist.geo.air.df)
anova(m.interaction)

# Obtain slopes
m.interaction$coefficients
m.lst <- lstrends(m.interaction, "site", var="geo")

# Compare slopes
pairs(m.lst)
```

```
# compare slopes for temporal distance decay between hwy33 air and kare
air (parabola)
# (see if land use is a significant interaction term)

# Make lm and anova table with "site" as interaction term
m.interaction = lm(dist ~ time*site + I(time^2)*site, data =
d.dist.time.air.df)
anova(m.interaction)

# Obtain slopes
m.interaction$coefficients
m.lst <- lstrends(m.interaction, "site", var="geo")

# Compare slopes
pairs(m.lst)




### Linear Mixed Effects Model (Onygenales Abundance)

# load libraries
library(lme4)
library(lmerTest)
library(multcomp)
library(lsmeans)
library(pbkrtest)
library(MuMIn)
library(vegan)

# load data
d = read.csv("d.combined.genus.onygenales.csv")
d.meta = d[,1:9]

# add factor for sitetype
d.meta$sitetype = paste(d.meta$site, d.meta$type, sep = " ")

# add factor for sitetype
d.meta$sitetype = paste(d.meta$site, d.meta$type, sep = " ")

# extract numeric data for number wrangling
d.numeric = d[,10:(ncol(d))]

# sum total abundance for each sample
total.abundance = rowSums(d.numeric)

# make new dataframe
d.total = d.meta
d.total$Onygenales = rowSums(d.numeric)
```

```
# define variables
# note: Site = "Land Use", site = "Site", year = "Year", month = "Month",
type = "Medium"
y = d.total$Onygenales
month= d.total$month
sitetype = d.total$sitetype

# fit model with varying intercepts for month and type and fixed effect for
site
lmer_fit_REML = lmer(y ~ sitetype + (1|month), REML=T)

# extract coefficients
coefs = round(data.frame(coef(summary(lmer_fit_REML))), 3)
coefs

# fit alternative model
lmer_fit = lmer(y ~ sitetype + (1|month), REML=F)

# fit null model
lmer_fit_null = lmer(y ~ (1|month), REML=F)

# compare models using log-likelihood ratio
anova(lmer_fit, lmer_fit_null)


# multiple comparison with glht (z-statistic, less conservative)
summary(glht(lmer_fit_REML,mcp(sitetype="Tukey")))

# multiple comparison with lsmeans (t-statistic, more conservative,
kenwood-rogers)
lsmeans(lmer_fit_REML, pairwise ~ sitetype)









### Linear Mixed Effects Model (Plant Pathogen Guild)

# load libraries
library(lme4)
library(lmerTest)
library(multcomp)
library(lsmeans)
library(pbkrtest)
library(MuMIn)
library(vegan)
library(reshape2)

# load data
```

```
d = read.csv("d.combined.guilds.csv")

# remove rows containing no guilds
d = d[which(rowSums(d[,9:dim(d)[2]]) != 0),]

d.matrix = as.matrix(d[,9:dim(d)[2]])

# remove any guilds not representing at least 1% of the community across
all samples
d.matrix = d.matrix[,(colSums(d.matrix)/sum(colSums(d.matrix))) >= .01]

# convert data to percent abundance
d.matrix = prop.table(d.matrix, 1)

# load meta data
d.meta = d[,1:8]

# standardize date column
d.meta$date = strptime((paste(d.meta$day, d.meta$month, d.meta$year)),
format = "%e %B %Y")

# make numeric month column
d.meta$month.numeric = format(d.meta$date, "%m")


# aggregate data
d.aggregate = aggregate(d.matrix, by = list(d.meta$month, d.meta$site,
d.meta$type), mean)
names(d.aggregate)[1:3] = c("month", "site", "type")

# change factor names for plotting
d.aggregate[d.aggregate$site!="kare",]$site = paste("Hwy33-",
d.aggregate[d.aggregate$site!="kare",]$site, sep = "")
d.aggregate[d.aggregate$site=="kare",]$site = "KARE"
d.aggregate[d.aggregate$type=="air",]$type = "Air"
d.aggregate[d.aggregate$type=="soil",]$type = "Soil"

# melt data
d.melt = melt(d.aggregate, id.vars = list("month", "site", "type"))

# add numeric month vector
d.melt$month.numeric = as.factor(match(d.melt$month, month.name))

# add abbreviated month vector
d.melt$month.abv = factor(substr(d.melt$month, 1, 3), levels =
substr(month.name, 1, 3))

# replace . with space in guild names for clearer visualization
d.melt$variable = gsub("\\.", " ", d.melt$variable)

# make air only dataframe
```

```
d.melt.air = d.melt[which(d.melt$type=="Air"),]

# reorder months so nov and dec are 1st
d.melt.air$month.numeric = as.numeric(d.melt.air$month.numeric)
d.melt.air$month.numeric = d.melt.air$month.numeric + 2
d.melt.air[which(d.melt.air$month.numeric == 13),]$month.numeric = 1
d.melt.air[which(d.melt.air$month.numeric == 14),]$month.numeric = 2

# make plant pathogen only graph
d.melt.air.plant = d.melt.air[which(d.melt.air$variable=="Plant
Pathogen"),]

# make plant pathogen only graph with only may - oct
d.melt.air.plant.summer = d.melt.air.plant[which(d.melt.air.plant$month
%in% month.name[5:10]),]

# adjust d.meta
# reorder months so nov and dec are 1st
d.meta$month.numeric = as.numeric(d.meta$month.numeric)
d.meta$month.numeric = d.meta$month.numeric + 2
d.meta[which(d.meta$month.numeric == 13),]$month.numeric = 1
d.meta[which(d.meta$month.numeric == 14),]$month.numeric = 2

# make air only matrix
d.matrix.air = d.matrix[which(d.meta$type=="air"),]

# make air only meta
d.meta.air = d.meta[which(d.meta$type=="air"),]

# change factor names for plotting (d.meta.air)
d.meta.air[d.meta.air$site!="kare",]$site = paste("Hwy33-",
d.meta.air[d.meta.air$site!="kare",]$site, sep = "")
d.meta.air[d.meta.air$site=="kare",]$site = "KARE"
d.meta.air[d.meta.air$type=="air",]$type = "Air"

# make air only matrix (summer)
d.matrix.air.summer= d.matrix.air[which(d.meta.air$month %in%
month.name[5:10]),]

# make air only meta (summer)
d.meta.air.summer= d.meta.air[which(d.meta.air$month %in%
month.name[5:10]),]

# statistics

# define variables
y = d.matrix.air.summer[,4]
month= d.meta.air.summer$month.numeric
site = as.factor(d.meta.air.summer$site)

# fit linear model
```

```
lm_fit = lm(y ~ month + site)
summary(lm_fit)

# fit model with varying intercepts for month and type and fixed effect for
site
lmer_fit_REML = lmer(y ~ month + (1|site), REML=T)

# extract coefficients
coefs = round(data.frame(coef(summary(lmer_fit_REML))), 3)
coefs

# fit alternative model
lmer_fit = lmer(y ~ month + (1|site), REML=F)

# fit null model
lmer_fit_null = lmer(y ~ (1|site), REML=F)

# compare models using log-likelihood ratio
model_compare_1 = anova(lmer_fit, lmer_fit_null)
model_compare_1

# extract p, marginal and conditional R^2 values
p = round(model_compare_1[2,8], 3)
r2m = round(r.squaredGLMM(lmer_fit)[1], 3)
r2c = round(r.squaredGLMM(lmer_fit)[2], 3)

#make labels for p and r^2 values
rp0 = as.expression(" " ~ " " ~ " ")
rp1 = as.expression(bquote({r^{2}}[m] ~ "=" ~ .(format(r2m, digits = 2))))
rp2 = as.expression(bquote({r^{2}}[c] ~ "=" ~ .(format(r2c, digits = 2))))
#rp3 = as.expression(bquote(p[lme] ~ "=" ~ .(format(p, digits = 2))))
rp3 = as.expression(bquote(p[lme] ~ "<" ~ .(format(0.001, digits = 2))))
rp = c(rp3, rp2, rp1)

# multiple comparison with glht (z-statistic, less conservative)
multiple_glht = summary(glht(lmer_fit_REML,mcp(site="Tukey")))
multiple_glht[1]

# multiple comparison with lsmeans (t-statistic, more conservative,
kenwood-rogers)
multiple_lsmeans = as.data.frame(lsmeans(lmer_fit_REML, pairwise~site)
$contrasts)
multiple_lsmeans[,2:6] = apply(multiple_lsmeans[,2:6], 2, function (x)
{round(x, 3)})
colnames(multiple_lsmeans) = c("", "Estimate", "se", "df", "t", "p")
rownames(multiple_lsmeans) = multiple_lsmeans[,1]
multiple_lsmeans = multiple_lsmeans[,-c(1,3)]
multiple_lsmeans$p[c(1,3,4,6)] = "<0.001"
multiple_lsmeans
```

Metadata for:

The air mycobiome is decoupled from the soil mycobiome in the California San Joaquin Valley

Robert Wagner, Liliam Montoya, Cheng Gao, Jennifer R. Head, Justin Remais, John W. Taylor

sample	land.use	site	sampling.medium	year	month	day
0724185S01	Agricultural	KARE	Soil	2018	July	24
0724185S02	Agricultural	KARE	Soil	2018	July	24
0724185S05	Agricultural	KARE	Soil	2018	July	24
0724185S06	Agricultural	KARE	Soil	2018	July	24
0724185S11	Agricultural	KARE	Soil	2018	July	24
0724185S12	Agricultural	KARE	Soil	2018	July	24
0724185S13	Agricultural	KARE	Soil	2018	July	24
0724185S14	Agricultural	KARE	Soil	2018	July	24
0724185S17	Agricultural	KARE	Soil	2018	July	24
0724185S18	Agricultural	KARE	Soil	2018	July	24
0724185S19	Agricultural	KARE	Soil	2018	July	24
0724185S20	Agricultural	KARE	Soil	2018	July	24
0821185S01	Agricultural	KARE	Soil	2018	August	21
0821185S02	Agricultural	KARE	Soil	2018	August	21
0821185S03	Agricultural	KARE	Soil	2018	August	21
0821185S04	Agricultural	KARE	Soil	2018	August	21
0821185S05	Agricultural	KARE	Soil	2018	August	21
0821185S06	Agricultural	KARE	Soil	2018	August	21
0821185S12	Agricultural	KARE	Soil	2018	August	21
0821185S13	Agricultural	KARE	Soil	2018	August	21
0821185S14	Agricultural	KARE	Soil	2018	August	21
0821185S15	Agricultural	KARE	Soil	2018	August	21
0821185S16	Agricultural	KARE	Soil	2018	August	21
0821185S17	Agricultural	KARE	Soil	2018	August	21
0821185S18	Agricultural	KARE	Soil	2018	August	21
0821185S19	Agricultural	KARE	Soil	2018	August	21
0821185S20	Agricultural	KARE	Soil	2018	August	21
0821185S21	Agricultural	KARE	Soil	2018	August	21
0821185S22	Agricultural	KARE	Soil	2018	August	21
0821185S27	Agricultural	KARE	Soil	2018	August	21
0821185S28	Agricultural	KARE	Soil	2018	August	21
0821185S29	Agricultural	KARE	Soil	2018	August	21
0821185S30	Agricultural	KARE	Soil	2018	August	21
0821185S31	Agricultural	KARE	Soil	2018	August	21
0821185S32	Agricultural	KARE	Soil	2018	August	21
0823187S01	Agricultural	KARE	Soil	2018	August	23
0823187S02	Agricultural	KARE	Soil	2018	August	23
0823187S03	Agricultural	KARE	Soil	2018	August	23
0823187S04	Agricultural	KARE	Soil	2018	August	23
0823187S11	Agricultural	KARE	Soil	2018	August	23
0823187S12	Agricultural	KARE	Soil	2018	August	23
0823187S15	Agricultural	KARE	Soil	2018	August	23
0823187S16	Agricultural	KARE	Soil	2018	August	23
0823187S19	Agricultural	KARE	Soil	2018	August	23
0823187S20	Agricultural	KARE	Soil	2018	August	23
0823187S21	Agricultural	KARE	Soil	2018	August	23
0823187S22	Agricultural	KARE	Soil	2018	August	23
0823187S27	Agricultural	KARE	Soil	2018	August	23
0823187S28	Agricultural	KARE	Soil	2018	August	23
0823187S29	Agricultural	KARE	Soil	2018	August	23
0823187S30	Agricultural	KARE	Soil	2018	August	23
0823187S31	Agricultural	KARE	Soil	2018	August	23
0823187S32	Agricultural	KARE	Soil	2018	August	23
0828189S01	Agricultural	KARE	Soil	2018	August	28

0828189S02	Agricultural	KARE	Soil	2018	August	28
0828189S03	Agricultural	KARE	Soil	2018	August	28
0828189S04	Agricultural	KARE	Soil	2018	August	28
0828189S05	Agricultural	KARE	Soil	2018	August	28
0828189S06	Agricultural	KARE	Soil	2018	August	28
0828189S11	Agricultural	KARE	Soil	2018	August	28
0828189S12	Agricultural	KARE	Soil	2018	August	28
0828189S13	Agricultural	KARE	Soil	2018	August	28
0828189S14	Agricultural	KARE	Soil	2018	August	28
0828189S15	Agricultural	KARE	Soil	2018	August	28
0828189S16	Agricultural	KARE	Soil	2018	August	28
0828189S17	Agricultural	KARE	Soil	2018	August	28
0828189S18	Agricultural	KARE	Soil	2018	August	28
0828189S19	Agricultural	KARE	Soil	2018	August	28
0828189S20	Agricultural	KARE	Soil	2018	August	28
0828189S21	Agricultural	KARE	Soil	2018	August	28
0828189S22	Agricultural	KARE	Soil	2018	August	28
0828189S27	Agricultural	KARE	Soil	2018	August	28
0828189S28	Agricultural	KARE	Soil	2018	August	28
0828189S29	Agricultural	KARE	Soil	2018	August	28
0828189S30	Agricultural	KARE	Soil	2018	August	28
0828189S31	Agricultural	KARE	Soil	2018	August	28
0828189S32	Agricultural	KARE	Soil	2018	August	28
0925180S27	Agricultural	KARE	Soil	2018	September	25
0925180S28	Agricultural	KARE	Soil	2018	September	25
0925180S29	Agricultural	KARE	Soil	2018	September	25
0925180S31	Agricultural	KARE	Soil	2018	September	25
0925183S32	Agricultural	KARE	Soil	2018	September	25
0925189S30	Agricultural	KARE	Soil	2018	September	25
1	Undeveloped	Hwy33-2	Soil	2017	November	8
10	Undeveloped	Hwy33-2	Soil	2017	November	8
100	Undeveloped	Hwy33-8	Soil	2018	February	15
1002185S01	Agricultural	KARE	Soil	2018	October	2
1002185S02	Agricultural	KARE	Soil	2018	October	2
1002185S03	Agricultural	KARE	Soil	2018	October	2
1002185S04	Agricultural	KARE	Soil	2018	October	2
1002185S05	Agricultural	KARE	Soil	2018	October	2
1002185S11	Agricultural	KARE	Soil	2018	October	2
1002185S12	Agricultural	KARE	Soil	2018	October	2
1002185S13	Agricultural	KARE	Soil	2018	October	2
1002185S14	Agricultural	KARE	Soil	2018	October	2
1002185S15	Agricultural	KARE	Soil	2018	October	2
1002185S16	Agricultural	KARE	Soil	2018	October	2
1002185S17	Agricultural	KARE	Soil	2018	October	2
1002185S19	Agricultural	KARE	Soil	2018	October	2
1002185S21	Agricultural	KARE	Soil	2018	October	2
1002185S22	Agricultural	KARE	Soil	2018	October	2
101	Undeveloped	Hwy33-2	Soil	2018	March	17
102	Undeveloped	Hwy33-2	Soil	2018	March	17
103	Undeveloped	Hwy33-2	Soil	2018	March	17
104	Undeveloped	Hwy33-3	Soil	2018	March	17
105	Undeveloped	Hwy33-3	Soil	2018	March	17
106	Undeveloped	Hwy33-3	Soil	2018	March	17
107	Undeveloped	Hwy33-4	Soil	2018	March	17
108	Undeveloped	Hwy33-4	Soil	2018	March	17
109	Undeveloped	Hwy33-4	Soil	2018	March	17
11	Undeveloped	Hwy33-2	Soil	2017	November	8
110	Undeveloped	Hwy33-7	Soil	2018	March	17
111	Undeveloped	Hwy33-7	Soil	2018	March	17
112	Undeveloped	Hwy33-7	Soil	2018	March	17
113	Undeveloped	Hwy33-8	Soil	2018	March	17
114	Undeveloped	Hwy33-8	Soil	2018	March	17
115	Undeveloped	Hwy33-8	Soil	2018	March	17
116	Undeveloped	Hwy33-2	Soil	2018	April	19
117	Undeveloped	Hwy33-2	Soil	2018	April	19
118	Undeveloped	Hwy33-2	Soil	2018	April	19
119	Undeveloped	Hwy33-3	Soil	2018	April	19
12	Undeveloped	Hwy33-2	Soil	2017	November	8
120	Undeveloped	Hwy33-3	Soil	2018	April	19

121	Undeveloped	Hwy33-3	Soil	2018	April	19
122	Undeveloped	Hwy33-4	Soil	2018	April	19
123	Undeveloped	Hwy33-4	Soil	2018	April	19
124	Undeveloped	Hwy33-4	Soil	2018	April	19
125	Undeveloped	Hwy33-7	Soil	2018	April	19
126	Undeveloped	Hwy33-7	Soil	2018	April	19
127	Undeveloped	Hwy33-7	Soil	2018	April	19
128	Undeveloped	Hwy33-8	Soil	2018	April	19
129	Undeveloped	Hwy33-8	Soil	2018	April	19
13	Undeveloped	Hwy33-2	Soil	2017	November	8
130	Undeveloped	Hwy33-8	Soil	2018	April	19
131	Undeveloped	Hwy33-2	Soil	2018	May	17
132	Undeveloped	Hwy33-2	Soil	2018	May	17
133	Undeveloped	Hwy33-2	Soil	2018	May	17
134	Undeveloped	Hwy33-2	Soil	2018	May	17
135	Undeveloped	Hwy33-2	Soil	2018	May	17
136	Undeveloped	Hwy33-2	Soil	2018	May	17
137	Undeveloped	Hwy33-3	Soil	2018	May	17
138	Undeveloped	Hwy33-3	Soil	2018	May	17
139	Undeveloped	Hwy33-3	Soil	2018	May	17
14	Undeveloped	Hwy33-2	Soil	2017	November	8
140	Undeveloped	Hwy33-3	Soil	2018	May	17
141	Undeveloped	Hwy33-3	Soil	2018	May	17
142	Undeveloped	Hwy33-3	Soil	2018	May	17
143	Undeveloped	Hwy33-4	Soil	2018	May	17
144	Undeveloped	Hwy33-4	Soil	2018	May	17
145	Undeveloped	Hwy33-4	Soil	2018	May	17
146	Undeveloped	Hwy33-7	Soil	2018	May	17
147	Undeveloped	Hwy33-7	Soil	2018	May	17
148	Undeveloped	Hwy33-7	Soil	2018	May	17
149	Undeveloped	Hwy33-8	Soil	2018	May	17
15	Undeveloped	Hwy33-2	Soil	2017	November	8
150	Undeveloped	Hwy33-8	Soil	2018	May	17
151	Undeveloped	Hwy33-8	Soil	2018	May	17
152	Undeveloped	Hwy33-2	Soil	2018	June	19
153	Undeveloped	Hwy33-2	Soil	2018	June	19
154	Undeveloped	Hwy33-2	Soil	2018	June	19
155	Undeveloped	Hwy33-3	Soil	2018	June	19
156	Undeveloped	Hwy33-3	Soil	2018	June	19
157	Undeveloped	Hwy33-3	Soil	2018	June	19
158	Undeveloped	Hwy33-4	Soil	2018	June	19
159	Undeveloped	Hwy33-4	Soil	2018	June	19
16	Undeveloped	Hwy33-3	Soil	2017	November	8
160	Undeveloped	Hwy33-4	Soil	2018	June	19
161	Undeveloped	Hwy33-7	Soil	2018	June	19
162	Undeveloped	Hwy33-7	Soil	2018	June	19
163	Undeveloped	Hwy33-7	Soil	2018	June	19
164	Undeveloped	Hwy33-8	Soil	2018	June	19
165	Undeveloped	Hwy33-8	Soil	2018	June	19
166	Undeveloped	Hwy33-8	Soil	2018	June	19
167	Undeveloped	Hwy33-2	Soil	2018	July	25
168	Undeveloped	Hwy33-2	Soil	2018	July	25
169	Undeveloped	Hwy33-2	Soil	2018	July	25
17	Undeveloped	Hwy33-3	Soil	2017	November	8
170	Undeveloped	Hwy33-3	Soil	2018	July	25
171	Undeveloped	Hwy33-3	Soil	2018	July	25
172	Undeveloped	Hwy33-3	Soil	2018	July	25
173	Undeveloped	Hwy33-4	Soil	2018	July	25
174	Undeveloped	Hwy33-4	Soil	2018	July	25
175	Undeveloped	Hwy33-4	Soil	2018	July	25
176	Undeveloped	Hwy33-7	Soil	2018	July	25
177	Undeveloped	Hwy33-7	Soil	2018	July	25
178	Undeveloped	Hwy33-7	Soil	2018	July	25
179	Undeveloped	Hwy33-8	Soil	2018	July	25
18	Undeveloped	Hwy33-3	Soil	2017	November	8
180	Undeveloped	Hwy33-8	Soil	2018	July	25
181	Undeveloped	Hwy33-8	Soil	2018	July	25
182	Undeveloped	Hwy33-2	Soil	2018	August	23
183	Undeveloped	Hwy33-2	Soil	2018	August	23

184	Undeveloped	Hwy33-2	Soil	2018	August	23
185	Undeveloped	Hwy33-3	Soil	2018	August	23
186	Undeveloped	Hwy33-3	Soil	2018	August	23
187	Undeveloped	Hwy33-3	Soil	2018	August	23
188	Undeveloped	Hwy33-4	Soil	2018	August	23
189	Undeveloped	Hwy33-4	Soil	2018	August	23
19	Undeveloped	Hwy33-3	Soil	2017	November	8
190	Undeveloped	Hwy33-4	Soil	2018	August	23
191	Undeveloped	Hwy33-7	Soil	2018	August	23
192	Undeveloped	Hwy33-7	Soil	2018	August	23
193	Undeveloped	Hwy33-7	Soil	2018	August	23
194	Undeveloped	Hwy33-8	Soil	2018	August	23
195	Undeveloped	Hwy33-8	Soil	2018	August	23
196	Undeveloped	Hwy33-8	Soil	2018	August	23
197	Undeveloped	Hwy33-8	Soil	2018	August	23
198	Undeveloped	Hwy33-8	Soil	2018	August	23
199	Undeveloped	Hwy33-8	Soil	2018	August	23
2	Undeveloped	Hwy33-2	Soil	2017	November	8
20	Undeveloped	Hwy33-3	Soil	2017	November	8
200	Undeveloped	Hwy33-8	Soil	2018	August	23
201	Undeveloped	Hwy33-8	Soil	2018	August	23
202	Undeveloped	Hwy33-8	Soil	2018	August	23
203	Undeveloped	Hwy33-2	Soil	2018	September	23
204	Undeveloped	Hwy33-2	Soil	2018	September	23
205	Undeveloped	Hwy33-2	Soil	2018	September	23
206	Undeveloped	Hwy33-2	Soil	2018	September	23
207	Undeveloped	Hwy33-2	Soil	2018	September	23
208	Undeveloped	Hwy33-2	Soil	2018	September	23
209	Undeveloped	Hwy33-3	Soil	2018	September	23
21	Undeveloped	Hwy33-3	Soil	2017	November	8
210	Undeveloped	Hwy33-3	Soil	2018	September	23
211	Undeveloped	Hwy33-3	Soil	2018	September	23
212	Undeveloped	Hwy33-3	Soil	2018	September	23
213	Undeveloped	Hwy33-3	Soil	2018	September	23
214	Undeveloped	Hwy33-3	Soil	2018	September	23
215	Undeveloped	Hwy33-4	Soil	2018	September	23
216	Undeveloped	Hwy33-4	Soil	2018	September	23
217	Undeveloped	Hwy33-4	Soil	2018	September	23
218	Undeveloped	Hwy33-7	Soil	2018	September	23
219	Undeveloped	Hwy33-7	Soil	2018	September	23
22	Undeveloped	Hwy33-3	Soil	2017	November	8
220	Undeveloped	Hwy33-7	Soil	2018	September	23
221	Undeveloped	Hwy33-8	Soil	2018	September	23
222	Undeveloped	Hwy33-8	Soil	2018	September	23
223	Undeveloped	Hwy33-8	Soil	2018	September	23
224	Undeveloped	Hwy33-2	Soil	2018	October	23
225	Undeveloped	Hwy33-2	Soil	2018	October	23
226	Undeveloped	Hwy33-2	Soil	2018	October	23
227	Undeveloped	Hwy33-3	Soil	2018	October	23
228	Undeveloped	Hwy33-3	Soil	2018	October	23
229	Undeveloped	Hwy33-3	Soil	2018	October	23
23	Undeveloped	Hwy33-3	Soil	2017	November	8
230	Undeveloped	Hwy33-4	Soil	2018	October	23
231	Undeveloped	Hwy33-4	Soil	2018	October	23
232	Undeveloped	Hwy33-4	Soil	2018	October	23
233	Undeveloped	Hwy33-7	Soil	2018	October	23
234	Undeveloped	Hwy33-7	Soil	2018	October	23
235	Undeveloped	Hwy33-7	Soil	2018	October	23
24	Undeveloped	Hwy33-3	Soil	2017	November	8
25	Undeveloped	Hwy33-3	Soil	2017	November	8
251	Undeveloped	Hwy33-8	Soil	2018	October	23
252	Undeveloped	Hwy33-8	Soil	2018	October	23
253	Undeveloped	Hwy33-8	Soil	2018	October	23
26	Undeveloped	Hwy33-4	Soil	2017	November	8
27	Undeveloped	Hwy33-4	Soil	2017	November	8
28	Undeveloped	Hwy33-4	Soil	2017	November	8
29	Undeveloped	Hwy33-4	Soil	2017	November	8
3	Undeveloped	Hwy33-2	Soil	2017	November	8
30	Undeveloped	Hwy33-4	Soil	2017	November	8

31	Undeveloped	Hwy33-4	Soil	2017	November	8
32	Undeveloped	Hwy33-4	Soil	2017	November	8
33	Undeveloped	Hwy33-4	Soil	2017	November	8
34	Undeveloped	Hwy33-4	Soil	2017	November	8
35	Undeveloped	Hwy33-4	Soil	2017	November	8
36	Undeveloped	Hwy33-7	Soil	2017	November	8
37	Undeveloped	Hwy33-7	Soil	2017	November	8
38	Undeveloped	Hwy33-7	Soil	2017	November	8
39	Undeveloped	Hwy33-7	Soil	2017	November	8
4	Undeveloped	Hwy33-2	Soil	2017	November	8
40	Undeveloped	Hwy33-7	Soil	2017	November	8
41	Undeveloped	Hwy33-7	Soil	2017	November	8
42	Undeveloped	Hwy33-7	Soil	2017	November	8
43	Undeveloped	Hwy33-7	Soil	2017	November	8
44	Undeveloped	Hwy33-7	Soil	2017	November	8
45	Undeveloped	Hwy33-7	Soil	2017	November	8
46	Undeveloped	Hwy33-8	Soil	2017	November	8
47	Undeveloped	Hwy33-8	Soil	2017	November	8
48	Undeveloped	Hwy33-8	Soil	2017	November	8
49	Undeveloped	Hwy33-8	Soil	2017	November	8
5	Undeveloped	Hwy33-2	Soil	2017	November	8
50	Undeveloped	Hwy33-8	Soil	2017	November	8
51	Undeveloped	Hwy33-8	Soil	2017	November	8
52	Undeveloped	Hwy33-8	Soil	2017	November	8
53	Undeveloped	Hwy33-8	Soil	2017	November	8
54	Undeveloped	Hwy33-8	Soil	2017	November	8
55	Undeveloped	Hwy33-8	Soil	2017	November	8
56	Undeveloped	Hwy33-2	Soil	2017	December	14
57	Undeveloped	Hwy33-2	Soil	2017	December	14
58	Undeveloped	Hwy33-2	Soil	2017	December	14
59	Undeveloped	Hwy33-3	Soil	2017	December	14
6	Undeveloped	Hwy33-2	Soil	2017	November	8
60	Undeveloped	Hwy33-3	Soil	2017	December	14
61	Undeveloped	Hwy33-3	Soil	2017	December	14
62	Undeveloped	Hwy33-4	Soil	2017	December	14
63	Undeveloped	Hwy33-4	Soil	2017	December	14
64	Undeveloped	Hwy33-4	Soil	2017	December	14
65	Undeveloped	Hwy33-7	Soil	2017	December	14
66	Undeveloped	Hwy33-7	Soil	2017	December	14
67	Undeveloped	Hwy33-7	Soil	2017	December	14
68	Undeveloped	Hwy33-8	Soil	2017	December	14
69	Undeveloped	Hwy33-8	Soil	2017	December	14
7	Undeveloped	Hwy33-2	Soil	2017	November	8
70	Undeveloped	Hwy33-8	Soil	2017	December	14
71	Undeveloped	Hwy33-2	Soil	2018	January	18
72	Undeveloped	Hwy33-2	Soil	2018	January	18
73	Undeveloped	Hwy33-3	Soil	2018	January	18
74	Undeveloped	Hwy33-3	Soil	2018	January	18
75	Undeveloped	Hwy33-3	Soil	2018	January	18
76	Undeveloped	Hwy33-3	Soil	2018	January	18
77	Undeveloped	Hwy33-4	Soil	2018	January	18
78	Undeveloped	Hwy33-4	Soil	2018	January	18
79	Undeveloped	Hwy33-4	Soil	2018	January	18
8	Undeveloped	Hwy33-2	Soil	2017	November	8
80	Undeveloped	Hwy33-7	Soil	2018	January	18
81	Undeveloped	Hwy33-7	Soil	2018	January	18
82	Undeveloped	Hwy33-7	Soil	2018	January	18
83	Undeveloped	Hwy33-8	Soil	2018	January	18
84	Undeveloped	Hwy33-8	Soil	2018	January	18
85	Undeveloped	Hwy33-8	Soil	2018	January	18
86	Undeveloped	Hwy33-2	Soil	2018	February	15
87	Undeveloped	Hwy33-2	Soil	2018	February	15
88	Undeveloped	Hwy33-2	Soil	2018	February	15
89	Undeveloped	Hwy33-3	Soil	2018	February	15
9	Undeveloped	Hwy33-2	Soil	2017	November	8
90	Undeveloped	Hwy33-3	Soil	2018	February	15
91	Undeveloped	Hwy33-3	Soil	2018	February	15
92	Undeveloped	Hwy33-4	Soil	2018	February	15
93	Undeveloped	Hwy33-4	Soil	2018	February	15

94	Undeveloped	Hwy33-4	Soil	2018	February	15
95	Undeveloped	Hwy33-7	Soil	2018	February	15
96	Undeveloped	Hwy33-7	Soil	2018	February	15
97	Undeveloped	Hwy33-7	Soil	2018	February	15
98	Undeveloped	Hwy33-8	Soil	2018	February	15
99	Undeveloped	Hwy33-8	Soil	2018	February	15
Y16TP00S1	Agricultural	KARE	Soil	2016	May	20
Y16TP00S11	Agricultural	KARE	Soil	2016	May	20
Y16TP00S12	Agricultural	KARE	Soil	2016	May	20
Y16TP00S13	Agricultural	KARE	Soil	2016	May	20
Y16TP00S14	Agricultural	KARE	Soil	2016	May	20
Y16TP00S15	Agricultural	KARE	Soil	2016	May	20
Y16TP00S16	Agricultural	KARE	Soil	2016	May	20
Y16TP00S17	Agricultural	KARE	Soil	2016	May	20
Y16TP00S18	Agricultural	KARE	Soil	2016	May	20
Y16TP00S19	Agricultural	KARE	Soil	2016	May	20
Y16TP00S2	Agricultural	KARE	Soil	2016	May	20
Y16TP00S20	Agricultural	KARE	Soil	2016	May	20
Y16TP00S21	Agricultural	KARE	Soil	2016	May	20
Y16TP00S22	Agricultural	KARE	Soil	2016	May	20
Y16TP00S3	Agricultural	KARE	Soil	2016	May	20
Y16TP00S4	Agricultural	KARE	Soil	2016	May	20
Y16TP00S5	Agricultural	KARE	Soil	2016	May	20
Y16TP00S6	Agricultural	KARE	Soil	2016	May	20
Y16TP01S1	Agricultural	KARE	Soil	2016	June	8
Y16TP01S11	Agricultural	KARE	Soil	2016	June	8
Y16TP01S12	Agricultural	KARE	Soil	2016	June	8
Y16TP01S19	Agricultural	KARE	Soil	2016	June	8
Y16TP01S2	Agricultural	KARE	Soil	2016	June	8
Y16TP01S20	Agricultural	KARE	Soil	2016	June	8
Y16TP02S1	Agricultural	KARE	Soil	2016	June	15
Y16TP02S11	Agricultural	KARE	Soil	2016	June	15
Y16TP02S12	Agricultural	KARE	Soil	2016	June	15
Y16TP02S19	Agricultural	KARE	Soil	2016	June	15
Y16TP02S2	Agricultural	KARE	Soil	2016	June	15
Y16TP02S20	Agricultural	KARE	Soil	2016	June	15
Y16TP03S1	Agricultural	KARE	Soil	2016	June	22
Y16TP03S11	Agricultural	KARE	Soil	2016	June	22
Y16TP03S12	Agricultural	KARE	Soil	2016	June	22
Y16TP03S13	Agricultural	KARE	Soil	2016	June	22
Y16TP03S14	Agricultural	KARE	Soil	2016	June	22
Y16TP03S17	Agricultural	KARE	Soil	2016	June	22
Y16TP03S18	Agricultural	KARE	Soil	2016	June	22
Y16TP03S19	Agricultural	KARE	Soil	2016	June	22
Y16TP03S2	Agricultural	KARE	Soil	2016	June	22
Y16TP03S20	Agricultural	KARE	Soil	2016	June	22
Y16TP03S5	Agricultural	KARE	Soil	2016	June	22
Y16TP03S6	Agricultural	KARE	Soil	2016	June	22
Y16TP04S1	Agricultural	KARE	Soil	2016	June	29
Y16TP04S11	Agricultural	KARE	Soil	2016	June	29
Y16TP04S12	Agricultural	KARE	Soil	2016	June	29
Y16TP04S13	Agricultural	KARE	Soil	2016	June	29
Y16TP04S14	Agricultural	KARE	Soil	2016	June	29
Y16TP04S17	Agricultural	KARE	Soil	2016	June	29
Y16TP04S18	Agricultural	KARE	Soil	2016	June	29
Y16TP04S19	Agricultural	KARE	Soil	2016	June	29
Y16TP04S2	Agricultural	KARE	Soil	2016	June	29
Y16TP04S20	Agricultural	KARE	Soil	2016	June	29
Y16TP04S5	Agricultural	KARE	Soil	2016	June	29
Y16TP04S6	Agricultural	KARE	Soil	2016	June	29
Y16TP05S1	Agricultural	KARE	Soil	2016	July	6
Y16TP05S11	Agricultural	KARE	Soil	2016	July	6
Y16TP05S12	Agricultural	KARE	Soil	2016	July	6
Y16TP05S13	Agricultural	KARE	Soil	2016	July	6
Y16TP05S17	Agricultural	KARE	Soil	2016	July	6
Y16TP05S18	Agricultural	KARE	Soil	2016	July	6
Y16TP05S19	Agricultural	KARE	Soil	2016	July	6
Y16TP05S2	Agricultural	KARE	Soil	2016	July	6
Y16TP05S20	Agricultural	KARE	Soil	2016	July	6

Y16TP05S5	Agricultural	KARE	Soil	2016	July	6
Y16TP05S6	Agricultural	KARE	Soil	2016	July	6
Y16TP06S1	Agricultural	KARE	Soil	2016	July	13
Y16TP06S11	Agricultural	KARE	Soil	2016	July	13
Y16TP06S12	Agricultural	KARE	Soil	2016	July	13
Y16TP06S13	Agricultural	KARE	Soil	2016	July	13
Y16TP06S14	Agricultural	KARE	Soil	2016	July	13
Y16TP06S17	Agricultural	KARE	Soil	2016	July	13
Y16TP06S18	Agricultural	KARE	Soil	2016	July	13
Y16TP06S19	Agricultural	KARE	Soil	2016	July	13
Y16TP06S2	Agricultural	KARE	Soil	2016	July	13
Y16TP06S20	Agricultural	KARE	Soil	2016	July	13
Y16TP06S5	Agricultural	KARE	Soil	2016	July	13
Y16TP06S6	Agricultural	KARE	Soil	2016	July	13
Y16TP07S1	Agricultural	KARE	Soil	2016	July	20
Y16TP07S11	Agricultural	KARE	Soil	2016	July	20
Y16TP07S12	Agricultural	KARE	Soil	2016	July	20
Y16TP07S13	Agricultural	KARE	Soil	2016	July	20
Y16TP07S14	Agricultural	KARE	Soil	2016	July	20
Y16TP07S17	Agricultural	KARE	Soil	2016	July	20
Y16TP07S18	Agricultural	KARE	Soil	2016	July	20
Y16TP07S19	Agricultural	KARE	Soil	2016	July	20
Y16TP07S2	Agricultural	KARE	Soil	2016	July	20
Y16TP07S20	Agricultural	KARE	Soil	2016	July	20
Y16TP07S5	Agricultural	KARE	Soil	2016	July	20
Y16TP07S6	Agricultural	KARE	Soil	2016	July	20
Y16TP08S1	Agricultural	KARE	Soil	2016	July	27
Y16TP08S11	Agricultural	KARE	Soil	2016	July	27
Y16TP08S12	Agricultural	KARE	Soil	2016	July	27
Y16TP08S13	Agricultural	KARE	Soil	2016	July	27
Y16TP08S14	Agricultural	KARE	Soil	2016	July	27
Y16TP08S15	Agricultural	KARE	Soil	2016	July	27
Y16TP08S16	Agricultural	KARE	Soil	2016	July	27
Y16TP08S17	Agricultural	KARE	Soil	2016	July	27
Y16TP08S18	Agricultural	KARE	Soil	2016	July	27
Y16TP08S19	Agricultural	KARE	Soil	2016	July	27
Y16TP08S2	Agricultural	KARE	Soil	2016	July	27
Y16TP08S20	Agricultural	KARE	Soil	2016	July	27
Y16TP08S21	Agricultural	KARE	Soil	2016	July	27
Y16TP08S22	Agricultural	KARE	Soil	2016	July	27
Y16TP08S3	Agricultural	KARE	Soil	2016	July	27
Y16TP08S4	Agricultural	KARE	Soil	2016	July	27
Y16TP08S5	Agricultural	KARE	Soil	2016	July	27
Y16TP08S6	Agricultural	KARE	Soil	2016	July	27
Y16TP09S1	Agricultural	KARE	Soil	2016	August	3
Y16TP09S11	Agricultural	KARE	Soil	2016	August	3
Y16TP09S12	Agricultural	KARE	Soil	2016	August	3
Y16TP09S13	Agricultural	KARE	Soil	2016	August	3
Y16TP09S14	Agricultural	KARE	Soil	2016	August	3
Y16TP09S15	Agricultural	KARE	Soil	2016	August	3
Y16TP09S16	Agricultural	KARE	Soil	2016	August	3
Y16TP09S17	Agricultural	KARE	Soil	2016	August	3
Y16TP09S18	Agricultural	KARE	Soil	2016	August	3
Y16TP09S19	Agricultural	KARE	Soil	2016	August	3
Y16TP09S2	Agricultural	KARE	Soil	2016	August	3
Y16TP09S20	Agricultural	KARE	Soil	2016	August	3
Y16TP09S21	Agricultural	KARE	Soil	2016	August	3
Y16TP09S22	Agricultural	KARE	Soil	2016	August	3
Y16TP09S3	Agricultural	KARE	Soil	2016	August	3
Y16TP09S4	Agricultural	KARE	Soil	2016	August	3
Y16TP09S5	Agricultural	KARE	Soil	2016	August	3
Y16TP09S6	Agricultural	KARE	Soil	2016	August	3
Y16TP10S1	Agricultural	KARE	Soil	2016	August	10
Y16TP10S11	Agricultural	KARE	Soil	2016	August	10
Y16TP10S12	Agricultural	KARE	Soil	2016	August	10
Y16TP10S13	Agricultural	KARE	Soil	2016	August	10
Y16TP10S14	Agricultural	KARE	Soil	2016	August	10
Y16TP10S15	Agricultural	KARE	Soil	2016	August	10
Y16TP10S16	Agricultural	KARE	Soil	2016	August	10

Y16TP10S17	Agricultural	KARE	Soil	2016	August	10
Y16TP10S18	Agricultural	KARE	Soil	2016	August	10
Y16TP10S19	Agricultural	KARE	Soil	2016	August	10
Y16TP10S2	Agricultural	KARE	Soil	2016	August	10
Y16TP10S20	Agricultural	KARE	Soil	2016	August	10
Y16TP10S21	Agricultural	KARE	Soil	2016	August	10
Y16TP10S22	Agricultural	KARE	Soil	2016	August	10
Y16TP10S3	Agricultural	KARE	Soil	2016	August	10
Y16TP10S4	Agricultural	KARE	Soil	2016	August	10
Y16TP10S5	Agricultural	KARE	Soil	2016	August	10
Y16TP10S6	Agricultural	KARE	Soil	2016	August	10
Y16TP11S1	Agricultural	KARE	Soil	2016	August	17
Y16TP11S11	Agricultural	KARE	Soil	2016	August	17
Y16TP11S12	Agricultural	KARE	Soil	2016	August	17
Y16TP11S13	Agricultural	KARE	Soil	2016	August	17
Y16TP11S14	Agricultural	KARE	Soil	2016	August	17
Y16TP11S15	Agricultural	KARE	Soil	2016	August	17
Y16TP11S16	Agricultural	KARE	Soil	2016	August	17
Y16TP11S17	Agricultural	KARE	Soil	2016	August	17
Y16TP11S18	Agricultural	KARE	Soil	2016	August	17
Y16TP11S19	Agricultural	KARE	Soil	2016	August	17
Y16TP11S2	Agricultural	KARE	Soil	2016	August	17
Y16TP11S20	Agricultural	KARE	Soil	2016	August	17
Y16TP11S21	Agricultural	KARE	Soil	2016	August	17
Y16TP11S22	Agricultural	KARE	Soil	2016	August	17
Y16TP11S3	Agricultural	KARE	Soil	2016	August	17
Y16TP11S4	Agricultural	KARE	Soil	2016	August	17
Y16TP11S5	Agricultural	KARE	Soil	2016	August	17
Y16TP11S6	Agricultural	KARE	Soil	2016	August	17
Y16TP12S1	Agricultural	KARE	Soil	2016	August	24
Y16TP12S11	Agricultural	KARE	Soil	2016	August	24
Y16TP12S12	Agricultural	KARE	Soil	2016	August	24
Y16TP12S13	Agricultural	KARE	Soil	2016	August	24
Y16TP12S14	Agricultural	KARE	Soil	2016	August	24
Y16TP12S15	Agricultural	KARE	Soil	2016	August	24
Y16TP12S16	Agricultural	KARE	Soil	2016	August	24
Y16TP12S17	Agricultural	KARE	Soil	2016	August	24
Y16TP12S18	Agricultural	KARE	Soil	2016	August	24
Y16TP12S19	Agricultural	KARE	Soil	2016	August	24
Y16TP12S2	Agricultural	KARE	Soil	2016	August	24
Y16TP12S20	Agricultural	KARE	Soil	2016	August	24
Y16TP12S21	Agricultural	KARE	Soil	2016	August	24
Y16TP12S22	Agricultural	KARE	Soil	2016	August	24
Y16TP12S3	Agricultural	KARE	Soil	2016	August	24
Y16TP12S4	Agricultural	KARE	Soil	2016	August	24
Y16TP12S5	Agricultural	KARE	Soil	2016	August	24
Y16TP12S6	Agricultural	KARE	Soil	2016	August	24
Y16TP13S1	Agricultural	KARE	Soil	2016	August	31
Y16TP13S11	Agricultural	KARE	Soil	2016	August	31
Y16TP13S12	Agricultural	KARE	Soil	2016	August	31
Y16TP13S13	Agricultural	KARE	Soil	2016	August	31
Y16TP13S14	Agricultural	KARE	Soil	2016	August	31
Y16TP13S15	Agricultural	KARE	Soil	2016	August	31
Y16TP13S16	Agricultural	KARE	Soil	2016	August	31
Y16TP13S17	Agricultural	KARE	Soil	2016	August	31
Y16TP13S18	Agricultural	KARE	Soil	2016	August	31
Y16TP13S19	Agricultural	KARE	Soil	2016	August	31
Y16TP13S2	Agricultural	KARE	Soil	2016	August	31
Y16TP13S20	Agricultural	KARE	Soil	2016	August	31
Y16TP13S21	Agricultural	KARE	Soil	2016	August	31
Y16TP13S22	Agricultural	KARE	Soil	2016	August	31
Y16TP13S4	Agricultural	KARE	Soil	2016	August	31
Y16TP13S5	Agricultural	KARE	Soil	2016	August	31
Y16TP13S6	Agricultural	KARE	Soil	2016	August	31
Y16TP14S1	Agricultural	KARE	Soil	2016	September	7
Y16TP14S11	Agricultural	KARE	Soil	2016	September	7
Y16TP14S12	Agricultural	KARE	Soil	2016	September	7
Y16TP14S13	Agricultural	KARE	Soil	2016	September	7
Y16TP14S14	Agricultural	KARE	Soil	2016	September	7

Y16TP14S15	Agricultural	KARE	Soil	2016	September	7
Y16TP14S19	Agricultural	KARE	Soil	2016	September	7
Y16TP14S2	Agricultural	KARE	Soil	2016	September	7
Y16TP14S20	Agricultural	KARE	Soil	2016	September	7
Y16TP14S21	Agricultural	KARE	Soil	2016	September	7
Y16TP14S22	Agricultural	KARE	Soil	2016	September	7
Y16TP14S3	Agricultural	KARE	Soil	2016	September	7
Y16TP14S4	Agricultural	KARE	Soil	2016	September	7
Y16TP14S5	Agricultural	KARE	Soil	2016	September	7
Y16TP15S1	Agricultural	KARE	Soil	2016	September	14
Y16TP15S11	Agricultural	KARE	Soil	2016	September	14
Y16TP15S13	Agricultural	KARE	Soil	2016	September	14
Y16TP15S14	Agricultural	KARE	Soil	2016	September	14
Y16TP15S15	Agricultural	KARE	Soil	2016	September	14
Y16TP15S16	Agricultural	KARE	Soil	2016	September	14
Y16TP15S17	Agricultural	KARE	Soil	2016	September	14
Y16TP15S18	Agricultural	KARE	Soil	2016	September	14
Y16TP15S19	Agricultural	KARE	Soil	2016	September	14
Y16TP15S2	Agricultural	KARE	Soil	2016	September	14
Y16TP15S20	Agricultural	KARE	Soil	2016	September	14
Y16TP15S21	Agricultural	KARE	Soil	2016	September	14
Y16TP15S22	Agricultural	KARE	Soil	2016	September	14
Y16TP15S3	Agricultural	KARE	Soil	2016	September	14
Y16TP15S4	Agricultural	KARE	Soil	2016	September	14
Y16TP15S5	Agricultural	KARE	Soil	2016	September	14
Y16TP15S6	Agricultural	KARE	Soil	2016	September	14
Y16TP16S1	Agricultural	KARE	Soil	2016	September	21
Y16TP16S11	Agricultural	KARE	Soil	2016	September	21
Y16TP16S12	Agricultural	KARE	Soil	2016	September	21
Y16TP16S13	Agricultural	KARE	Soil	2016	September	21
Y16TP16S14	Agricultural	KARE	Soil	2016	September	21
Y16TP16S15	Agricultural	KARE	Soil	2016	September	21
Y16TP16S16	Agricultural	KARE	Soil	2016	September	21
Y16TP16S18	Agricultural	KARE	Soil	2016	September	21
Y16TP16S19	Agricultural	KARE	Soil	2016	September	21
Y16TP16S2	Agricultural	KARE	Soil	2016	September	21
Y16TP16S20	Agricultural	KARE	Soil	2016	September	21
Y16TP16S21	Agricultural	KARE	Soil	2016	September	21
Y16TP16S22	Agricultural	KARE	Soil	2016	September	21
Y16TP16S3	Agricultural	KARE	Soil	2016	September	21
Y16TP16S4	Agricultural	KARE	Soil	2016	September	21
Y16TP16S5	Agricultural	KARE	Soil	2016	September	21
Y16TP16S6	Agricultural	KARE	Soil	2016	September	21
Y16TP17S1	Agricultural	KARE	Soil	2016	September	28
Y16TP17S11	Agricultural	KARE	Soil	2016	September	28
Y16TP17S12	Agricultural	KARE	Soil	2016	September	28
Y16TP17S13	Agricultural	KARE	Soil	2016	September	28
Y16TP17S14	Agricultural	KARE	Soil	2016	September	28
Y16TP17S2	Agricultural	KARE	Soil	2016	September	28
Y16TP17S3	Agricultural	KARE	Soil	2016	September	28
Y16TP17S4	Agricultural	KARE	Soil	2016	September	28
Y16TP17S5	Agricultural	KARE	Soil	2016	September	28
Y16TP17S6	Agricultural	KARE	Soil	2016	September	28
Y171011Hwy2a	Undeveloped	Hwy33-2	Air	2017	November	8
Y171011Hwy2b	Undeveloped	Hwy33-2	Air	2017	November	8
Y171011Hwy2c	Undeveloped	Hwy33-2	Air	2017	November	8
Y171011Hwy3a	Undeveloped	Hwy33-3	Air	2017	November	8
Y171011Hwy3b	Undeveloped	Hwy33-3	Air	2017	November	8
Y171011Hwy3c	Undeveloped	Hwy33-3	Air	2017	November	8
Y171011Hwy4a	Undeveloped	Hwy33-4	Air	2017	November	8
Y171011Hwy4b	Undeveloped	Hwy33-4	Air	2017	November	8
Y171011Hwy4c	Undeveloped	Hwy33-4	Air	2017	November	8
Y171011Hwy7a	Undeveloped	Hwy33-7	Air	2017	November	8
Y171011Hwy7b	Undeveloped	Hwy33-7	Air	2017	November	8
Y171011Hwy7c	Undeveloped	Hwy33-7	Air	2017	November	8
Y171011Hwy8a	Undeveloped	Hwy33-8	Air	2017	November	8
Y171011Hwy8b	Undeveloped	Hwy33-8	Air	2017	November	8
Y171108Hwy2a	Undeveloped	Hwy33-2	Air	2017	December	14
Y171108Hwy2b	Undeveloped	Hwy33-2	Air	2017	December	14

Y171108Hwy2c	Undeveloped	Hwy33-2	Air	2017	December	14
Y171108Hwy3a	Undeveloped	Hwy33-3	Air	2017	December	14
Y171108Hwy3b	Undeveloped	Hwy33-3	Air	2017	December	14
Y171108Hwy3c	Undeveloped	Hwy33-3	Air	2017	December	14
Y171108Hwy4a	Undeveloped	Hwy33-4	Air	2017	December	14
Y171108Hwy4b	Undeveloped	Hwy33-4	Air	2017	December	14
Y171108Hwy4c	Undeveloped	Hwy33-4	Air	2017	December	14
Y171108Hwy7a	Undeveloped	Hwy33-7	Air	2017	December	14
Y171108Hwy7b	Undeveloped	Hwy33-7	Air	2017	December	14
Y171108Hwy8a	Undeveloped	Hwy33-8	Air	2017	December	14
Y171108Hwy8b	Undeveloped	Hwy33-8	Air	2017	December	14
Y171214Hwy2a	Undeveloped	Hwy33-2	Air	2018	January	18
Y171214Hwy2b	Undeveloped	Hwy33-2	Air	2018	January	18
Y171214Hwy2c	Undeveloped	Hwy33-2	Air	2018	January	18
Y171214Hwy3a	Undeveloped	Hwy33-3	Air	2018	January	18
Y171214Hwy3b	Undeveloped	Hwy33-3	Air	2018	January	18
Y171214Hwy3c	Undeveloped	Hwy33-3	Air	2018	January	18
Y171214Hwy4a	Undeveloped	Hwy33-4	Air	2018	January	18
Y171214Hwy4b	Undeveloped	Hwy33-4	Air	2018	January	18
Y171214Hwy4c	Undeveloped	Hwy33-4	Air	2018	January	18
Y171214Hwy7a	Undeveloped	Hwy33-7	Air	2018	January	18
Y171214Hwy7b	Undeveloped	Hwy33-7	Air	2018	January	18
Y171214Hwy8a	Undeveloped	Hwy33-8	Air	2018	January	18
Y171214Hwy8b	Undeveloped	Hwy33-8	Air	2018	January	18
Y171214Hwy8c	Undeveloped	Hwy33-8	Air	2018	January	18
Y17A1170913	Agricultural	KARE	Air	2017	September	13
Y17A1171011	Agricultural	KARE	Air	2017	October	11
Y17A2170913	Agricultural	KARE	Air	2017	September	13
Y17A2171011	Agricultural	KARE	Air	2017	October	11
Y17A4170913	Agricultural	KARE	Air	2017	September	13
Y17A4171011	Agricultural	KARE	Air	2017	October	11
Y17A8170913	Agricultural	KARE	Air	2017	September	13
Y17A8171011	Agricultural	KARE	Air	2017	October	11
Y17B1170913	Agricultural	KARE	Air	2017	September	13
Y17B1171011	Agricultural	KARE	Air	2017	October	11
Y17B2170913	Agricultural	KARE	Air	2017	September	13
Y17B2171011	Agricultural	KARE	Air	2017	October	11
Y17B4170913	Agricultural	KARE	Air	2017	September	13
Y17B4171011	Agricultural	KARE	Air	2017	October	11
Y17B8170913	Agricultural	KARE	Air	2017	September	13
Y17B8171011	Agricultural	KARE	Air	2017	October	11
Y17C1170913	Agricultural	KARE	Air	2017	September	13
Y17C1171011	Agricultural	KARE	Air	2017	October	11
Y17C2170913	Agricultural	KARE	Air	2017	September	13
Y17C2171011	Agricultural	KARE	Air	2017	October	11
Y17C4170913	Agricultural	KARE	Air	2017	September	13
Y17C4171011	Agricultural	KARE	Air	2017	October	11
Y17C8170913	Agricultural	KARE	Air	2017	September	13
Y17C8171011	Agricultural	KARE	Air	2017	October	11
Y17P0170913	Agricultural	KARE	Air	2017	September	13
Y17P0171011	Agricultural	KARE	Air	2017	October	11
Y17TP02S02	Agricultural	KARE	Soil	2017	June	28
Y17TP02S06	Agricultural	KARE	Soil	2017	June	28
Y17TP02S13	Agricultural	KARE	Soil	2017	June	28
Y17TP02S30	Agricultural	KARE	Soil	2017	June	28
Y17TP03S02	Agricultural	KARE	Soil	2017	July	5
Y17TP03S06	Agricultural	KARE	Soil	2017	July	5
Y17TP03S11	Agricultural	KARE	Soil	2017	July	5
Y17TP03S13	Agricultural	KARE	Soil	2017	July	5
Y17TP03S16	Agricultural	KARE	Soil	2017	July	5
Y17TP03S19	Agricultural	KARE	Soil	2017	July	5
Y17TP04S02	Agricultural	KARE	Soil	2017	July	12
Y17TP04S06	Agricultural	KARE	Soil	2017	July	12
Y17TP04S11	Agricultural	KARE	Soil	2017	July	12
Y17TP04S13	Agricultural	KARE	Soil	2017	July	12
Y17TP04S18	Agricultural	KARE	Soil	2017	July	12
Y17TP04S19	Agricultural	KARE	Soil	2017	July	12
Y17TP05S02	Agricultural	KARE	Soil	2017	July	19
Y17TP05S06	Agricultural	KARE	Soil	2017	July	19

Y17TP05S11	Agricultural	KARE	Soil	2017	July	19
Y17TP05S13	Agricultural	KARE	Soil	2017	July	19
Y17TP05S18	Agricultural	KARE	Soil	2017	July	19
Y17TP05S19	Agricultural	KARE	Soil	2017	July	19
Y17TP05S27	Agricultural	KARE	Soil	2017	July	19
Y17TP05S30	Agricultural	KARE	Soil	2017	July	19
Y17TP06S02	Agricultural	KARE	Soil	2017	July	26
Y17TP06S06	Agricultural	KARE	Soil	2017	July	26
Y17TP06S11	Agricultural	KARE	Soil	2017	July	26
Y17TP06S13	Agricultural	KARE	Soil	2017	July	26
Y17TP06S18	Agricultural	KARE	Soil	2017	July	26
Y17TP06S19	Agricultural	KARE	Soil	2017	July	26
Y17TP07S02	Agricultural	KARE	Soil	2017	August	2
Y17TP07S06	Agricultural	KARE	Soil	2017	August	2
Y17TP07S11	Agricultural	KARE	Soil	2017	August	2
Y17TP07S13	Agricultural	KARE	Soil	2017	August	2
Y17TP07S18	Agricultural	KARE	Soil	2017	August	2
Y17TP07S19	Agricultural	KARE	Soil	2017	August	2
Y17TP0808S02	Agricultural	KARE	Soil	2017	August	9
Y17TP0808S06	Agricultural	KARE	Soil	2017	August	9
Y17TP0808S11	Agricultural	KARE	Soil	2017	August	9
Y17TP0808S13	Agricultural	KARE	Soil	2017	August	9
Y17TP0808S18	Agricultural	KARE	Soil	2017	August	9
Y17TP0808S19	Agricultural	KARE	Soil	2017	August	9
Y17TP0824S02	Agricultural	KARE	Soil	2017	August	9
Y17TP0824S06	Agricultural	KARE	Soil	2017	August	9
Y17TP0824S11	Agricultural	KARE	Soil	2017	August	9
Y17TP0824S13	Agricultural	KARE	Soil	2017	August	9
Y17TP0824S18	Agricultural	KARE	Soil	2017	August	9
Y17TP0824S19	Agricultural	KARE	Soil	2017	August	9
Y17TP0848S02	Agricultural	KARE	Soil	2017	August	9
Y17TP0848S06	Agricultural	KARE	Soil	2017	August	9
Y17TP0848S11	Agricultural	KARE	Soil	2017	August	9
Y17TP0848S13	Agricultural	KARE	Soil	2017	August	9
Y17TP0848S18	Agricultural	KARE	Soil	2017	August	9
Y17TP0848S19	Agricultural	KARE	Soil	2017	August	9
Y17TP0896S02	Agricultural	KARE	Soil	2017	August	9
Y17TP0896S06	Agricultural	KARE	Soil	2017	August	9
Y17TP0896S11	Agricultural	KARE	Soil	2017	August	9
Y17TP0896S13	Agricultural	KARE	Soil	2017	August	9
Y17TP0896S18	Agricultural	KARE	Soil	2017	August	9
Y17TP0896S19	Agricultural	KARE	Soil	2017	August	9
Y17TP08S02	Agricultural	KARE	Soil	2017	August	9
Y17TP08S06	Agricultural	KARE	Soil	2017	August	9
Y17TP08S11	Agricultural	KARE	Soil	2017	August	9
Y17TP08S13	Agricultural	KARE	Soil	2017	August	9
Y17TP08S18	Agricultural	KARE	Soil	2017	August	9
Y17TP08S19	Agricultural	KARE	Soil	2017	August	9
Y17TP08S27	Agricultural	KARE	Soil	2017	August	9
Y17TP0948S02	Agricultural	KARE	Soil	2017	August	16
Y17TP0948S03	Agricultural	KARE	Soil	2017	August	16
Y17TP0948S11	Agricultural	KARE	Soil	2017	August	16
Y17TP0948S16	Agricultural	KARE	Soil	2017	August	16
Y17TP0948S19	Agricultural	KARE	Soil	2017	August	16
Y17TP0948S22	Agricultural	KARE	Soil	2017	August	16
Y17TP0996S02	Agricultural	KARE	Soil	2017	August	16
Y17TP0996S03	Agricultural	KARE	Soil	2017	August	16
Y17TP0996S11	Agricultural	KARE	Soil	2017	August	16
Y17TP0996S16	Agricultural	KARE	Soil	2017	August	16
Y17TP0996S19	Agricultural	KARE	Soil	2017	August	16
Y17TP0996S22	Agricultural	KARE	Soil	2017	August	16
Y17TP09S02	Agricultural	KARE	Soil	2017	August	16
Y17TP09S03	Agricultural	KARE	Soil	2017	August	16
Y17TP09S06	Agricultural	KARE	Soil	2017	August	16
Y17TP09S11	Agricultural	KARE	Soil	2017	August	16
Y17TP09S13	Agricultural	KARE	Soil	2017	August	16
Y17TP09S16	Agricultural	KARE	Soil	2017	August	16
Y17TP09S18	Agricultural	KARE	Soil	2017	August	16
Y17TP09S19	Agricultural	KARE	Soil	2017	August	16

Y17TP09S22	Agricultural	KARE	Soil	2017	August	16
Y17TP09S25	Agricultural	KARE	Soil	2017	August	16
Y17TP09S27	Agricultural	KARE	Soil	2017	August	16
Y17TP09S30	Agricultural	KARE	Soil	2017	August	16
Y17TP10S02	Agricultural	KARE	Soil	2017	August	23
Y17TP10S03	Agricultural	KARE	Soil	2017	August	23
Y17TP10S06	Agricultural	KARE	Soil	2017	August	23
Y17TP10S11	Agricultural	KARE	Soil	2017	August	23
Y17TP10S13	Agricultural	KARE	Soil	2017	August	23
Y17TP10S16	Agricultural	KARE	Soil	2017	August	23
Y17TP10S18	Agricultural	KARE	Soil	2017	August	23
Y17TP10S19	Agricultural	KARE	Soil	2017	August	23
Y17TP10S22	Agricultural	KARE	Soil	2017	August	23
Y17TP10S25	Agricultural	KARE	Soil	2017	August	23
Y17TP10S27	Agricultural	KARE	Soil	2017	August	23
Y17TP10S30	Agricultural	KARE	Soil	2017	August	23
Y17TP11S02	Agricultural	KARE	Soil	2017	August	30
Y17TP11S03	Agricultural	KARE	Soil	2017	August	30
Y17TP11S06	Agricultural	KARE	Soil	2017	August	30
Y17TP11S11	Agricultural	KARE	Soil	2017	August	30
Y17TP11S13	Agricultural	KARE	Soil	2017	August	30
Y17TP11S16	Agricultural	KARE	Soil	2017	August	30
Y17TP11S18	Agricultural	KARE	Soil	2017	August	30
Y17TP11S19	Agricultural	KARE	Soil	2017	August	30
Y17TP11S22	Agricultural	KARE	Soil	2017	August	30
Y17TP12S02	Agricultural	KARE	Soil	2017	September	6
Y17TP12S03	Agricultural	KARE	Soil	2017	September	6
Y17TP12S11	Agricultural	KARE	Soil	2017	September	6
Y17TP12S13	Agricultural	KARE	Soil	2017	September	6
Y17TP12S16	Agricultural	KARE	Soil	2017	September	6
Y17TP12S18	Agricultural	KARE	Soil	2017	September	6
Y17TP12S19	Agricultural	KARE	Soil	2017	September	6
Y17TP12S22	Agricultural	KARE	Soil	2017	September	6
Y17TP13S13	Agricultural	KARE	Soil	2017	September	13
Y17TP13S16	Agricultural	KARE	Soil	2017	September	13
Y17TP13S18	Agricultural	KARE	Soil	2017	September	13
Y17TP13S19	Agricultural	KARE	Soil	2017	September	13
Y17TP13S22	Agricultural	KARE	Soil	2017	September	13
Y17TP13S27	Agricultural	KARE	Soil	2017	September	13
Y17TP13S30	Agricultural	KARE	Soil	2017	September	13
Y17TP15S02	Agricultural	KARE	Soil	2017	September	20
Y17TP15S03	Agricultural	KARE	Soil	2017	September	20
Y17TP15S06	Agricultural	KARE	Soil	2017	September	20
Y17TP15S11	Agricultural	KARE	Soil	2017	September	20
Y17TP15S16	Agricultural	KARE	Soil	2017	September	20
Y17TP15S18	Agricultural	KARE	Soil	2017	September	20
Y17TP15S19	Agricultural	KARE	Soil	2017	September	20
Y17TP15S22	Agricultural	KARE	Soil	2017	September	20
Y17TP17S02	Agricultural	KARE	Soil	2017	October	4
Y17TP17S03	Agricultural	KARE	Soil	2017	October	4
Y17TP17S06	Agricultural	KARE	Soil	2017	October	4
Y17TP17S11	Agricultural	KARE	Soil	2017	October	4
Y17TP17S13	Agricultural	KARE	Soil	2017	October	4
Y17TP17S16	Agricultural	KARE	Soil	2017	October	4
Y17TP17S18	Agricultural	KARE	Soil	2017	October	4
Y17TP17S19	Agricultural	KARE	Soil	2017	October	4
Y17TP17S22	Agricultural	KARE	Soil	2017	October	4
Y17TP17S25	Agricultural	KARE	Soil	2017	October	4
Y17TP17S27	Agricultural	KARE	Soil	2017	October	4
Y17TP17S30	Agricultural	KARE	Soil	2017	October	4
Y180118Hwy2a	Undeveloped	Hwy33-2	Air	2018	February	15
Y180118Hwy2b	Undeveloped	Hwy33-2	Air	2018	February	15
Y180118Hwy2c	Undeveloped	Hwy33-2	Air	2018	February	15
Y180118Hwy3a	Undeveloped	Hwy33-3	Air	2018	February	15
Y180118Hwy3b	Undeveloped	Hwy33-3	Air	2018	February	15
Y180118Hwy3c	Undeveloped	Hwy33-3	Air	2018	February	15
Y180118Hwy4a	Undeveloped	Hwy33-4	Air	2018	February	15
Y180118Hwy4b	Undeveloped	Hwy33-4	Air	2018	February	15
Y180118Hwy4c	Undeveloped	Hwy33-4	Air	2018	February	15

Y180118Hwy7a	Undeveloped	Hwy33-7	Air	2018	February	15
Y180118Hwy7b	Undeveloped	Hwy33-7	Air	2018	February	15
Y180118Hwy7c	Undeveloped	Hwy33-7	Air	2018	February	15
Y180118Hwy8a	Undeveloped	Hwy33-8	Air	2018	February	15
Y180118Hwy8b	Undeveloped	Hwy33-8	Air	2018	February	15
Y180118Hwy8c	Undeveloped	Hwy33-8	Air	2018	February	15
Y180215Hwy2a	Undeveloped	Hwy33-2	Air	2018	March	17
Y180215Hwy2b	Undeveloped	Hwy33-2	Air	2018	March	17
Y180215Hwy2c	Undeveloped	Hwy33-2	Air	2018	March	17
Y180215Hwy3a	Undeveloped	Hwy33-3	Air	2018	March	17
Y180215Hwy3b	Undeveloped	Hwy33-3	Air	2018	March	17
Y180215Hwy3c	Undeveloped	Hwy33-3	Air	2018	March	17
Y180215Hwy4a	Undeveloped	Hwy33-4	Air	2018	March	17
Y180215Hwy4b	Undeveloped	Hwy33-4	Air	2018	March	17
Y180215Hwy4c	Undeveloped	Hwy33-4	Air	2018	March	17
Y180215Hwy7a	Undeveloped	Hwy33-7	Air	2018	March	17
Y180215Hwy7b	Undeveloped	Hwy33-7	Air	2018	March	17
Y180215Hwy7c	Undeveloped	Hwy33-7	Air	2018	March	17
Y180215Hwy8a	Undeveloped	Hwy33-8	Air	2018	March	17
Y180215Hwy8b	Undeveloped	Hwy33-8	Air	2018	March	17
Y180215Hwy8c	Undeveloped	Hwy33-8	Air	2018	March	17
Y180317Hwy2a	Undeveloped	Hwy33-2	Air	2018	April	19
Y180317Hwy2c	Undeveloped	Hwy33-2	Air	2018	April	19
Y180317Hwy3a	Undeveloped	Hwy33-3	Air	2018	April	19
Y180317Hwy3b	Undeveloped	Hwy33-3	Air	2018	April	19
Y180317Hwy3c	Undeveloped	Hwy33-3	Air	2018	April	19
Y180317Hwy4a	Undeveloped	Hwy33-4	Air	2018	April	19
Y180317Hwy4b	Undeveloped	Hwy33-4	Air	2018	April	19
Y180317Hwy4c	Undeveloped	Hwy33-4	Air	2018	April	19
Y180317Hwy7a	Undeveloped	Hwy33-7	Air	2018	April	19
Y180317Hwy7b	Undeveloped	Hwy33-7	Air	2018	April	19
Y180317Hwy7c	Undeveloped	Hwy33-7	Air	2018	April	19
Y180317Hwy8a	Undeveloped	Hwy33-8	Air	2018	April	19
Y180317Hwy8b	Undeveloped	Hwy33-8	Air	2018	April	19
Y180317Hwy8c	Undeveloped	Hwy33-8	Air	2018	April	19
Y180419Hwy2a	Undeveloped	Hwy33-2	Air	2018	May	17
Y180419Hwy2b	Undeveloped	Hwy33-2	Air	2018	May	17
Y180419Hwy2c	Undeveloped	Hwy33-2	Air	2018	May	17
Y180419Hwy3a	Undeveloped	Hwy33-3	Air	2018	May	17
Y180419Hwy3b	Undeveloped	Hwy33-3	Air	2018	May	17
Y180419Hwy3c	Undeveloped	Hwy33-3	Air	2018	May	17
Y180419Hwy4a	Undeveloped	Hwy33-4	Air	2018	May	17
Y180419Hwy4b	Undeveloped	Hwy33-4	Air	2018	May	17
Y180419Hwy4c	Undeveloped	Hwy33-4	Air	2018	May	17
Y180419Hwy7a	Undeveloped	Hwy33-7	Air	2018	May	17
Y180419Hwy7b	Undeveloped	Hwy33-7	Air	2018	May	17
Y180419Hwy7c	Undeveloped	Hwy33-7	Air	2018	May	17
Y180419Hwy8a	Undeveloped	Hwy33-8	Air	2018	May	17
Y180419Hwy8b	Undeveloped	Hwy33-8	Air	2018	May	17
Y180419Hwy8c	Undeveloped	Hwy33-8	Air	2018	May	17
Y180517Hwy2a	Undeveloped	Hwy33-2	Air	2018	June	19
Y180517Hwy2b	Undeveloped	Hwy33-2	Air	2018	June	19
Y180517Hwy2c	Undeveloped	Hwy33-2	Air	2018	June	19
Y180517Hwy3a	Undeveloped	Hwy33-3	Air	2018	June	19
Y180517Hwy3b	Undeveloped	Hwy33-3	Air	2018	June	19
Y180517Hwy3c	Undeveloped	Hwy33-3	Air	2018	June	19
Y180517Hwy4a	Undeveloped	Hwy33-4	Air	2018	June	19
Y180517Hwy4b	Undeveloped	Hwy33-4	Air	2018	June	19
Y180517Hwy4c	Undeveloped	Hwy33-4	Air	2018	June	19
Y180517Hwy7a	Undeveloped	Hwy33-7	Air	2018	June	19
Y180517Hwy7b	Undeveloped	Hwy33-7	Air	2018	June	19
Y180517Hwy7c	Undeveloped	Hwy33-7	Air	2018	June	19
Y180517Hwy8a	Undeveloped	Hwy33-8	Air	2018	June	19
Y180517Hwy8b	Undeveloped	Hwy33-8	Air	2018	June	19
Y180517Hwy8c	Undeveloped	Hwy33-8	Air	2018	June	19
Y180616Hwy2a	Undeveloped	Hwy33-2	Air	2018	July	25
Y180616Hwy2b	Undeveloped	Hwy33-2	Air	2018	July	25
Y180616Hwy2c	Undeveloped	Hwy33-2	Air	2018	July	25
Y180616Hwy3a	Undeveloped	Hwy33-3	Air	2018	July	25

Y180616Hwy3b	Undeveloped	Hwy33-3	Air	2018	July	25
Y180616Hwy3c	Undeveloped	Hwy33-3	Air	2018	July	25
Y180616Hwy4a	Undeveloped	Hwy33-4	Air	2018	July	25
Y180616Hwy4b	Undeveloped	Hwy33-4	Air	2018	July	25
Y180616Hwy4c	Undeveloped	Hwy33-4	Air	2018	July	25
Y180616Hwy7a	Undeveloped	Hwy33-7	Air	2018	July	25
Y180616Hwy7b	Undeveloped	Hwy33-7	Air	2018	July	25
Y180616Hwy7c	Undeveloped	Hwy33-7	Air	2018	July	25
Y180616Hwy8a	Undeveloped	Hwy33-8	Air	2018	July	25
Y180616Hwy8b	Undeveloped	Hwy33-8	Air	2018	July	25
Y180616Hwy8c	Undeveloped	Hwy33-8	Air	2018	July	25
Y180816Hwy2a	Undeveloped	Hwy33-2	Air	2018	August	23
Y180816Hwy2b	Undeveloped	Hwy33-2	Air	2018	August	23
Y180816Hwy2c	Undeveloped	Hwy33-2	Air	2018	August	23
Y180816Hwy3a	Undeveloped	Hwy33-3	Air	2018	August	23
Y180816Hwy3b	Undeveloped	Hwy33-3	Air	2018	August	23
Y180816Hwy3c	Undeveloped	Hwy33-3	Air	2018	August	23
Y180816Hwy4a	Undeveloped	Hwy33-4	Air	2018	August	23
Y180816Hwy4b	Undeveloped	Hwy33-4	Air	2018	August	23
Y180816Hwy4c	Undeveloped	Hwy33-4	Air	2018	August	23
Y180816Hwy7a	Undeveloped	Hwy33-7	Air	2018	August	23
Y180816Hwy7b	Undeveloped	Hwy33-7	Air	2018	August	23
Y180816Hwy7c	Undeveloped	Hwy33-7	Air	2018	August	23
Y180816Hwy8a	Undeveloped	Hwy33-8	Air	2018	August	23
Y180816Hwy8b	Undeveloped	Hwy33-8	Air	2018	August	23
Y180816Hwy8c	Undeveloped	Hwy33-8	Air	2018	August	23
Y180916Hwy2a	Undeveloped	Hwy33-2	Air	2018	September	23
Y180916Hwy2b	Undeveloped	Hwy33-2	Air	2018	September	23
Y180916Hwy2c	Undeveloped	Hwy33-2	Air	2018	September	23
Y180916Hwy3a	Undeveloped	Hwy33-3	Air	2018	September	23
Y180916Hwy3b	Undeveloped	Hwy33-3	Air	2018	September	23
Y180916Hwy3c	Undeveloped	Hwy33-3	Air	2018	September	23
Y180916Hwy4a	Undeveloped	Hwy33-4	Air	2018	September	23
Y180916Hwy4b	Undeveloped	Hwy33-4	Air	2018	September	23
Y180916Hwy4c	Undeveloped	Hwy33-4	Air	2018	September	23
Y180916Hwy7a	Undeveloped	Hwy33-7	Air	2018	September	23
Y180916Hwy7b	Undeveloped	Hwy33-7	Air	2018	September	23
Y180916Hwy7c	Undeveloped	Hwy33-7	Air	2018	September	23
Y180916Hwy8a	Undeveloped	Hwy33-8	Air	2018	September	23
Y180916Hwy8b	Undeveloped	Hwy33-8	Air	2018	September	23
Y180916Hwy8c	Undeveloped	Hwy33-8	Air	2018	September	23
Y181016Hwy2a	Undeveloped	Hwy33-2	Air	2018	October	23
Y181016Hwy2b	Undeveloped	Hwy33-2	Air	2018	October	23
Y181016Hwy2c	Undeveloped	Hwy33-2	Air	2018	October	23
Y181016Hwy3a	Undeveloped	Hwy33-3	Air	2018	October	23
Y181016Hwy3b	Undeveloped	Hwy33-3	Air	2018	October	23
Y181016Hwy3c	Undeveloped	Hwy33-3	Air	2018	October	23
Y181016Hwy4a	Undeveloped	Hwy33-4	Air	2018	October	23
Y181016Hwy4b	Undeveloped	Hwy33-4	Air	2018	October	23
Y181016Hwy4c	Undeveloped	Hwy33-4	Air	2018	October	23
Y181016Hwy7a	Undeveloped	Hwy33-7	Air	2018	October	23
Y181016Hwy7b	Undeveloped	Hwy33-7	Air	2018	October	23
Y181016Hwy7c	Undeveloped	Hwy33-7	Air	2018	October	23
Y181016Hwy8a	Undeveloped	Hwy33-8	Air	2018	October	23
Y181016Hwy8b	Undeveloped	Hwy33-8	Air	2018	October	23
Y181016Hwy8c	Undeveloped	Hwy33-8	Air	2018	October	23
Y18A10503	Agricultural	KARE	Air	2018	May	3
Y18A10601	Agricultural	KARE	Air	2018	June	1
Y18A10726	Agricultural	KARE	Air	2018	July	26
Y18A10823	Agricultural	KARE	Air	2018	August	23
Y18A10925	Agricultural	KARE	Air	2018	September	25
Y18A20503	Agricultural	KARE	Air	2018	May	3
Y18A20601	Agricultural	KARE	Air	2018	June	1
Y18A20726	Agricultural	KARE	Air	2018	July	26
Y18A20823	Agricultural	KARE	Air	2018	August	23
Y18A20925	Agricultural	KARE	Air	2018	September	25
Y18A40503	Agricultural	KARE	Air	2018	May	3
Y18A40601	Agricultural	KARE	Air	2018	June	1
Y18A40726	Agricultural	KARE	Air	2018	July	26

Y18A40823	Agricultural	KARE	Air	2018	August	23
Y18A40925	Agricultural	KARE	Air	2018	September	25
Y18A80503	Agricultural	KARE	Air	2018	May	3
Y18A80601	Agricultural	KARE	Air	2018	June	1
Y18A80726	Agricultural	KARE	Air	2018	July	26
Y18A80823	Agricultural	KARE	Air	2018	August	23
Y18A80925	Agricultural	KARE	Air	2018	September	25
Y18B10503	Agricultural	KARE	Air	2018	May	3
Y18B10601	Agricultural	KARE	Air	2018	June	1
Y18B10726	Agricultural	KARE	Air	2018	July	26
Y18B10823	Agricultural	KARE	Air	2018	August	23
Y18B10925	Agricultural	KARE	Air	2018	September	25
Y18B20503	Agricultural	KARE	Air	2018	May	3
Y18B20601	Agricultural	KARE	Air	2018	June	1
Y18B20726	Agricultural	KARE	Air	2018	July	26
Y18B20823	Agricultural	KARE	Air	2018	August	23
Y18B20925	Agricultural	KARE	Air	2018	September	25
Y18B40503	Agricultural	KARE	Air	2018	May	3
Y18B40601	Agricultural	KARE	Air	2018	June	1
Y18B40726	Agricultural	KARE	Air	2018	July	26
Y18B40823	Agricultural	KARE	Air	2018	August	23
Y18B40925	Agricultural	KARE	Air	2018	September	25
Y18B80503	Agricultural	KARE	Air	2018	May	3
Y18B80601	Agricultural	KARE	Air	2018	June	1
Y18B80726	Agricultural	KARE	Air	2018	July	26
Y18B80823	Agricultural	KARE	Air	2018	August	23
Y18B80925	Agricultural	KARE	Air	2018	September	25
Y18C10503	Agricultural	KARE	Air	2018	May	3
Y18C10601	Agricultural	KARE	Air	2018	June	1
Y18C10726	Agricultural	KARE	Air	2018	July	26
Y18C10823	Agricultural	KARE	Air	2018	August	23
Y18C10925	Agricultural	KARE	Air	2018	September	25
Y18C20503	Agricultural	KARE	Air	2018	May	3
Y18C20601	Agricultural	KARE	Air	2018	June	1
Y18C20726	Agricultural	KARE	Air	2018	July	26
Y18C20823	Agricultural	KARE	Air	2018	August	23
Y18C20925	Agricultural	KARE	Air	2018	September	25
Y18C40503	Agricultural	KARE	Air	2018	May	3
Y18C40601	Agricultural	KARE	Air	2018	June	1
Y18C40726	Agricultural	KARE	Air	2018	July	26
Y18C40823	Agricultural	KARE	Air	2018	August	23
Y18C40925	Agricultural	KARE	Air	2018	September	25
Y18C80503	Agricultural	KARE	Air	2018	May	3
Y18C80726	Agricultural	KARE	Air	2018	July	26
Y18C80823	Agricultural	KARE	Air	2018	August	23
Y18C80925	Agricultural	KARE	Air	2018	September	25
Y18P00503	Agricultural	KARE	Air	2018	May	3
Y18P00601	Agricultural	KARE	Air	2018	June	1
Y18P00726	Agricultural	KARE	Air	2018	July	26
Y18P00823	Agricultural	KARE	Air	2018	August	23
Y18P00925	Agricultural	KARE	Air	2018	September	25

3239